NATIONAL AERONAUTICS AND SPACE ADMINISTRATION

Technical Report 32-1584

Performance Characterization Tests of Three 0.44-N (0.1-lbf) Hydrazine Catalytic Thrusters

P. I. Moynihan

R. A. Bjorklund

JET PROPULSION LABORATORY

CALIFORNIA INSTITUTE OF TECHNOLOGY

PASADENA, CALIFORNIA

September 1, 1973

NATIONAL AERONAUTICS AND SPACE ADMINISTRATION

Technical Report 32-1584

Performance Characterization Tests of Three 0.44-N (0.1-lbf) Hydrazine Catalytic Thrusters

P. I. Moynihan
R. A. Bjorklund

JET PROPULSION LABORATORY
CALIFORNIA INSTITUTE OF TECHNOLOGY
PASADENA, CALIFORNIA

September 1, 1973

Prepared Under Contract No. NAS 7-100
National Aeronautics and Space Administration

Preface

The work described in this report was sponsored by the National Aeronautics and Space Administration Office of Advanced Research and Technology and was performed by the Propulsion Division of the Jet Propulsion Laboratory.

Acknowledgment

The authors wish to extend their gratitude to Mrs. Judy Foster for her skill and perseverance in handling and reducing the enormous volumes of data that were generated by this test program.

Contents

Contents (contd)

Tables

Figures

Contents (contd)

Figures (contd)

Contents (contd)

Figures (contd)

Contents (contd)

Figures (contd)

Abstract

The 0.44-N (0.1-lbf) class of hydrazine catalytic thruster has been evaluated at the Jet Propulsion Laboratory to assess its capability for spacecraft limit-cycle attitude control with thruster pulse durations on the order of 10 ms. Dynamic-environment and limit-cycle simulation tests were performed on three commercially available thruster/valve assemblies, purchased from three different manufacturers. The results indicate that this class of thruster can sustain a launch environment and, when properly temperature-conditioned, can perform limit-cycle operations over the anticipated life span of a multi-year mission. The minimum operating temperature for very short pulse durations was determined for each thruster. Pulsing life tests were then conducted on each thruster under a thermally controlled condition which maintained the catalyst bed at both a nominal 93°C (200°F) and 205°C (400°F). These were the temperatures believed to be slightly below and very near the minimum recommended operating temperature, respectively. The ensuing life tests ranged from 1×10^5 to 2.5×10^5 pulses at these temperatures, as would be required for spacecraft limit-cycle attitude control applications.

Performance Characterization Tests of Three 0.44-N (0.1 lbf) Hydrazine Catalytic Thrusters

I. Introduction and Background

As experience was gained during earlier attitude propulsion system programs (Ref. 1) with 0.44-N (0.1-lbf)[1] hydrazine thrusters, it became increasingly apparent that there was insufficient knowledge of the minimum-impulse capabilities of these thrusters for spacecraft attitude-control limit-cycle applications. A demonstration of limit-cycle proficiency for the 0.44-N (0.1-lbf) hydrazine thruster class would also provide a mass-limited spacecraft, such as those for outer planet missions, with the option of an all-liquid-fed mass expulsion system completely contained within a common propulsion module.

Although the minimum hydrazine thruster *on*-time required of previous Jet Propulsion Laboratory (JPL) programs was 0.1 s, the disturbing question of the actual minimum impulse capabilities remained. An early impulse bit definition experiment (Ref. 2), which was performed at temperatures of 21°C (70°F) and 149°C (300°F), was a precursor to the more extensive investigation of spacecraft limit-cycle applicability reported herein.

In this report, the results of both environmental tests and attitude-control limit-cycle simulation tests are presented for three thruster designs.

In early 1971, JPL had procured two 0.44-N (0.1-lbf) hydrazine catalytic thrusters from each of three manufacturers of these units (Hamilton Standard, Marquardt, and Rocket Research) for the Thermoelectric Outer Planet Spacecraft (TOPS) attitude propulsion subsystem feasibility demonstration program. One thruster of each set (see Fig. 1) had undergone an exhaustive test program (Ref. 1) to demonstrate the capability of this class of thrusters to meet the primary attitude propulsion requirements for a 10-year outer-planets mission with three planet encounters.

[1]Values in English units are included in parentheses after the values in SI (International System) units if the English units were used in the measurements or calculations.

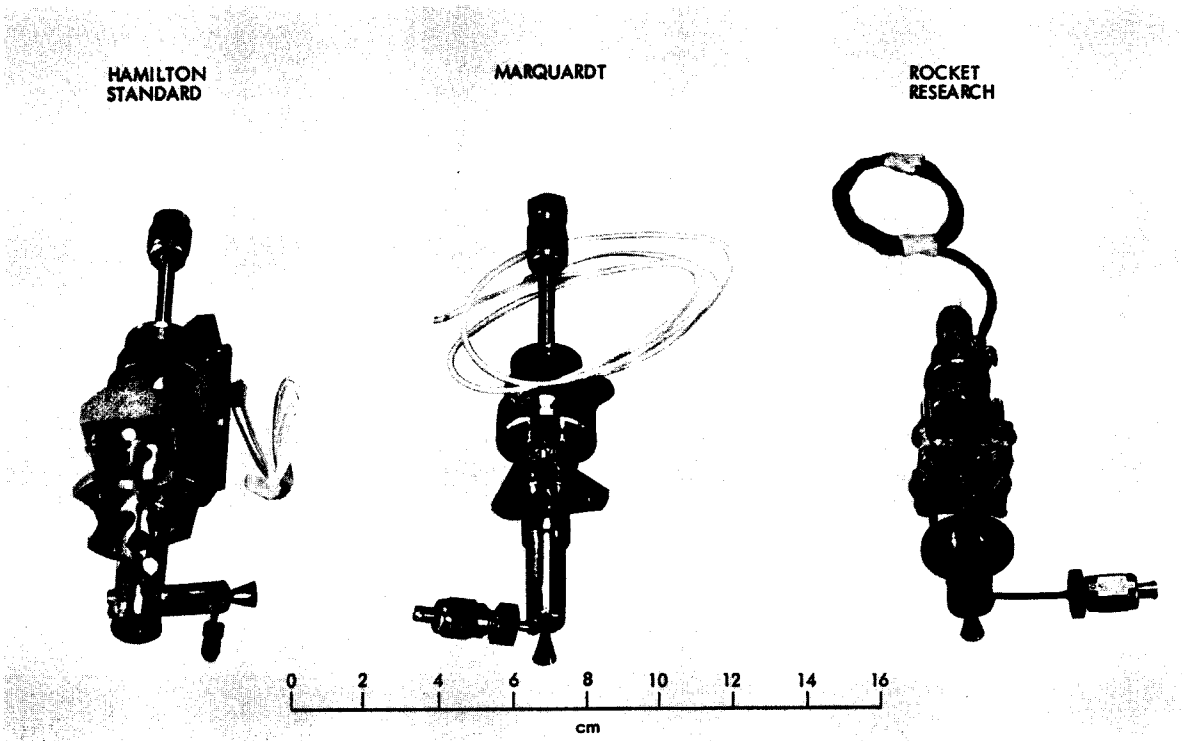

Fig. 1. The 0.44-N (1-lbf) thrusters tested in this program

The second thruster of each set was subsequently scheduled to undergo extensive environmental dynamics testing indicative of the anticipated launch environment, followed by the test program described herein. For all three thrusters, the environmental dynamics test was preceded by a performance characterization test and followed by a performance validation test to detect any performance changes.

Following the environmental dynamics tests, several tests were conducted to define the lower catalyst bed temperature limits at which each thruster could operate in a pulse mode and still expect an increased catalyst bed life. The catalyst bed structural lifetime was expected to be markedly increased if all hydrazine decomposition reactions were to take place primarily on the outer surface of the porous, iridium-impregnated alumina catalyst particles (Shell 405). Assuming the required catalytic surface area to be inversely proportional to the bed temperature, there would be a lower temperature limit at which this exclusively outer-surface reaction would occur. For a spontaneous reaction to occur below this temperature, it would be necessary for the hydrazine to be absorbed into the porous catalyst particles in order to make contact with a greater surface area.

However, when the hydrazine is absorbed into the capillary-size catalyst pores as a liquid and is then vaporized and decomposed (or absorbed directly as a vapor and decomposed), pressures on the order of 1.38×10^7 N/m^2 (2000 psi) can be generated locally. These high pressures, coupled with large thermal gradients, cause fracturing of the ceramic catalyst particles and hence the generation of catalyst "fines" (see Fig. 2). As the fines are expelled from the thruster, the bed loosens, causing an increase in chamber pressure roughness, which aggravates bed erosion.

It is further theorized that the temperature at which the hydrazine starts to absorb into the catalyst particle prior to decomposition would be reflected by a change in impulse bit, response time, and chamber pressure profiles in such a way that any one, or a combination, of these parameters plotted as a function of temperature would reflect a change of slope of the curve at the temperature where the dissociation would be sustained solely on the outer surface of the catalyst particles, in a manner similar to that indicated by Fig. 3a. Data from earlier test series indicated that this slope change was expected to occur around 121°C (250°F). In a mode similar to that suggested by Fig. 3b, the catalyst bed life is expected to increase significantly as the lower temperature limit of the thruster is raised.

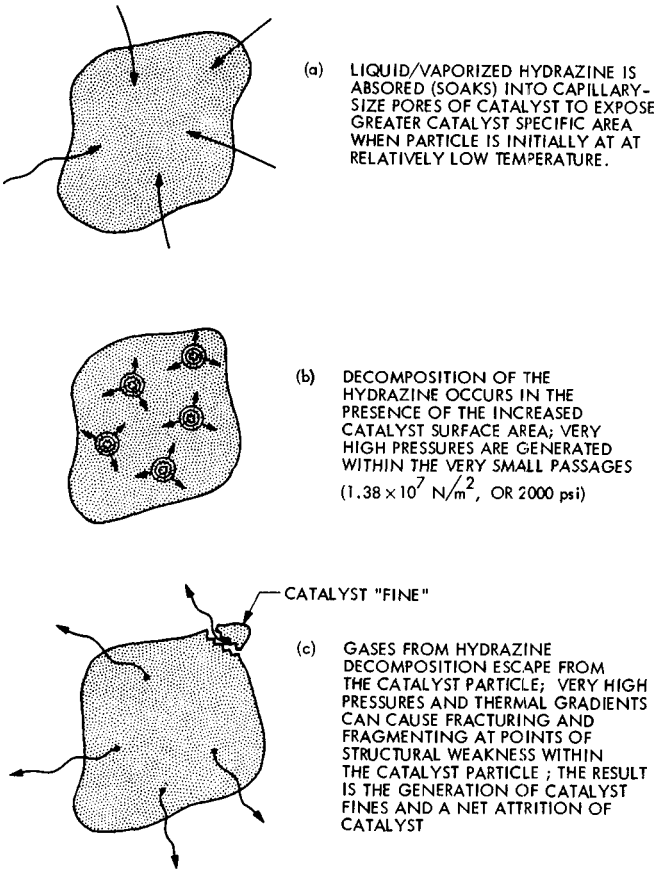

Fig. 2. Catalyst particle fracturing from low-temperature start

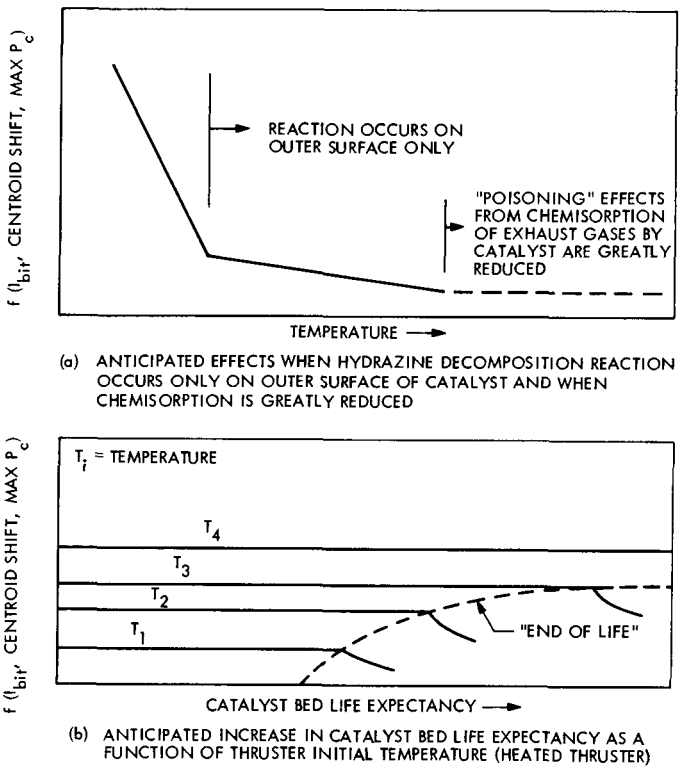

Fig. 3. Relationships between thruster initial temperature and catalyst bed life expectancy

Life tests simulating a spacecraft attitude-control limit-cycle mode operation were conducted after the tests defining the minimum operating temperature. The starting temperatures for the life tests were based on the results of the minimum operating temperature tests; initially, the life test starting temperatures were assigned as those values occurring very near the change in slope from the minimum temperature tests. However, as the life tests proceeded at these relatively low temperatures, a second anomaly independent of the established minimum operating temperature was observed in the form of a performance decay caused apparently by a temporary "poisoning" of the active catalyst sites from chemisorption of the exhaust product gases.

As presented pictorially in Fig. 4, this temporary poisoning appears to start with the primary reaction zone located close to the injector and renders the catalyst inactive at that point, causing the incoming hydrazine to migrate further downstream until an active site is encountered. This process continues until most of the active sites are consumed. The result is a marked performance loss and thrust decay. However, since chemisorption poisoning appears nearly completely reversible by a vacuum baking for a few hours at approximately 260°C (500°F), a second minimum operating temperature higher than that previously established for the catalyst's mechanical integrity is suggested to prevent, or at least retard, such poisoning. For the duty cycle selected for this test program, any starting temperature at or above 204°C (400°F) was considered sufficient.

II. Test Items

The three purchased 0.44-N (0.1-lbf) thrusters used in this program are identified in Table 1. All were of the monopropellant hydrazine type using either 25–30 mesh or 30–40 mesh Shell 405 ABSG spontaneous catalyst in the reactor beds. The Hamilton Standard (HS) and Rocket Research Corporation (RRC) thrusters incorporated a preloaded packed bed design, whereas the Marquardt (TMC) thruster utilized a spring-loaded bed. Each unit employed a different propellant injector design. The RRC thruster had a Rigimesh showerhead injector; the HS unit incorporated a short cone penetrant composed of an 85-mesh inner screen and a 200-mesh outer screen, and the TMC

Table 1. Nomenclature of the 0.44-N (0.1 lbf) hydrazine catalytic thruster assemblies tested

Thruster			
Manufacturer	Hamilton Standard Division United Aircraft Corp. Windsor Locks, Conn.	The Marquardt Co. Van Nuys, Calif.	Rocket Research Corp. Redmond, Wash.
Model No.	10-12	R-25A	MR-74 REA
Part No.	SYSK 75814	T-17412	25917-301-11
Serial No.	001	002A	02[a]
Valve			
Manufacturer	Parker-Hannifin Corp. Aerospace Group Los Angeles, Calif.	Parker-Hannifin Corp. Aerospace Group Los Angeles, Calif.	Moog Inc. Aerospace Div. East Aurora, N.Y.
Model No.	—	—	50X391
Part No.	5696050-101	5690054-101	010-58723-1
Serial No.	T064801	T095502	3

[a]Rocket Research Thruster S/N 01 was also used for one limit-cycle test series.

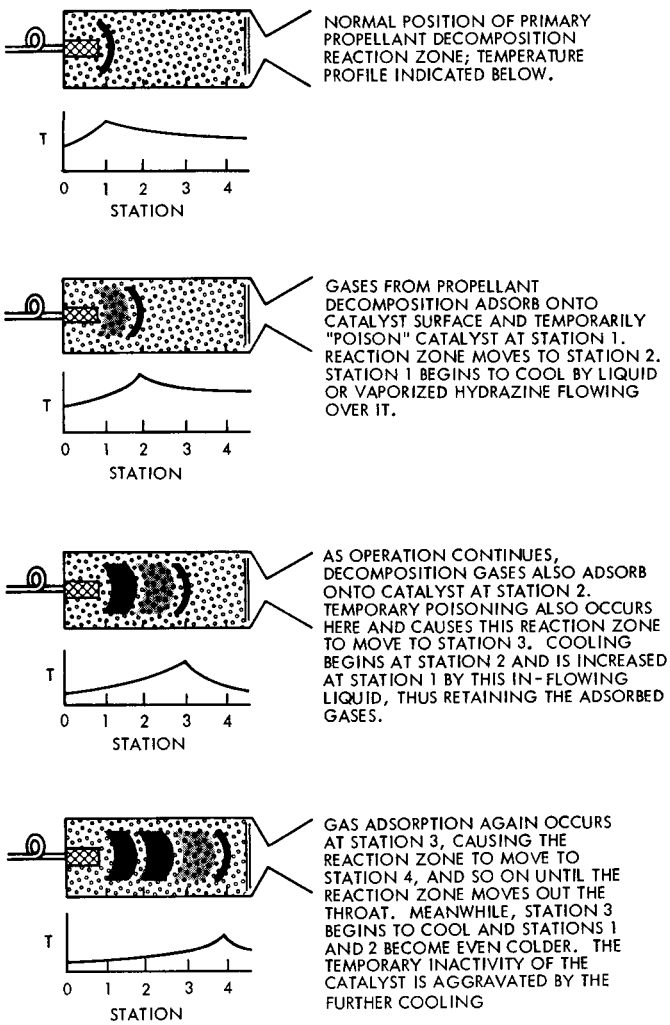

Fig. 4. Progression of reaction zone through catalyst bed during an extended-duration test

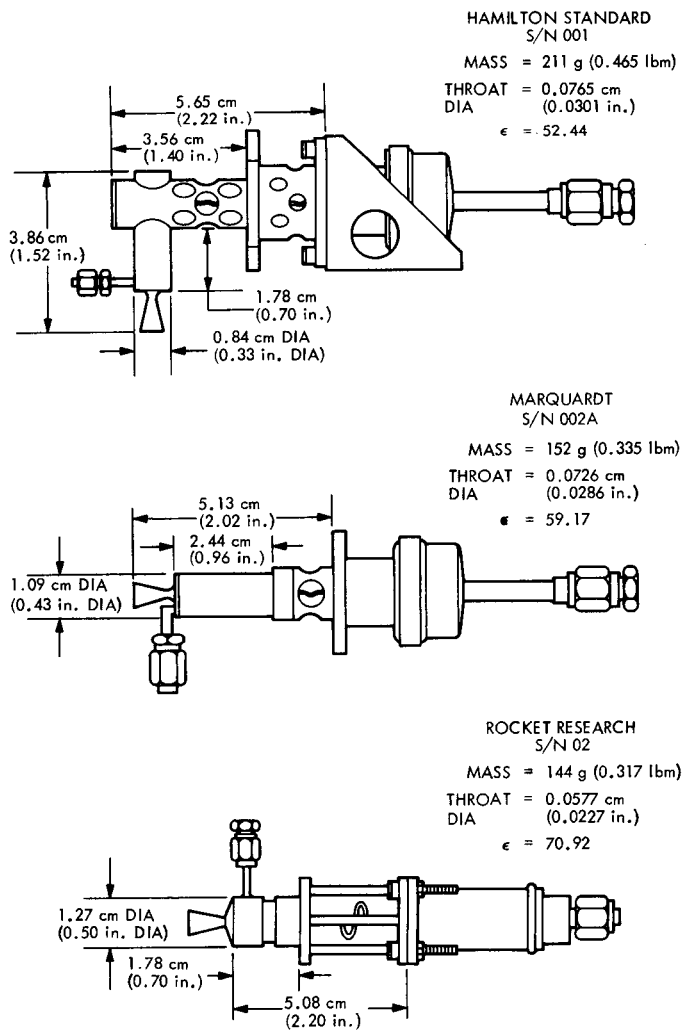

Fig. 5. Nominal dimensions and mass of 0.44-N (1-lbf) thrusters

thruster had a long penetrant tube made of 60-mesh screen. The propellant valves were all of the normally closed, coaxial solenoid, poppet type with TFE Teflon for the seat seal. Two assemblies, RRC and TMC, had the valves oriented in line with the thrust chamber, while the HS unit had the valve mounted perpendicular to the thrust chamber axis. The valves were normally activated with 28-V dc electrical power.

Nominal dimensions and weights of each thruster assembly are shown in the Fig. 5. A chamber pressure tap downstream of the catalyst bed was provided with each thruster assembly.

III. Test Facilities

All operations that were performed on the 0.44-N (0.1-lbf) thruster assemblies for this program (except for the environmental dynamics tests, which utilized a portion of the JPL spacecraft environmental laboratory) were conducted at JPL in a vacuum test facility that utilized the same engine support hardware, propellant feed system, test chamber, and vacuum pumping system that were reported in detail in Ref. 1. The test facility and test conditions are summarized in the following paragraphs.

A. Vacuum Test Facility

The actual test firings of the 0.44-N (0.1-lbf) monopropellant thrusters required a continuous vacuum of 133 N/m^2 (1 torr) or lower to accomplish the design performance and to prolong life. The vacuum test chamber utilized for this test program, shown in Fig. 6, had a volume of 2.3 m^3 (100 ft^3). The vacuum pumping system, with a capacity of 2.42 m^3/s (5100 ft^3/min), could maintain a nominal vacuum of 133 N/m^2 (1 torr) with an ultimate

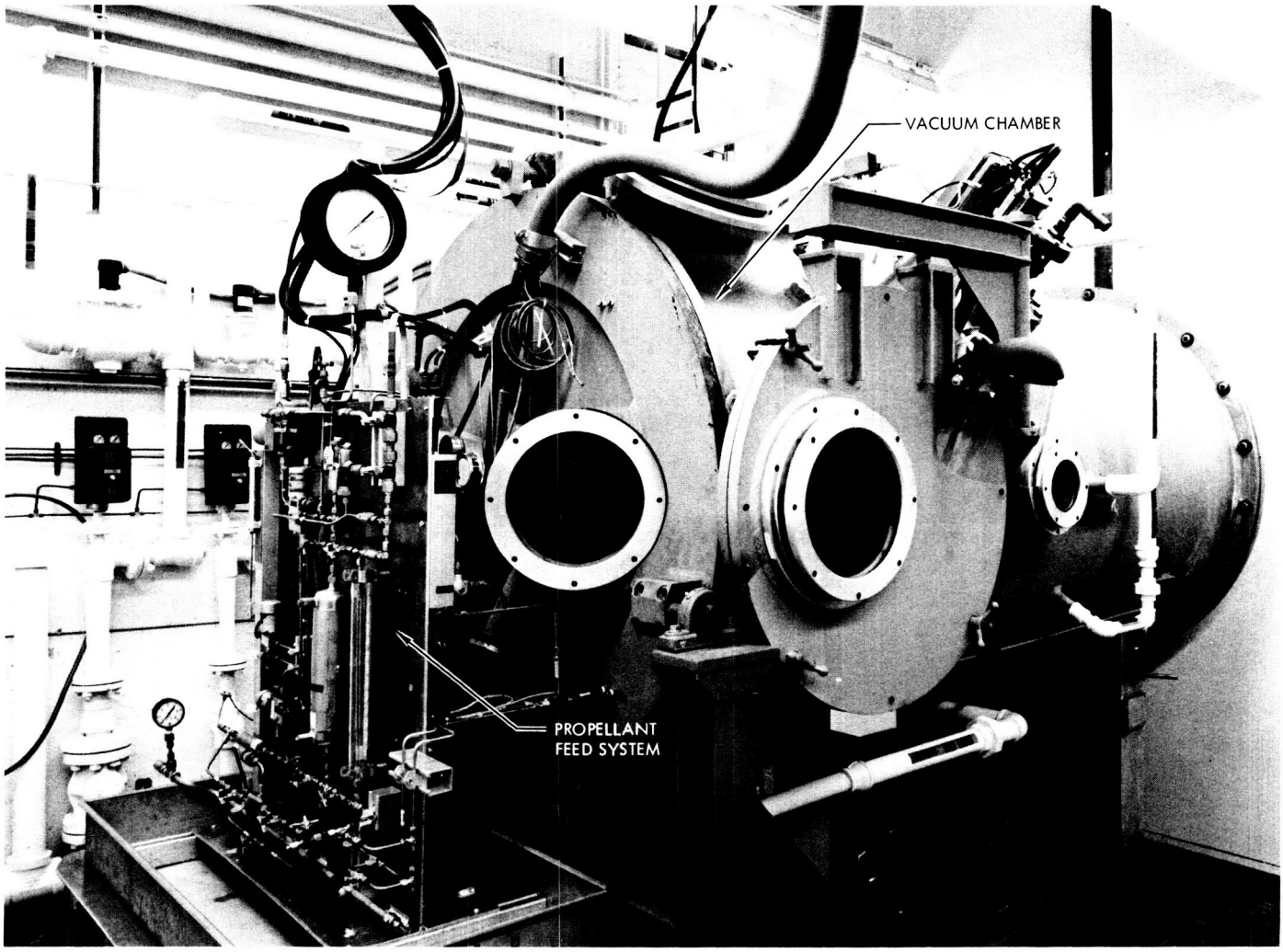

Fig. 6. Vacuum test chamber, JPL Vacuum Test Facility

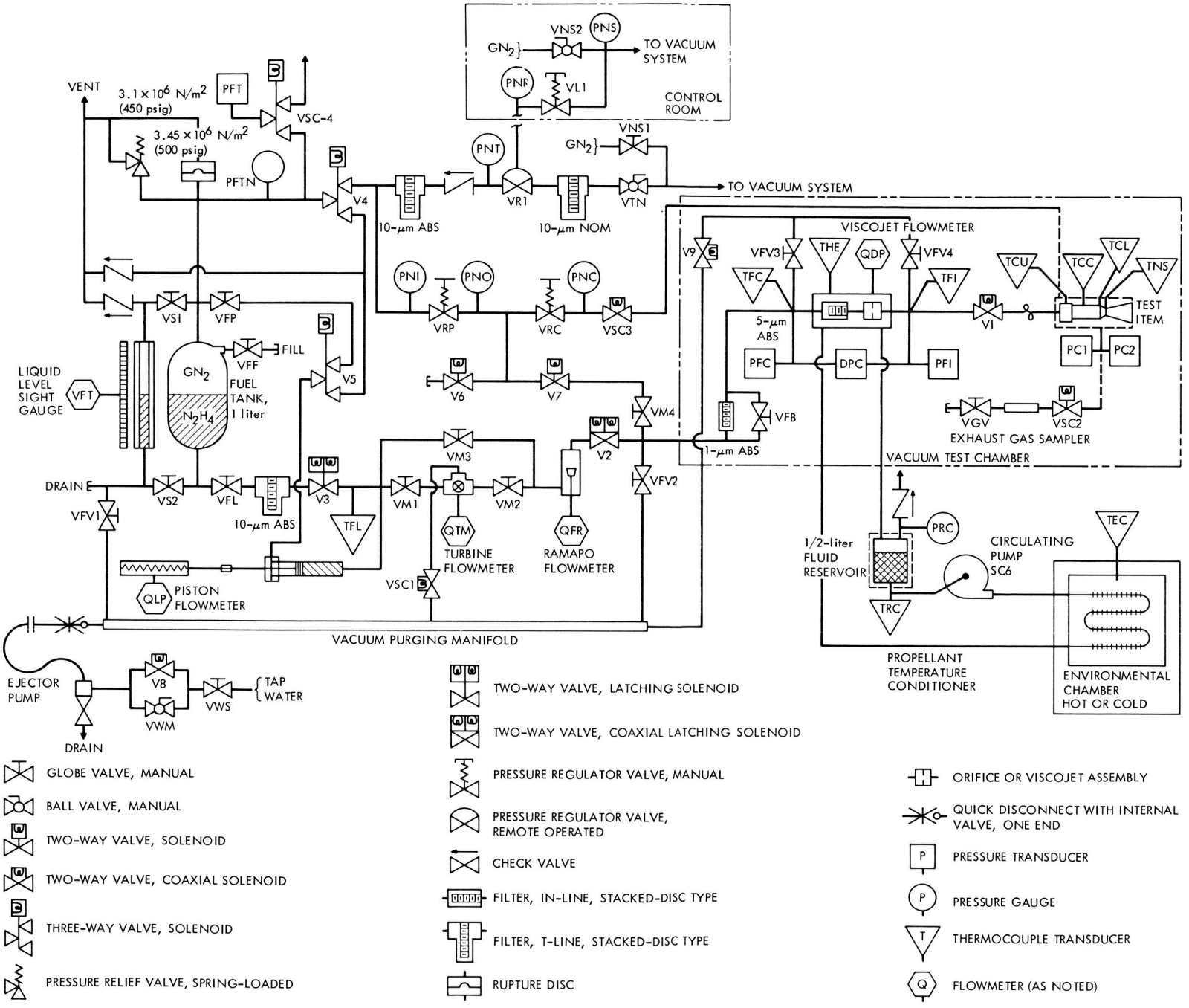

Fig. 7. Propellant system schematic diagram for small thruster tests

(no-flow) vacuum of 0.27 N/m^2 (2×10^{-3} torr). The pressure inside the test chamber could be raised to atmospheric pressure by allowing either ambient air or gaseous nitrogen to be vented in.

The hydrazine propellant feed system shown mounted on the vacuum chamber door carriage in Fig. 6 was nitrogen-gas-pressure regulated with a maximum operating pressure of 3493×10^3 N/m^2 (500 psig). The total liquid volume in the all-stainless-steel system was 1000 cm^3 (61 $in.^3$). A Viscojet ΔP flowmeter and an Omniflo turbine flowmeter were the primary and secondary means of measuring propellant flow rate.

Two Vacco stacked etched-disc-type filters were normally used in the propellant line. A 10-μm absolute filter preceded and protected the Omniflo turbine flowmeter and a 5-μm absolute filter was at the inlet of the Viscojet ΔP flowmeter. A third labyrinth type was added for experimental evaluation at a convenient point in the system. This filter, which had a 1-μm absolute rating, was manufactured to JPL specification by the Wintec Corporation, Los Angeles, Calif. The filter was installed at the start of this test program (Test 1354) but had to be removed later when it became plugged (Test 1530). During the time in service, 3 months and 19 days, it had filtered 7.88×10^3 cm^3 (4.80×10^3 $in.^3$) of hydrazine.

The propellant temperature conditioning, which ranged from 4.5 to 49.0°C (40 to 120°F), was accomplished by circulating a preconditioned mixture of water and ethylene glycol through a heat exchanger jacket that surrounded the 5-μm filter and Viscojet element. A schematic diagram depicting the pressurant and propellant feed system is presented in Fig. 7.

B. Instrumentation

The instrumentation systems incorporated into the vacuum test facility consisted of pressure transducers, thermocouples, signal conditioning units, and recording equipment. The pressure transducers used were as follows:

(1) Statham PA-208-TC, 0 to 3.45×10^6 N/m^2 (0–500 psia).

(2) Statham PL-280-TC, $\pm 1.73 \times 10^6$ N/m^2 ($\pm$250 psid).

(3) Taber 176, 0 to 3.45×10^6 N/m^2 (0–500 psig).

(4) Taber 217, 0 to 1.38×10^6 N/m^2 (0–200 psia).

(5) CVC Magnavac, 0 to 6.65×10^4 N/m^2 (0–500 torr).

The volumetric flowrate transducers were:

(1) Flow Technology Omniflo FTM-0.4-LJS.

(2) Lee Company Viscojet 38VL3CM (used in conjunction with the Statham PL-280-TC differential pressure transducer).

Chromel–alumel thermocouples (type K) were immersed into both the hydrazine and the heat transfer fluids to obtain direct readings of these temperatures; the temperatures of the thruster bodies and nozzles were obtained from chromel–alumel thermocouples that were spot-welded to the outer surfaces.

The pressure transducers were calibrated in the JPL Calibration Laboratory, whose procedures are traceable to the National Bureau of Standards (NBS). The flow rate transducers were calibrated both with water and with hydrazine. (The hydrazine calibration was performed in the test system.) Thermocouples were not calibrated but were made of wire obtained from spools certified by the JPL Calibration Laboratory.

The signal-conditioning equipment included the following units:

(1) Dynamics 6496 amplifier.

(2) Dynamics 7506 amplifier.

(3) Dynamics 6343 A bridge supply.

The recording instruments were divided between the low-speed type for slow transients or steady state data and the high-speed type for transient data. Critical parameters were recorded on both types for redundancy. The low-speed recorders were the Leeds and Northrup Type G and the Mosely 680 strip charts. The high-speed recorder was a 12-channel Honeywell Model 1912 oscillograph.

Data accuracy was improved by recording critical parameters used in performance calculations on the low-speed recorders. The reported thruster performance was obtained at steady state operating conditions. A listing of instrumentation test parameters, recording instruments, and the results of an error analysis calculated using the root-sum-square (rss) method is presented in Table 2.

C. Environmental Dynamics Test Facilities

1. Acoustic energy. The high-intensity acoustic energy test facility in which the thruster environmental test assemblies were evaluated was constructed primarily for testing the Mariner Mars 1971 spacecraft but has

Table 2. Summary of test instrumentation parameters

Symbol	Parameter description	Units	Full scale	Recorder	Maximum error
P_{ft}	Pressure, fuel tank	N/m^2 (psia)	3.448×10^6 (500)	Strip-chart	19.3×10^3 (2.8)
P_{fc}	Pressure, Viscojet inlet	N/m^2 (psia)	2.758×10^6 (400)	Oscillograph	79.9×10^3 (11.6)
ΔP_{fc}	Differential pressure, Viscojet	N/m^2 (psid)	2.069×10^6 (300)	Strip-chart, Oscillograph	25.5×10^3 (3.7) 61.4×10^3 (8.9)
P_{fi}	Pressure, fuel injector inlet	N/m^2 (psia)	2.758×10^6 (400)	Oscillograph	79.9×10^3 (11.6)
P_{c1}	Pressure, thrust chamber (Statham)	N/m^2 (psia)	3.448×10^6 (500)	Oscillograph	101.4×10^3 (14.7)
P_{c2}	Pressure, thrust chamber (Taber)	N/m^2 (psia)	1.379×10^6 (200)	Strip-chart, Oscillograph	8.9×10^3 (1.3) 39.4×10^3 (5.7)
P_{vc}	Pressure, vacuum test chamber	N/m^2 (psia)	186 (0.027)	Oscillograph	0.006 (0.001)
T_{fl}	Temperature, fuel line	°C (°F)	94 (200)	Strip-chart, Oscillograph	7.6 (4.2) 16.5 (9.0)
T_{fc}	Temperature, fuel capillary or Viscojet inlet	°C (°F)	94 (200)	Strip-chart, Oscillograph	7.6 (4.2) 16.5 (9.0)
T_{cl}	Temperature, thrust chamber lower wall	°C (°F)	1094 (2000)	Strip-chart, Oscillograph	12.3 (18.0) 40.1 (58.5)
T_{ns}	Temperature, nozzle throat surface	°C (°F)	1094 (2000)	Strip-chart, Oscillograph	12.3 (18.0) 40.1 (58.5)
$\dot{m}_o$	Mass flow rate, Omniflo turbine meter	g/s (mlbm/s)	0.395 (0.870)	Oscillograph	0.0015 (0.0034)
$\dot{m}_v$	Mass flow rate, Viscojet ΔP meter	g/s (mlbm/s)	0.395 (0.870)	Strip-chart, Oscillograph	0.0022 (0.0048) 0.0053 (0.0116)

broader range capabilities for future requirements. The 2.83×10^2 m^3 (10^4 ft^3) concrete reverberation chamber has steel-reinforced walls 0.46 m (18 in.) thick. The sound pressure is derived from two gaseous-nitrogen-driven exponential horns with a cutoff frequency of 50 Hz. The horn transducers are of the Ling Electropneumatic type EPT-94B, with a total acoustic power of 16 kW. The transducers are controlled by direct digital means over the frequency range of 1/3 octaves from 63 to 800 Hz. Energy above 800 Hz is generated by harmonic distortion within these horns. Six B & K Type 4133 microphones were used for the control channels, and an additional six for the recording channels. The system was calibrated before and after each test using the following listed sources, which are traceable to an NBS standard at a level of 124 dB:

(1) Pistonphone—B & K 4200.

(2) Reciprocity—B & K 4142.

(3) Noise source—B & K 4240.

(4) Sine source—GR 1562 A.

(5) High intensity—Whittaker PC 125 and B & K BBN910D.

2. Vibration. The environmental sinusoidal and random vibration testing was conducted using the Ling PP 175/240 KVA control system to drive one of two electrodynamic vibration exciters, an M. B. Electronics Model C-126 or a Ling Electronics Model 335. Both exciters have a frequency range capability of 5 to 2000 Hz with a maximum amplitude of 2.54 cm (1 in.) peak to peak. The first unit has a maximum force capability of 40,032 N (9,000 lbf), while the second can reach up to 77,840 N (17,500 lbf). Both are equipped with oil film granite slide tables in order to permit vibration in three orthogonal axes.

3. Shock. The shock testing was performed on a high-g shock machine designed and fabricated at JPL. This machine operates by rolling a 227-kg (500-lbm) steel carriage down an inclined plane onto an anvil upon which the test item is mounted. The g-level of shock is determined by the starting height of the carriage. The nature of the shock transmitted to the anvil is determined by a liquid spring or other resilient material placed on the anvil at the point of impact. Vertical and horizontal mounting surfaces on the anvil provide the orthogonal orientation axes for the test fixture. The intensity and shape of the shock are measured by accelerometers aligned with the

axis of applied shock, and the output is recorded on an oscilloscope equipped with a Polaroid camera.

4. Acceleration. Static acceleration testing was performed on a Genisco centrifuge. The arm length (radius) of the centrifuge was 1.22 m (4.0 ft). Maximum capability of this machine is 100 g, as determined by its speed of rotation.

IV. Environmental Effects Evaluation Tests

A. Objective

The objective of the environmental effects test program was to evaluate the three 0.44-N (0.1-lbf) thrusters, which JPL had purchased from Hamilton Standard, Marquardt, and Rocket Research, for their durability in withstanding the dynamic structural loads imposed on the spacecraft by typical launch vehicle staging, injection into the transfer orbit, and peripheral systems operation. The baseline performance of the thrusters was compared both before and after a series of environmental dynamic tests that were designed to simulate the more severe conditions, including sinusoidal and random vibrations, static acceleration, shock, and acoustic noise.

B. Test Plan

The test plan consisted of three test series performed consecutively on each thruster. They were identified as the characterization tests, environmental dynamics tests, and performance validation tests. All thruster operations were conducted with the thruster installed in a vacuum chamber and fed by ambient-temperature propellant. All environmental dynamics tests, however, were performed at the laboratory ambient pressure and temperature conditions. The specifications that were given for these three tests are outlined below.

1. Characterization tests. The characterization tests, which were conducted to define the thruster performance parameters, proceeded as follows:

(1) Each thruster was tested with supply tank pressures increasing from 6.9×10^5 N/m^2 (100 psig) to 2.75×10^6 N/m^2 (400 psig) in 3.45×10^5 N/m^2 (50 psi) increments, dwelling at each pressure for 60 s. (Hereafter, this is referred to as a "calibration" test.) The tank pressure required for a thrust level of 0.44 N (0.1 lbf) is established from the first test on each thruster.

(2) Each thruster was tested at the tank pressure selected to give a nominal thrust of 0.44 N (0.1 lbf) for 60 s steady state. An exhaust gas sample was taken during the last 10 s of operation before cutoff.

(3) Each thruster was pulsed 1000 times at the tank pressure selected to give a nominal thrust of 0.44 N (0.1 lbf). A duty cycle of 0.4 s *on* and 0.4 s *off* was used.

(4) The duty cycle was reduced to 0.2 s *on* and 0.2 s *off* and the thruster was pulsed 1000 times.

(5) The duty cycle was reduced to 0.15 s *on* and 0.15 s *off* and the thruster was pulsed 1000 times.

(6) The duty cycle was reduced to 0.1 s *on* and 0.9 s *off* and the thruster was pulsed 1000 times.

(7) The duty cycle was reduced to 0.07 s *on* and 0.7 s *off* and the thruster was pulsed 1000 times.

(8) The duty cycle was reduced to 0.05 s *on* and 0.5 s *off* and the thruster was pulsed 1000 times.

(9) The calibration test was repeated.

(10) The data were compared with the manufacturer's results.

2. Environmental dynamics tests. Although there was no requirement for any of these thrusters to meet an environmental dynamics spectrum at the time of purchase, it was decided that the one unit from each manufacturer that was selected for this test program would be subjected to an environmental dynamics test at JPL to ascertain any limitations that may result from a launch sequence. The Viking Orbiter specification (Ref. 3) was used as the background for these test requirements, which are indicated below. A closure was placed over the nozzle exit to retain any catalyst particles that may have been generated by the induced loads. Test requirements were as follows:

(1) *Sinusoidal vibration.* The thrusters shall withstand sinusoidal vibration throughout the frequency range from 5 to 2000 Hz. Excitation of the amplitude levels shown in Table 3 shall be applied to the longitudinal axis and both lateral axes at a sweep rate of two octaves per minute between 5 and 2000 Hz and back to 5 Hz.

(2) *Random vibration.* The thrusters shall withstand random vibration with the spectrum shown in Fig. 8 for 300 s duration in the longitudinal axis and both lateral axes. The vibration shall have a Gaussian amplitude distribution, except that instantaneous peak amplitudes greater than 3σ shall be suppressed. The shape shall be a flat power density of 1.0 g^2/Hz from 40 to 600 Hz with roll-off at 12 dB/octave from 600 to 2000 Hz; the spectrum

Table 3. Sinusoidal vibration amplitude levels

Frequency, Hz	Amplitude, g (peak)
5 to 2000	1.0
5 to 30	4.0
30 to 2000	10.0

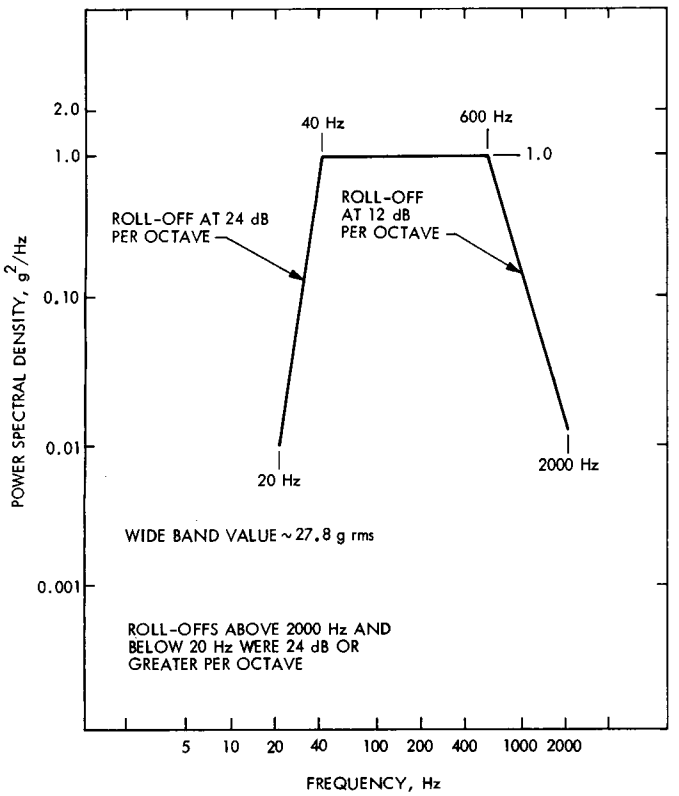

Fig. 8. Random vibration spectrum

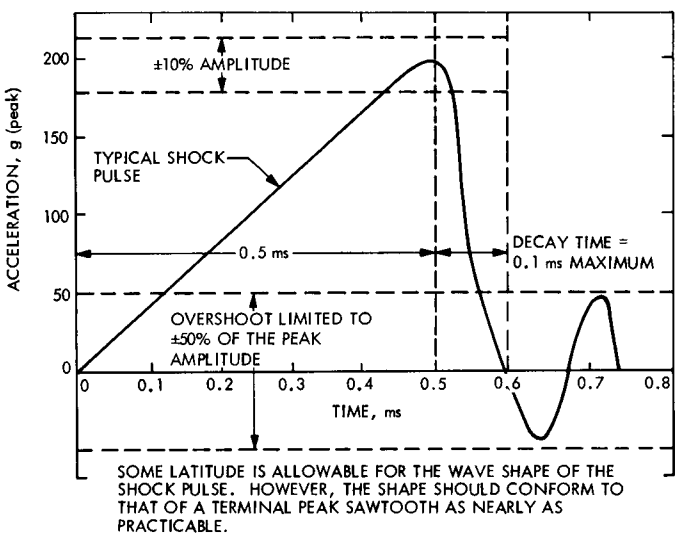

Fig. 9. Typical shock pulse

shall be rolled off at a rate of 24 dB/octave or greater. Requirements shall be the same for all axes. When the specified spectrum is obtained, the wideband level will be approximately 27.8 g rms.

(3) *Shock.* The thrusters shall withstand five shock pulses (shown in Fig. 9) in the longitudinal axis and both lateral axes for a total of 15 shock pulses.

(4) *Acceleration.* The thrusters shall withstand exposure to a 15-g (maximum) acceleration load when it is applied in each direction to the longitudinal axis and both lateral axes for a duration of 2 min per application.

(5) *Acoustic energy.* The thrusters shall withstand exposure to a reverberant acoustic field with an overall sound pressure level of 150 dB (ref. 2×10^{-5} N/m², or 0.0002 microbar) and 1/3-octave band sound pressure levels as defined in Table 4. The exposure duration shall be 5 min.

3. Performance validation tests. The performance validation tests, which were conducted after the environ-

Table 4. Acoustic sound pressure levels

1/3-octave band center frequency, Hz	Sound pressure level (ref. 2×10^{-5} N/m² 0.0002 μbar), dB	Tolerance, dB
40	130	+5 −16
50	132	+5 −8
63	134	±5
80	135	±5
100	136	±5
125	137	±4
160	138	±4
200	139	±4
250	139	±4
315	139	±4
400	139	±3
500	139	±3
630	139	±3
800	138	±3
1000	137	±3
1250	136	±2
1600	135	+2 −3
2000	134	+2 −4
2500	133	+2 −5
3150	132	+2 −6
4000	131	+1 −7
5000	130	+1 −8
6300	129	+1 −9
8000	128	+1 −10
10000	127	+1 −11

mental dynamics tests to determine whether any degradation had occurred, were performed as follows:

(1) The thrusters were inspected for any visible structural damage that might have been caused by the environmental dynamics tests. The nozzle exit closure was removed, and any particles that might have separated from the catalyst bed were collected, weighed, and sized.

(2) The characterization test series was repeated for each thruster.

(3) The performance data were compared for each thruster before and after the environmental dynamics tests.

C. Test Installation

For the characterization and performance validation tests, only one thruster was installed in the vacuum test chamber at any one time. Each thruster was mounted with the nozzle exits directed horizontally, as shown in Figs. 10–12. The thruster valve inlet was located at the

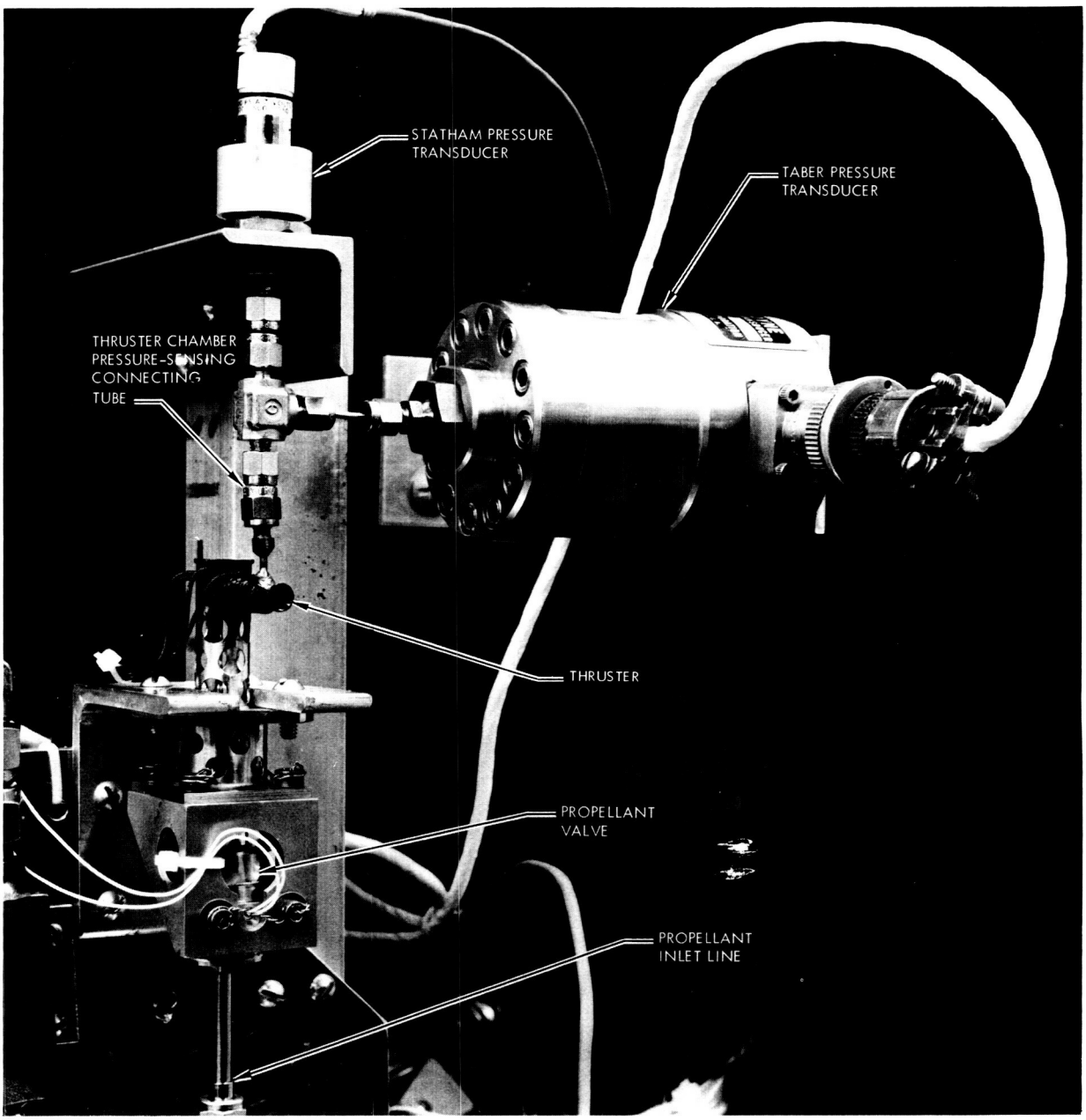

Fig. 10. Hamilton Standard thruster S/N 001 calibration test installation

high point in the propellant delivery system so as to minimize trapped gas bubbles and to facilitate the priming operation. Figure 10 shows the Hamilton Standard thruster installed with the solenoid valve axis in the vertical plane and the thrust chamber directly above. The transducers for measuring chamber pressure were positioned above the thruster and supported by separate mounting brackets. This figure, showing two transducers installed, presents the configuration used for steady state and calibration test operations. The larger Taber trans-

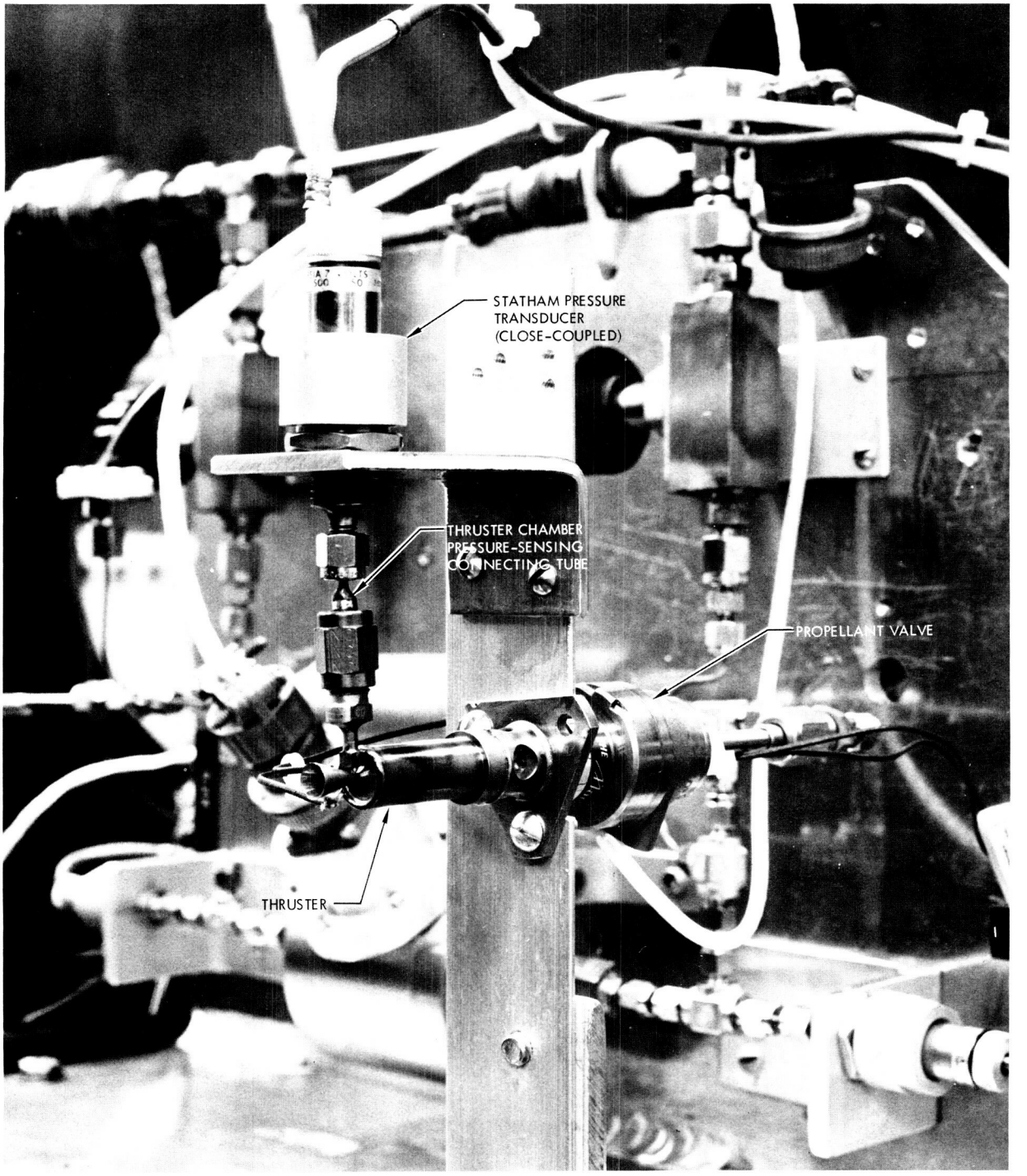

Fig. 11. Marquardt thruster S/N 002A pulse test installation

ducer was removed and the small Statham transducer was close-coupled to the thruster for all pulse mode duty cycles. Figures 11 and 12 show the Marquardt and Rocket Research thrusters, respectively, installed and arranged in the pulse mode configuration. Chromel–alumel (type K) thermocouples were attached by spot welding to the outer surface of the thruster. The thermocouple locations were typically at the exhaust nozzle throat, as well as the lower, middle, and upper chamber wall between the propellant injector head and the nozzle inlet. In most cases, it was not practical to attach a thermocouple on the inlet side of the injector head due either to inaccessibility or space limitation on these small thrusters. Thermal insulation or radiation shielding around the thrust chamber assemblies

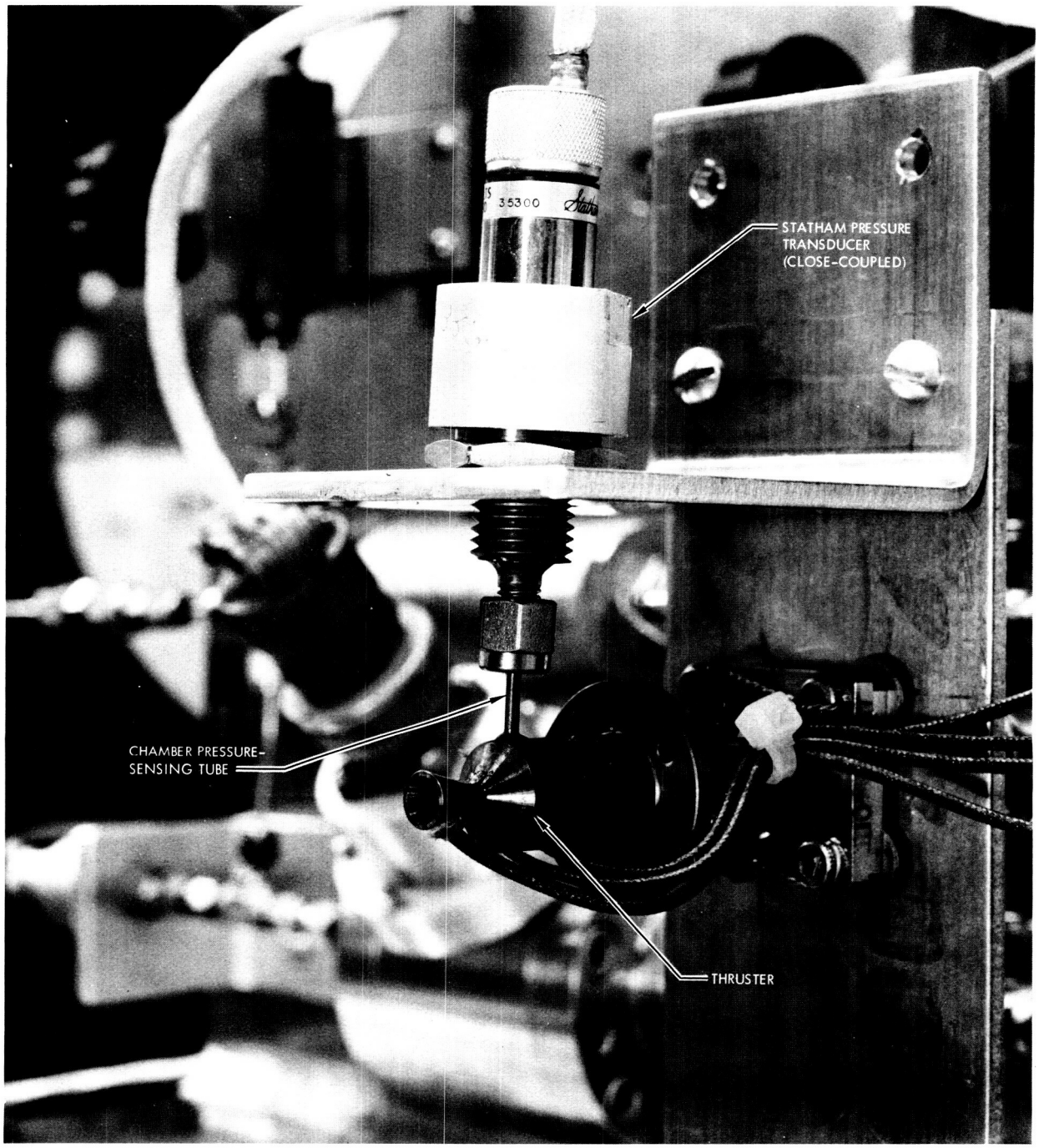

Fig. 12. Rocket Research thruster S/N 02 pulse test installation

was not considered necessary for this test program because all operations were conducted in a vacuum and at ambient starting temperatures.

A special test mounting fixture was fabricated to support all three thrusters simultaneously during the environmental dynamics test series. However, operating and scheduling difficulties developed which resulted in two separate test periods. The first test assembly contained the Hamilton Standard and the Rocket Research thrusters.

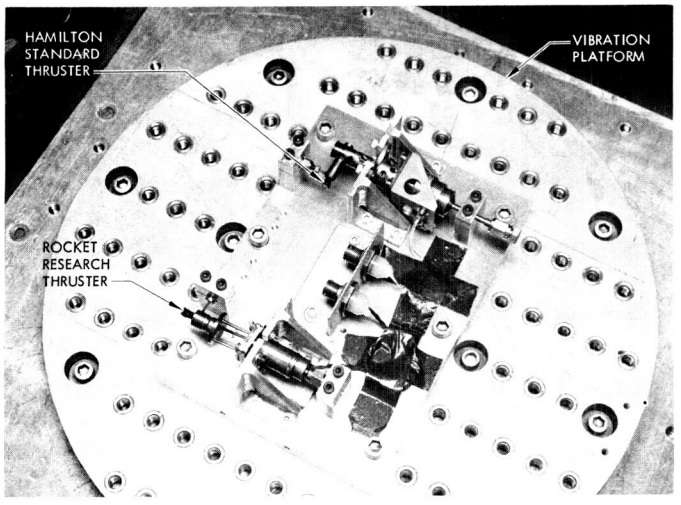

Fig. 13. First environmental dynamics test assembly, with the Hamilton Standard and Rocket Research thrusters mounted on the test fixture in the acceleration centrifuge

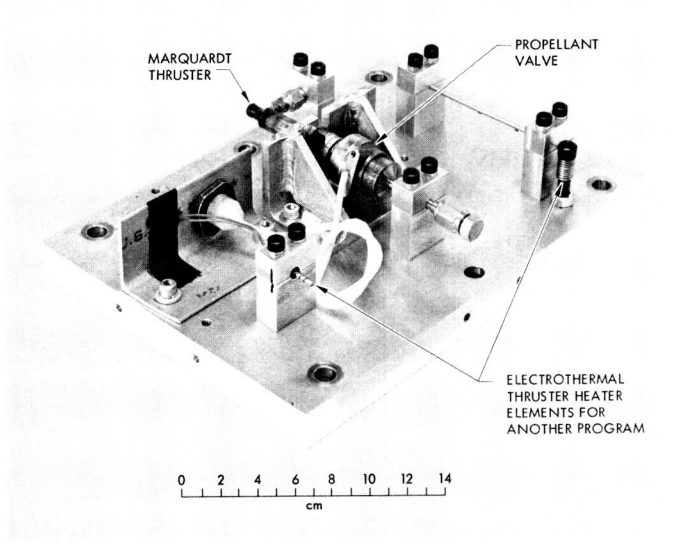

Fig. 14. Second environmental dynamics test assembly, with the Marquardt thruster and two heating elements mounted on the test fixture

A typical installation of this test setup, as it was mounted on the acceleration centrifuge, is shown in Fig. 13. Both thrusters were attached to the fixture by their normal mounting flanges, with additional supports provided at the chamber pressure taps and propellant valve inlet fittings. All attached thermocouples and pressure transducers were removed. The electrical connectors for the solenoid valves are shown mounted in the center of the fixture. The second test assembly consisted of the single remaining Marquardt thruster, along with two resistance heating elements, shown in Fig. 14. These heating elements were not associated with the catalytic thrusters, but were spares for two types of electrothermal thrusters that would eventually be subjected to similar qualification testing.

D. Test Procedure

The first step required before any test firing operations were conducted with the 0.44-N (0.1-lbf) thrusters was the priming and bleeding of the hydrazine propellant system. Normally, the gas-pressurized feed system is cycled between high- and low-pressure levels many times in the course of a test program. High-pressure gas in solution with the propellant tends to come out of solution at lower pressures, especially when the propellant saturation limit is approached, as indicated by Fig. 15. The gas can then become trapped at high points within the system. This trapped gas must be bled off, or vented, periodically (or, more ideally, prevented from forming in the first place) or a slow-responding system with the trapped gas acting like

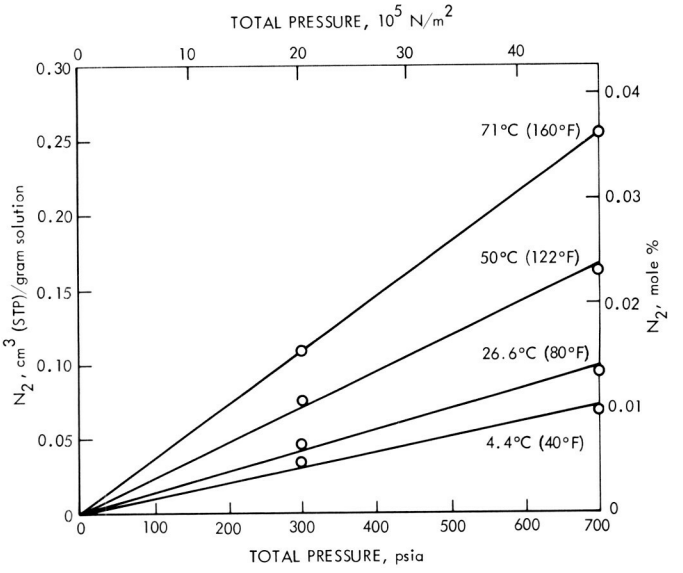

Fig. 15. Quantity of nitrogen in a saturated nitrogen–hydrazine solution, as a function of temperature and pressure

an accumulator will result. This condition is obviously undesirable for pulse mode operation. High-point bleed valves were provided in the propellant system for the purpose of venting any trapped gases, as seen in Fig. 7.

The next step in the procedure was to close the vacuum chamber and bring the pressure down to the range of 6.7×10^2 to 13.3×10^2 N/m^2 (5×10^{-3} to 10×10^{-3} torr). The propellant temperature conditioning system was also activated at the same time. When the vacuum level and temperature conditioning had stabilized, the pretest instrumentation calibration was then completed. Pressurization of the propellant system was the final step required before the thruster firing sequence could begin. A manual pressure regulator on the control console was used to adjust a remotely actuated, dome-loaded regulator installed in the nitrogen supply line. This method provided the quick and accurate control setting of tank pressure required for the thruster calibration tests.

Steady state thruster firings were controlled by manually switching *on* and *off*. For pulse mode operations, the switching was controlled by a solid state electronic repeat cycle relay. This relay was modified to incorporate two multi-turn potentiometers to increase the range and accuracy of the *on* and *off* time settings available. *On*-time range was limited from 0.008 to 1.0 s; however, the *off*-time range was extended from 0.01 to 16.5 s. The very short *on*-times were verified by an oscilloscope.

The characterization test series was performed in the manner and sequence specified above in Subsection B. The vacuum test chamber had to be opened at least three times for each thruster during this series of tests in order to change instrumentation and to install and remove the gas sample cylinder. Each time that a chamber opening was required, the chamber was vented up to atmospheric pressure with gaseous nitrogen, which not only cooled the thruster and prevented oxidation of the hot catalyst bed but also diluted any residual hydrogen that may have been present.

After each day's testing (on the non-24-hour per day test schedule), or at the completion of the final calibration test in the series, a post-test instrumentation calibration was conducted before the vacuum test chamber was vented up to ambient pressure. If the test series was completed, the thruster was removed. Hydrazine remaining in the thruster valve was flushed out with isopropyl alcohol, vacuum purged, and blown dry with gaseous nitrogen. The thruster assembly was then placed in a vacuum oven at 66°C (150°F) overnight for final drying.

The characterization test series had been completed on the Hamilton Standard and Rocket Research thrusters when the thermal stand-off injector tube on the Marquardt thruster was found to be plugged. The thruster had been installed for the characterization tests, but at no time was it possible to flow propellant through it. After efforts at JPL to relieve the blockage failed, the complete thruster assembly was returned to the manufacturer for inspection and rework.

Rather than delay the test program by waiting for the return of the Marquardt thruster, the Hamilton Standard and Rocket Research thrusters were prepared for the follow-on environmental dynamics testing. The skin temperature thermocouples were removed and the chamber pressure ports and the propellant inlet tubes were capped off. A transparent polyethylene plastic film closure held in place with a narrow strip of tape was placed over the nozzle exit to retain any catalyst particles that may have been generated. Both thrusters were then mounted on the test fixture described above in Subsection C.

All five tests in the environmental dynamics test series were conducted at laboratory ambient temperature and pressure conditions, which were normally approximately 21°C (70°F) and 98.6×10^3 N/m^2 (14.3 psia). The tests were performed in the following order:

(1) Acoustic energy.

(2) Sinusoidal vibration.

(3) Random vibration.

(4) Shock.

(5) Acceleration.

For the acoustic energy test, the text fixture was suspended with bungee elastic cables inside the reverberation chamber. Six microphones were positioned at varying locations around the test fixture to record sound amplitudes and frequencies. This test installation is shown in Fig. 16. Before the test, the sound system was calibrated with a calibration source traceable to an NBS standard level of 124 dB. The thrusters were subjected to an overall acoustic noise energy level of 150 dB (ref. 2×10^{-5} N/m^2, or 0.0002 microbar) for 5 min.

The test fixture with the installed thrusters was directly adaptable to the mounting bed of each dynamic testing machine. As a result, the progression through the environmental test series required a minimum of installation and instrumentation time. Both a control and a monitor accel-

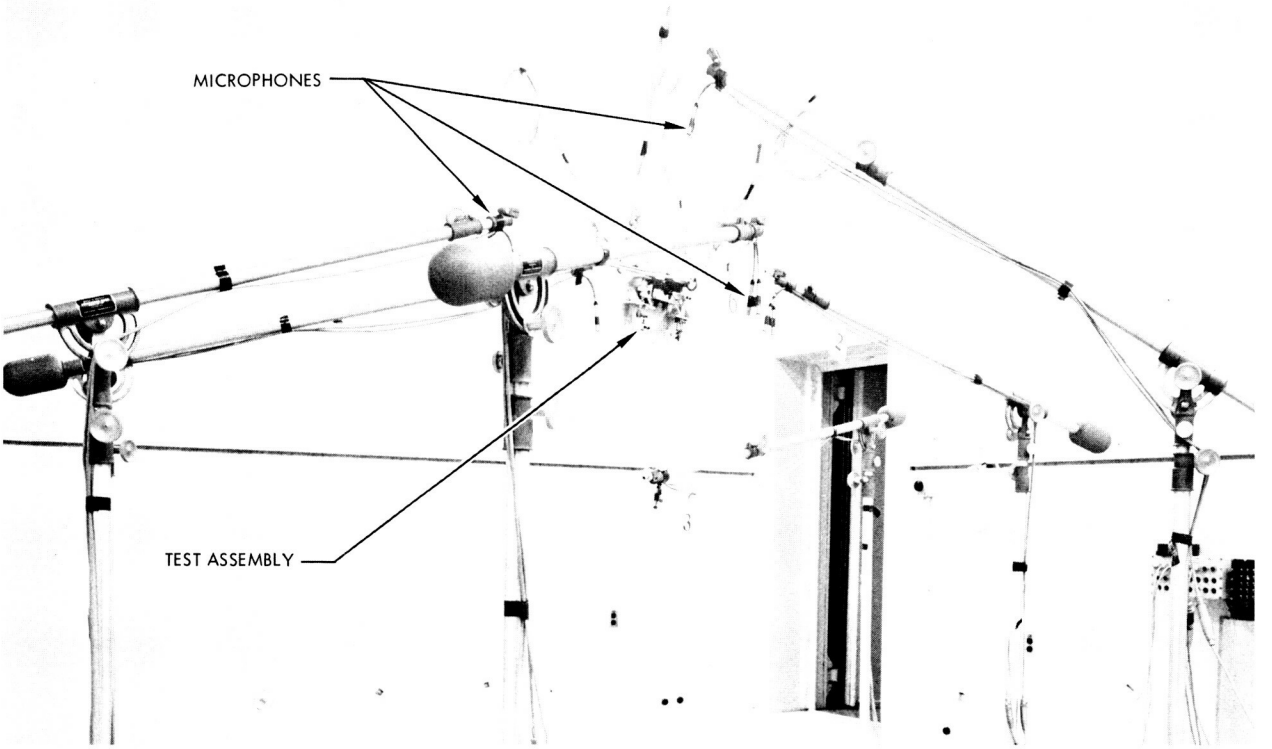

Fig. 16. Environmental dynamics test assembly installed in the reverberation chamber

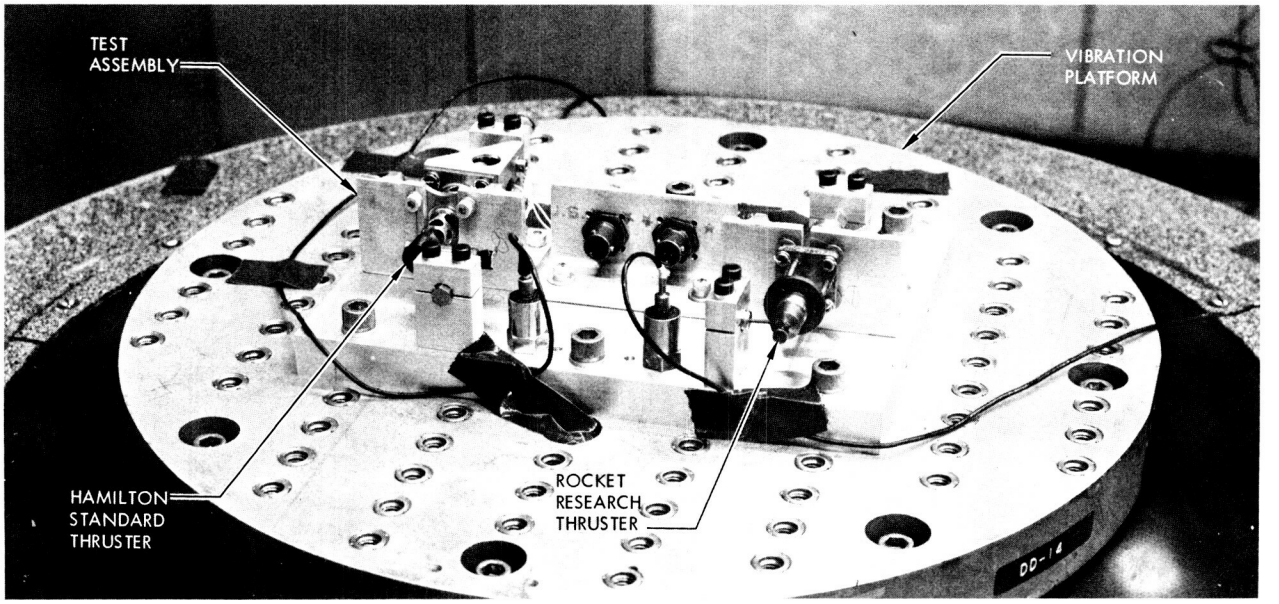

Fig. 17. Environmental dynamics test assembly installed on the electrodynamic shaker

erometer were mounted on the test fixture in a position aligned with the axis of applied force for the sinusoidal and random vibration test sequences. Figure 17 shows the test installation on the electrodynamic shaker for the vertical (z-axis) test. The vibration test series began with a low-level 1.0-g peak sinusoidal sweep. The recorded data were reviewed in order to determine resonant frequencies before proceeding with the high-g sweep. A stroboscope

was used to locate the source of potentially destructive resonant points on the test assembly. If no serious resonances occurred, the high-g sinusoidal and the random vibration test would be completed. The same procedure was followed for each of the three axes of orientation.

The longitudinal or x-axis of the test assembly was defined as the horizontal center line, through the coaxial solenoid valve, in line with the thruster catalyst bed, and perpendicular to the plane of the exhaust nozzle. The Hamilton Standard thruster was an exception to this because the valve center line and thruster catalyst bed are at 90 deg to each other. For this case the valve center line prevailed in order to maintain the spring-loaded armature of the coaxial solenoid valves all aligned in the same direction. The lateral or y-axis was 90 deg to the x-axis in the horizontal plane, while the vertical or z-axis was then perpendicular to the x–y plane. The test assembly is shown installed on the shock tester in Fig. 18. Five high-impact shocks, with a peak amplitude of 200 g, were applied in

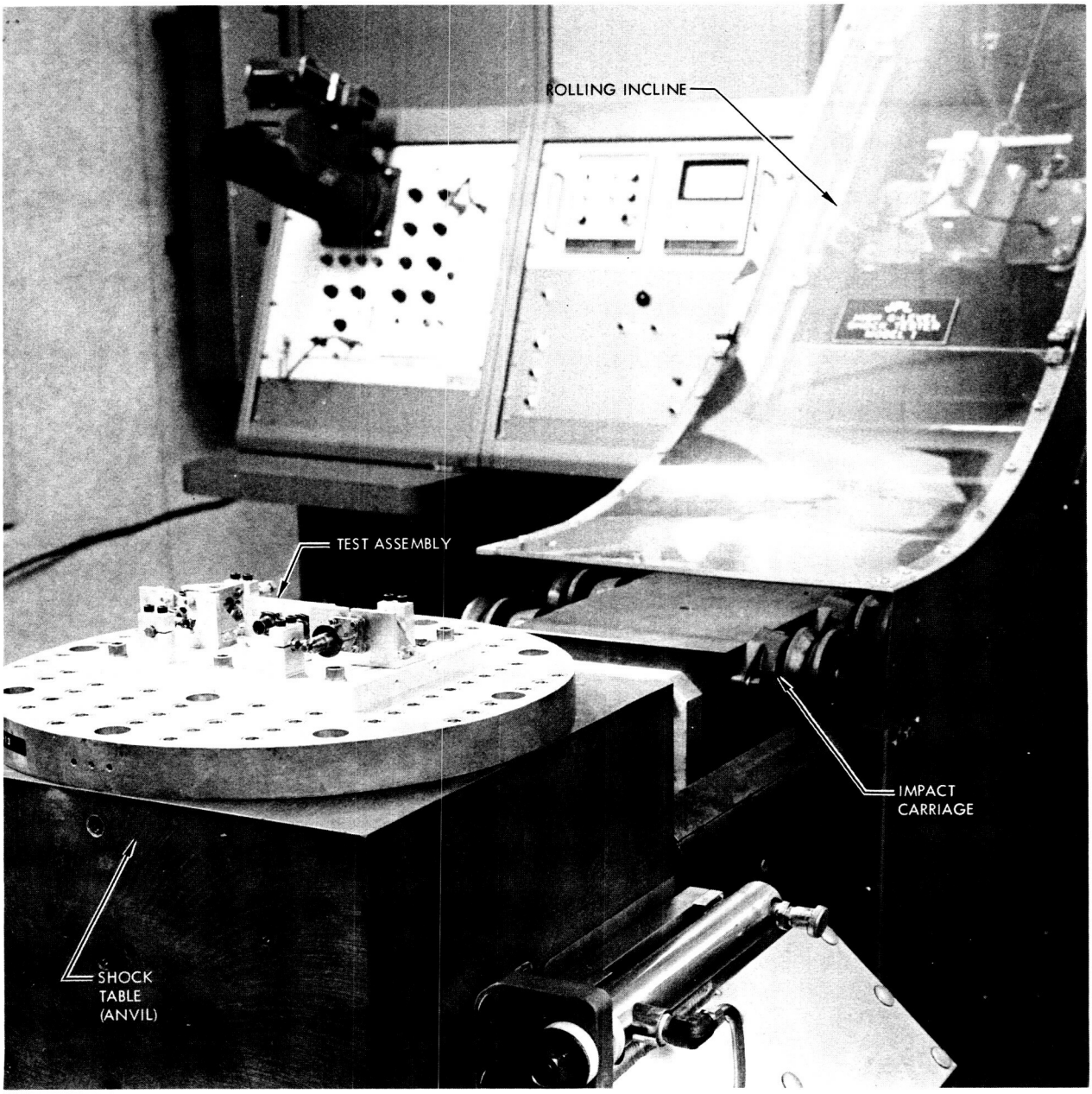

Fig. 18. Environmental dynamics test assembly installed on the shock tester

each axis for a total of 15 shocks. A control accelerometer with its center line aligned with the longitudinal axis of the impact carriage was mounted on the anvil.

The final test in the environmental dynamic series was a static acceleration of 15 g, maintained for a period of 120 s on each of the three axes. The weight of the test assembly was determined with a platform scale in order to balance the rotating arm of the centrifuge. (An installation of the test assembly in the centrifuge was shown previously in Fig. 13.)

The environmental dynamics test series on the first two thrusters was completed in only 2 days. This test series was repeated a month later on the Marquardt thruster after it was returned from the manufacturer and had successfully completed the characterization tests. Each thruster was carefully inspected for structural damage following the environmental tests. Thermocouples were reattached to the outer surfaces of the thruster body and the exhaust nozzle in preparation for the performance validation tests. Each thruster, in turn, was reinstalled in the vacuum facility for the post-environmental test performance validations. The same test procedure used in the characterization test was repeated on all three thrusters. A chronology of the thruster test history is given in Table 5. The results of the three-test series are presented in the following section.

Table 5. Thruster test history

Test number	Thruster and serial number	Type of test
1355	Hamilton Standard S/N 001	Calibration test (previbration)
1356		Gas sample
1357 to 1362		Pulse characterization tests
1363	Hamilton Standard S/N 001	Calibration test
1364	Rocket Research S/N 02	Calibration test (previbration)
1365		Gas sample
1366 to 1371		Pulse characterization tests
1372	Rocket Research S/N 02	Calibration test
1373 to 1381	Rocket Research S/N 01	Definition of limit cycle at 205 ±7°C (400 ±20°F)
1382 to 1394	Rocket Research S/N 01	205°C (400°F) limit-cycle mode (100,216 starts)

Table 5 (contd)

Test number	Thruster and serial number	Type of test
1395	Hamilton Standard S/N 001	Calibration test (post-vibration)
1396		Gas sample
1397 to 1406		Pulse characterization tests
1407	Hamilton Standard S/N 001	Calibration test (post-vibration)
1408	Rocket Research S/N 02	Calibration test (post-vibration)
1409		Gas sample
1410 to 1415		Characterization tests
1416	Rocket Research S/N 02	Calibration test (post-vibration)
1417	Marquardt S/N 002A	Calibration test (pre-vibration)
1418		Gas sample
1419 to 1424		Pulse characterization tests
1425		Calibration test (pre-vibration)
1426		Test terminated due to injector inlet flow restriction caused by swollen O-ring
1427	Marquardt S/N 002A	Steady state check
1428 to 1452	Rocket Research S/N 02	Definition of low-temperature limit
1453 to 1471	Hamilton Standard S/N 001	Definition of low-temperature limit
1472 to 1527	Rocket Research S/N 02	Definition of low-temperature limit
1528		93°C (200°F) limit-cycle life test
1529		Calibration test (pre-life-test)
1530		93°C (200°F) limit-cycle life test (1-μm filter plugged)
1531 to 1540		93°C (200°F) limit-cycle life test (1-μm filter bypassed)
1541		93°C (200°F) limit-cycle life test (removed 1-μm filter)
1543		93°C (200°F) limit-cycle life test completed (103,202 starts)

Table 5 (contd)

Test number	Thruster and serial number	Type of test
1544	Rocket Research S/N 02	Calibration test (post-life-test)
1545	Marquardt S/N 002A	Calibration test (post-vibration)
1546		Gas sample
1547 to 1552		Pulse characterization tests
1553		Calibration test (postvibration and pre-life-test)
1554		Checkout of low-temperature limit
1555 to 1557		93°C (200°F) limit-cycle life test
1558		Definition of low-temperature limit
1559 to 1570		93°C (200°F) limit-cycle life test (252,248 starts)
1571		Calibration test (post-life-test, facility valve VFL found partially closed)
1572	Marquardt S/N 002A	Gas sample
1573	Rocket Research S/N 01	Calibration test (post-life-test)
1574	Rocket Research S/N 01	Gas sample
1575	Marquardt S/N 002A-1	Calibration test (post-life-test and post-500°F-oven-heating for 48 h)
1576		Gas sample
1577		Performance verification for unplugging of injector tube
1578		Calibration test (pre-life-test)
1579		Gas sample
1580 to 1584		206°C (400°F) limit-cycle life tests (100,465 starts)
1585	Marquardt S/N 002A-1	Calibration test (injector tube partially plugged)

Table 5 (contd)

Test number	Thruster and serial number	Type of test
1586	Hamilton Standard S/N 001	Calibration test (post-life-test)
1587		Gas sample
1588		Limit-cycle life tests initiated but stopped to clean system facility filters (higher ΔP values observed from Test 1587)
1589		Calibration test (pre-life-test)
1590 to 1601		206°C (400°F) limit-cycle life tests (256,665 starts)
1602		Calibration test (post-life-test)
1603		Gas sample
1604		Gas sample to quantify presence of hydrazine
1605		
1606		
1607		Gas sample to quantify presence of hydrazine
1608		Gas sample to quantify presence of hydrazine and water
1609		Gas sample to quantify presence of hydrazine and water
1610	Hamilton Standard S/N 001	Standard gas sample

E. Performance Test Results

1. Hamilton Standard thruster. The first thruster to complete the environment dynamics evaluation test series was the Hamilton Standard S/N 001. Results of the calibration tests are presented in Fig. 19, where various performance parameters are plotted as a function of chamber pressure P_c. Test data from the two characterization (previbration) tests and the two performance validation (postvibration) tests are shown on the same graph. A comparison of the calibration performance before and after the environmental dynamics test series reveals essentially no change. There was, however, a 15% upward shift in measured thruster wall temperature. This was undoubtedly due to the removal and reinstallation of the spot-welded skin temperature thermocouples required to provide a clean configuration for the vibration tests. (A higher thermal resistance had apparently existed on the original thermocouple installation.) The data scatter in the chamber pressure roughness parameter, $\Delta P_c/\overline{P}_c$, is due primarily to the selection of the maximum deviation from the nominal P_c level. A single curve is shown drawn through the data, which encompasses the more significant parameters for each of the four tests.

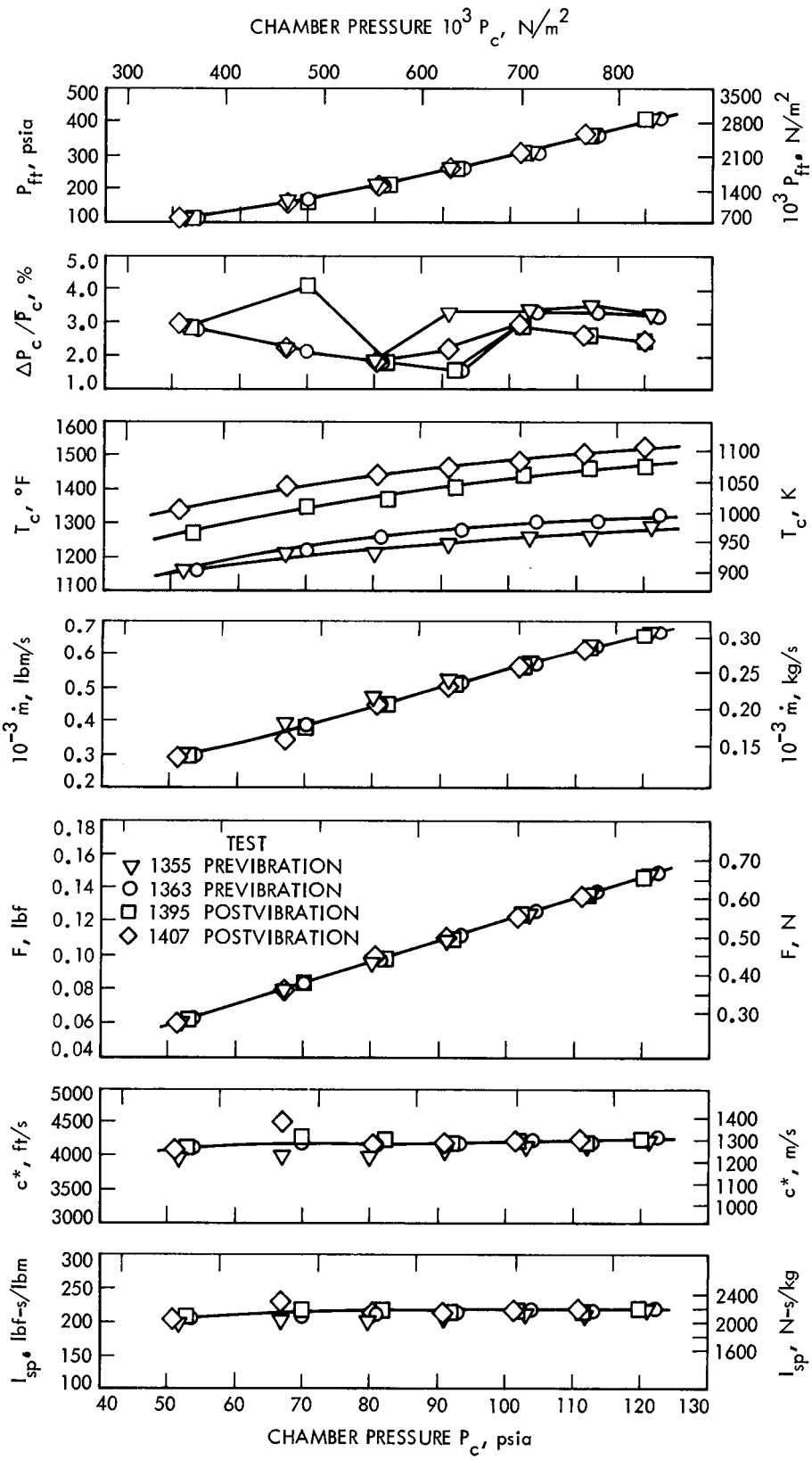

Fig. 19. Calibration test performance of Hamilton Standard thruster S/N 001 before and after vibration tests

The results of the 60-s steady state tests are listed in Table 6. The data point selected occurred after 40 or more seconds elapsed time, just after the thruster had reached thermal equilibrium and just before the exhaust gas sample was collected. Test 1356 was before and Test 1396 was after the environmental dynamics tests. A comparison of the detailed performance at this nominal 0.44-N (0.1-lbf) design thrust condition again shows essentially no change.

The oscillograph traces from Test 1356 are presented in Fig. 20, showing the typical start and stop transient pressure responses of the Hamilton Standard thruster recorded during a 60-s steady state firing. The chamber pressure exhibits an initial 10% overshoot, which levels off after 3 s. This peculiar behavior is suspected to be caused by thermal adjustments of the L-shaped, corrugated capillary injector inlet tube. Chamber pressure roughness appears to be very slight, primarily due to the damping effect of the larger volume Taber pressure transducer used to record P_c during this specific test. (Normally, the smaller-volume, close-coupled Statham pressure transducer was used to determine chamber pressure roughness.) Fuel injector (valve inlet) pressure P_{fi} and Viscojet differential pressure drop ΔP_{fc} show a similar 3-s time period to stabilize after a smooth start transient. The stop transient for chamber pressure is a sharp decay with no evidence of propellant boil-off "perks." By contrast, the fuel injector pressure and Viscojet pressure drop are slower to respond, requiring about 1 s to recover. This is a characteristic of the propellant feed system when pressurant gas is trapped in the transducer cavities, producing an accumulator effect and a soft-responding system.

A typical steady state temperature rise for the Hamilton Standard thruster is presented in Fig. 21. Both thrust chamber and nozzle throat skin temperatures are plotted as a function of engine operating time. A total of three thermocouples were attached to the wall of the thruster body. These were the upper, middle, and lower as referenced to the position along the catalyst bed in the direction of propellant flow. The lower chamber thermocouple T_{c1} recorded the maximum temperature during steady

Table 6. Nominal steady state performance at thruster design conditions before and after environmental dynamics test series

Parameter	Hamilton Standard S/N 001		Rocket Research S/N 02		Marquardt S/N 002A	
	Before	After	Before	After	Before	After
Test number	1356	1396	1365	1409	1418	1546
Lapsed time, s	45	42	44	40	55	45
Fuel tank pressure, 10^3 P_{ft}, N/m²	1682	1675	2364	2371	2171	2137
(lbf/in.²)	(244)	(243)	(343)	(344)	(315)	(310)
Fuel injector pressure, 10^3 P_{fi}, N/m²	772	765	1461	1509	1358	1434
(lbf/in.²)	(112)	(111)	(212)	(219)	(197)	(208)
Vacuum chamber pressure P_{vc}, N/m²	36.0	38.8	38.7	39.3	34.7	33.5
(torr)	(0.270)	(0.291)	(0.290)	(0.295)	(0.260)	(0.251)
Thruster chamber pressure, 10^3 P_c, N/m²	598.4	592.9	1023.9	1003.2	606.7	627.4
(lbf/in.²)	(86.8)	(86.0)	(148.5)	(145.5)	(88.0)	(91.0)
Thruster chamber temperature T_c, K	948	1017	914	839	989	950
(°F)	(1246)	(1371)	(1185)	(1050)	(1320)	(1250)
Nozzle temperature T_n, K	925	860	794	800	939	882
(°F)	(1215)	(1088)	(969)	(981)	(1230)	(1128)
Fuel flow rate, 10^{-3} $\dot{m}$, 10^{-3} kg/s	0.2231	0.2203	0.2173	0.2099	0.2044	0.2108
(lbm/s)	(0.4919)	(0.4856)	(0.4791)	(0.4628)	(0.4507)	(0.4648)
Nozzle throat area (hot), $10^{-6}A_{th}$, 10^{-3} m²	0.4693	0.4662	0.2655	0.2654	0.4238	0.4234
(in.²)	(0.7274)	(0.7226)	(0.4117)	(0.4113)	(0.6569)	(0.6562)
Thrust (calculated) F, N	0.4679	0.4612	0.4532	0.4430	0.4275	0.4417
(lbf)	(0.1052)	(0.1037)	(0.1019)	(0.0996)	(0.0961)	(0.0993)
Characteristic velocity c^*, m/s	1259	1255	1254	1268	1260	1250
(ft/s)	(4130)	(4118)	(4106)	(4161)	(4134)	(4102)
Specific impulse I_{sp}, N-s/kg	2098	2095	2085	2111	2091	2079
(lbf-s/lbm)	(213.9)	(213.6)	(212.6)	(215.3)	(213.2)	(212.0)
Thrust coefficient C_f	1.666	1.669	1.666	1.664	1.659	1.663

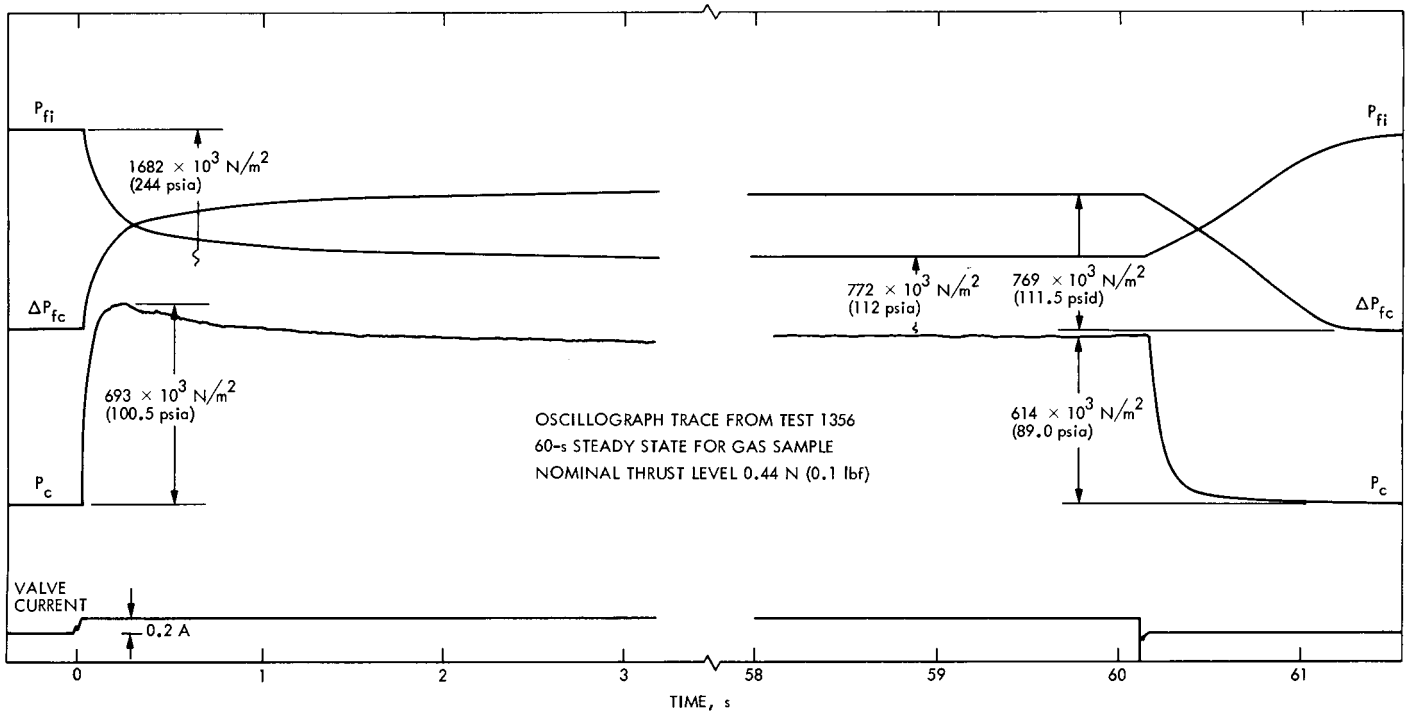

Fig. 20. Typical start and stop transient pressure response of the Hamilton Standard thruster S/N 001

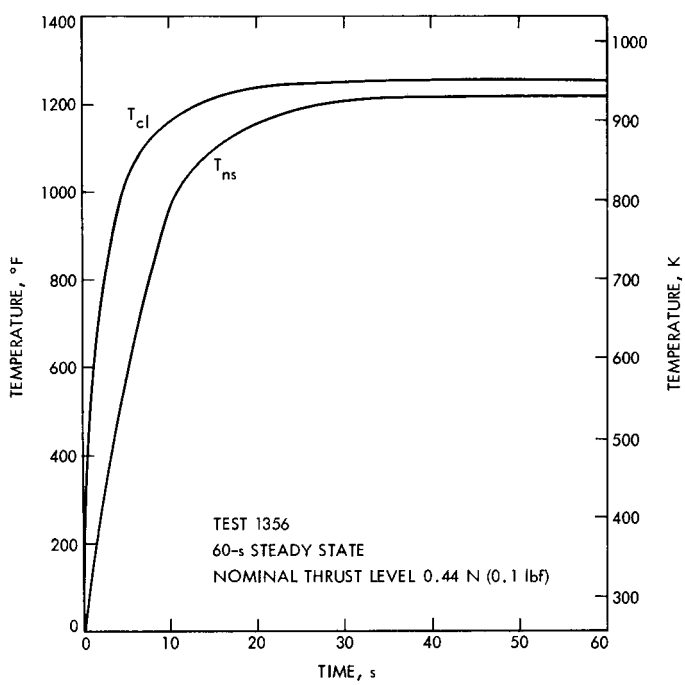

Fig. 21. Typical steady state temperature rise time for Hamilton Standard thruster S/N 001

state operation and is the one plotted in the figure. The nozzle throat temperature T_{ns} appears to lag the chamber temperature during the rise time. However, they both reach maximum levels after 35 s, with the nozzle throat equilibrium temperature only slightly lower than the thrust chamber temperature.

During the final seconds of a 60-s steady state firing, thruster exhaust gas samples were collected through the chamber pressure port into an evacuated 10-cm^3 valved stainless steel cylinder. Monometric and mass spectrometric analyses were performed on the gas sample by the method described in Ref. 4, p. 80. Through the use of the mole fraction ratio of hydrogen to ammonia from the volumetric analysis, the percentage of ammonia dissociation was determined by the method presented in Ref. 1. The results of the gas sample analysis and the determination of ammonia dissociation levels are listed in Table 7. The ammonia dissociation for the Hamilton Standard thruster ranges from 41.0 to 42.5% for this test series (Tests 1356 and 1395). A total of 25 μg of unreacted hydrazine (N_2H_4) was noted for Test 1356. One would expect that larger traces of unreacted hydrazine would be associated with the lower ammonia dissociation levels, although the

Table 7. Analysis of exhaust gas samples

Thruster and serial number	Test number	Condition	Composition[a]			Ammonia dissociation, %	Unreacted N_2H_4, μg
			N_2, %	H_2, %	NH_3, %		
Hamilton Standard S/N 001	1356	Previbration	29.3	36.2	34.4	41.0	25
	1396	Postvibration	30.1	36.5	33.2	42.5	<1
	1587	Pre-limit-cycle	28.4	36.4	34.7	41.0	5
	1603	Post-limit-cycle	25.6	34.4	40.0	36.0	30
Rocket Research S/N 01	988	Pre-limit-cycle	34.3	48.8	16.5	66.5	<1
	1574	Post-limit-cycle	33.1	51.5	14.7	70.5	<1
Rocket Research S/N 02	1365	Previbration	30.4	47.2	22.2	58.5	1
	1409	Postvibration	31.8	46.2	21.7	59.0	<1
Marquardt S/N 002A	1418	Previbration	28.6	36.5	34.8	41.5	11
	1546	Postvibration (Pre-limit-cycle)	28.2	38.3	33.0	42.0	5
	1572	Post-limit-cycle	30.9	40.3	28.6	48.0	<1
Marquardt S/N 002A-1	1576	Post-oven-cure	27.3	43.1	29.3	49.5	<1
	1579	Pre-limit-cycle	28.2	39.8	31.6	45.2	<1

[a]Small quantities of Ar, CH_4, and H_2O, which were also found in the gas samples, are not listed.

difference between 41 and 42.5% is not sufficient to explain the variation observed in Table 7. (This variation is most probably due to the sampling and analysis techniques.)

Thrust was not measured during this test program; instead, it was calculated by the method presented in the Appendix, using the gamma value (γ = ratio of heat capacities) derived from the ammonia dissociation level.

A comparison was made of the pulse mode chamber pressure profiles recorded on the oscillograph for the six different pulse duty cycles before and after the environmental dynamics test series. There was no significant difference in the comparable P_c profiles. However, a slight variation was noted from start to stop in any 1000 pulse tests. Figure 22 presents some typical pulse mode P_c profiles for the Hamilton Standard thruster at three representative duty cycles. Each test was started with the thrust chamber at or near ambient temperature. The first pulse is not shown because it was always much lower than nominal chamber pressure because of a foreshortened valve input signal which always occurred for the first output from the pulse generator that was being used for this phase of the test program. The second pulse was usually well-formed and only slightly below nominal pressure level. By the tenth pulse, nominal chamber pressure had been obtained, and the pressure remained fairly constant thereaft . . The upward trend noted in the prestart reference pressure at the beginning of each pulse is apparently due to a slow chamber pressure decay caused by propellant retention within the capillary injector tube. By the end of the final pulse, from 1.0 to 1.5 s were required for the chamber pressure to decay completely to the starting zero pressure. No thermal zero shift was noted as a result of transducer heating, even though the transducer was close-coupled to the thrust chamber pressure tap. The valve current trace shows the typical armature movement inflection during the increasing and decaying of the current, indicating the actual valve opening and closing responses.

2. Rocket Research thruster. The second thruster to complete the environmental dynamics evaluation test series was the Rocket Research thruster S/N 02. The results of the calibration performance tests are presented in Fig. 23. A comparison of the data before and after the environmental dynamics test indicates no change in performance. The values of specific impulse, characteristic velocity, and chamber pressure roughness are very similar to the range of values obtained for the other two thrusters.

Steady state performance at the nominal 0.44-N (0.1-lbf) design thrust condition is listed in Table 6. Again, there was no significant change before or after the vibration tests. The smaller exhaust nozzle throat on this thruster necessitates a higher fuel tank pressure and chamber pressure than either of the other two thrusters. Figure 24 depicts the typical start and stop pressure transients which were recorded during the 60-s gas sampling Test 1409. The chamber pressure trace shows a rapid rise

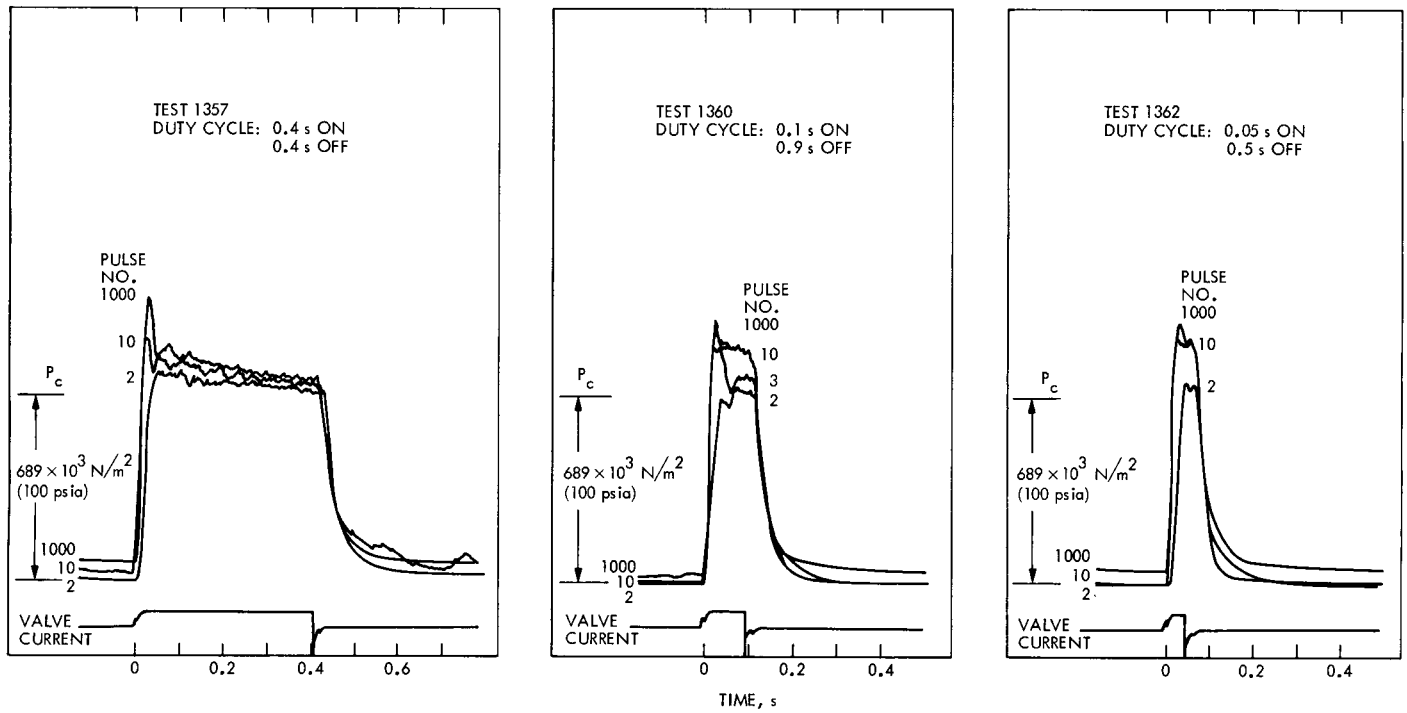

Fig. 22. Typical pulse mode chamber pressure profiles for Hamilton Standard thruster S/N 001 at 0.44-N (0.1-lbf) thrust

with no spike or overshoot. When the thruster experiences an ambient temperature start, nominal operating P_c is reached only after approximately 15 s of steady state firing. This delay is caused primarily by the time required to heat the heavy-walled thruster body. Chamber pressure decay is smooth, without boil-off "perks," and rapid, taking less than 1.0 s. Figure 25 indicates the variation of temperature as a function of time for this test. It is noted that chamber wall temperature and nozzle throat temperature were still increasing slightly after 60 s of operation.

The results of the exhaust gas sample analysis are listed in Table 7. As shown in this table, the Rocket Research thruster experienced an ammonia dissociation level around 59.0%, the highest of the three thrusters tested. This is further substantiated by its lower operating temperature, noted in Table 6, resulting from the endothermic ammonia dissociation reaction. The longer catalyst bed length incorporated into the design of this thruster produces this higher dissociation level, as well as a correspondingly lower amount of detected unreacted hydrazine.

Figure 26 presents chamber pressure profiles for three of the six pulse mode duty cycles that were demonstrated by the Rocket Research thruster. Since there was no appreciable change in pressure profile before or after the environmental dynamics tests, these pressure traces are considered typical for both pre- and post-vibration. When the pulse train is initiated from ambient temperature, the increase or stabilization of P_c profile is very much a function of duty cycle and the time to reach temperature equilibrium. For the 0.4-s *on*/0.4-s *off* duty cycle, the 10th pulse reached greater than 90% of nominal operating P_c. The shorter *on*-time duty cycles show 50% or less P_c rise by the 10th pulse. In general, the pressure profiles for this thruster are very clean, with sharp increases and decreases in P_c that improve with increased operating temperature.

3. Marquardt thruster. The third and final thruster to complete the environmental dynamics evaluation test series was the Marquardt S/N 002A. As stated earlier, since the initial attempts to fire this thruster (identified originally as S/N 001A) were unsuccessful because of a plugged injector tube, the thruster was returned to the manufacturer for inspection and repair. Detailed results of their investigation and refurbishing are reported in Ref. 5. Although the material plugging the injector tube was not identified, it was believed to be nonmetallic. The material was finally removed by disassembling the thruster and ultrasonically cleaning the injector tube in a heated, slightly alkaline detergent solution for several days. The refurbished thruster was reassembled with new catalyst and component parts from both thruster S/N 001A and

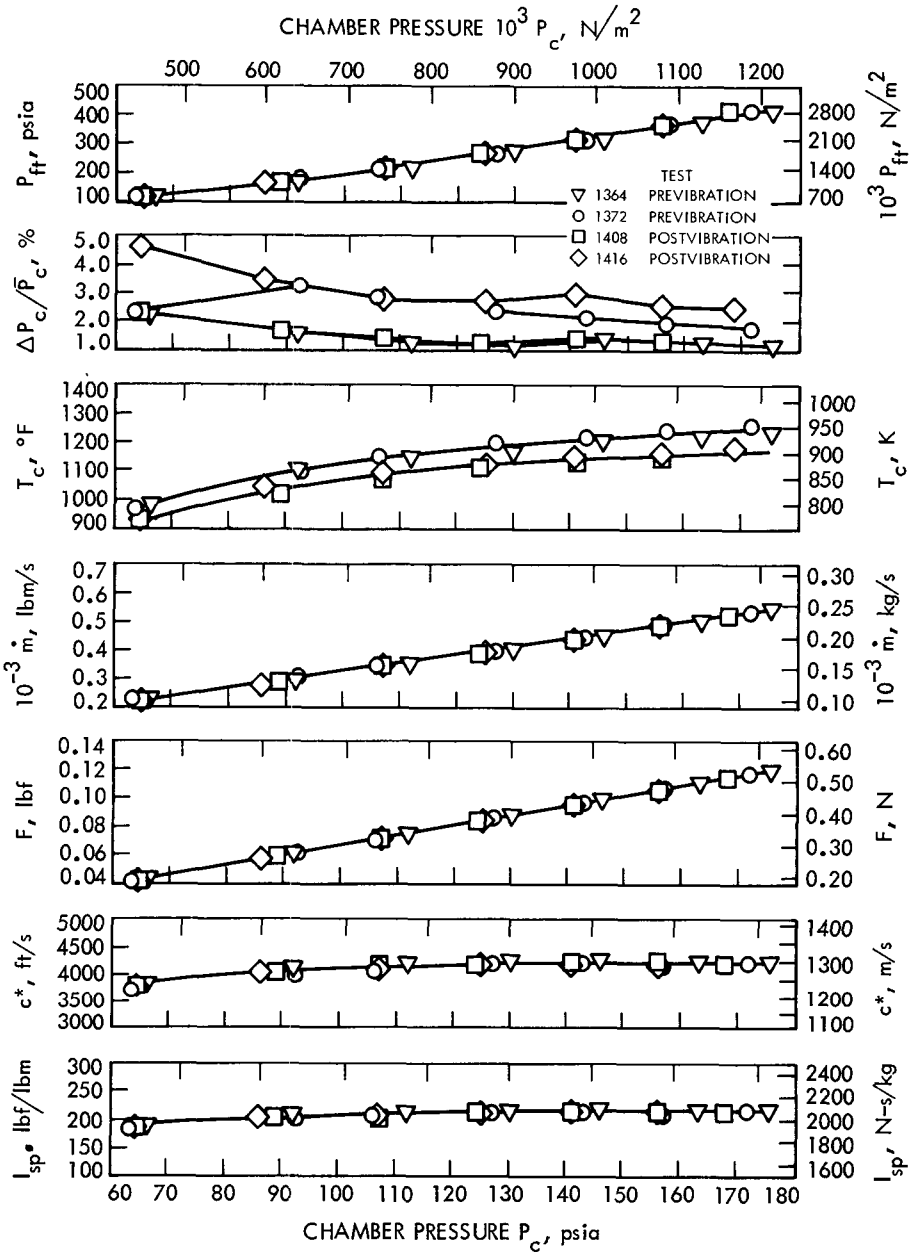

Fig. 23. Calibration test performance of Rocket Research thruster S/N 02 before and after vibration tests

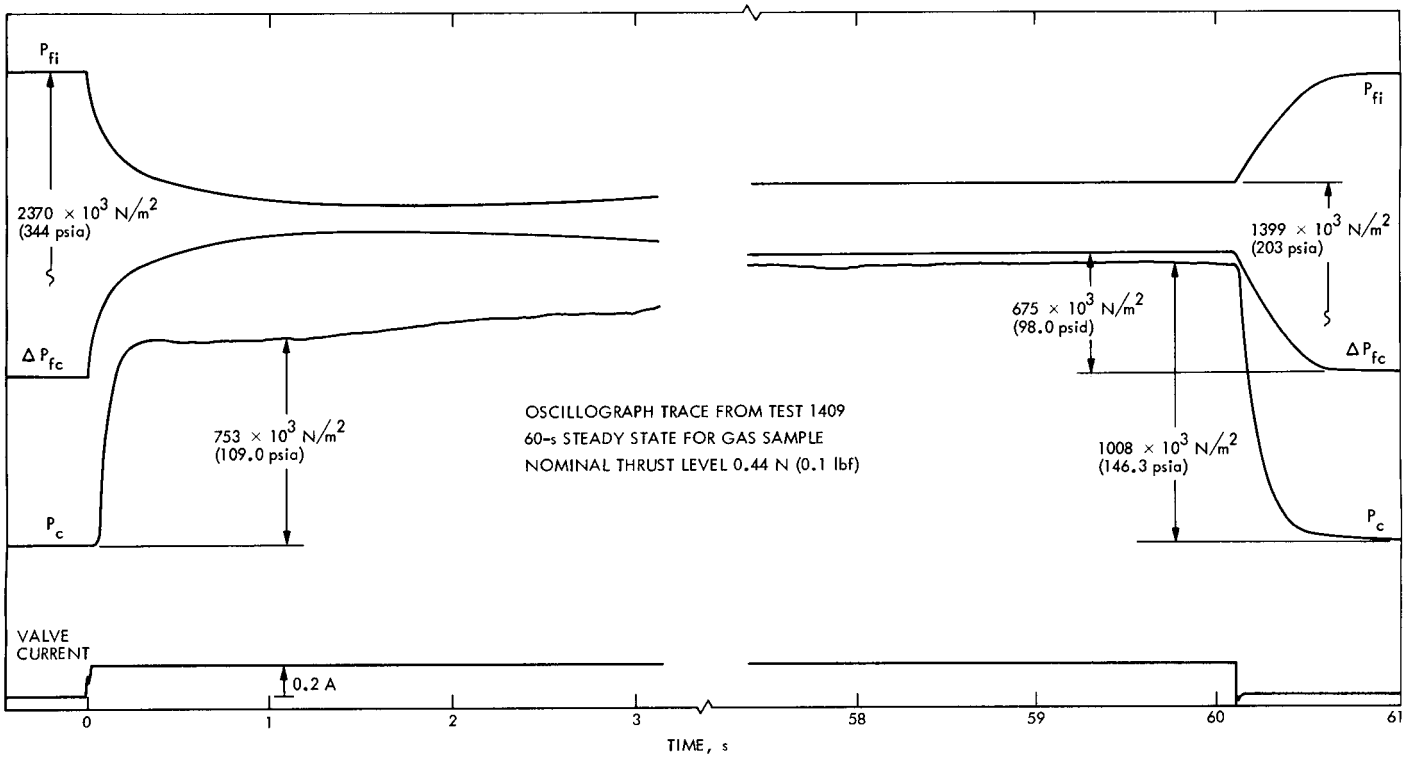

Fig. 24. Typical start and stop transient pressure response of the Rocket Research thruster S/N 02

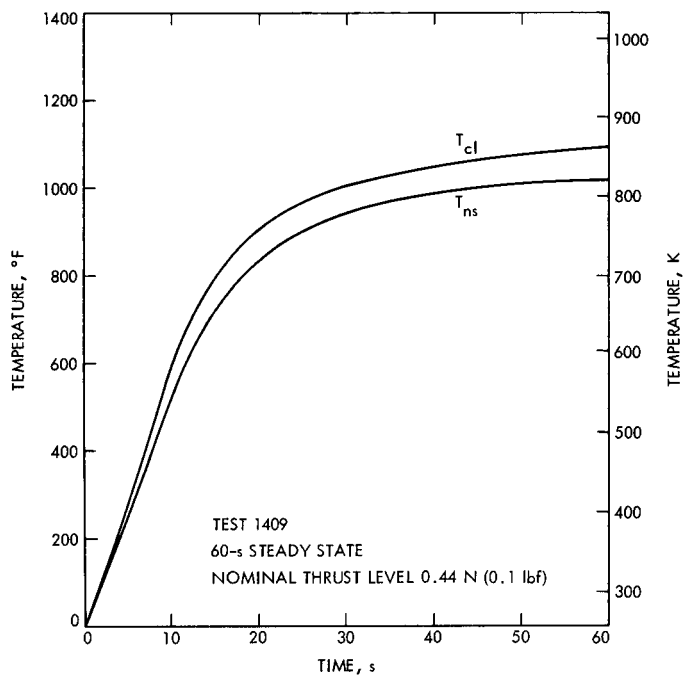

Fig. 25. Typical steady state temperature rise time for Rocket Research thruster S/N 02

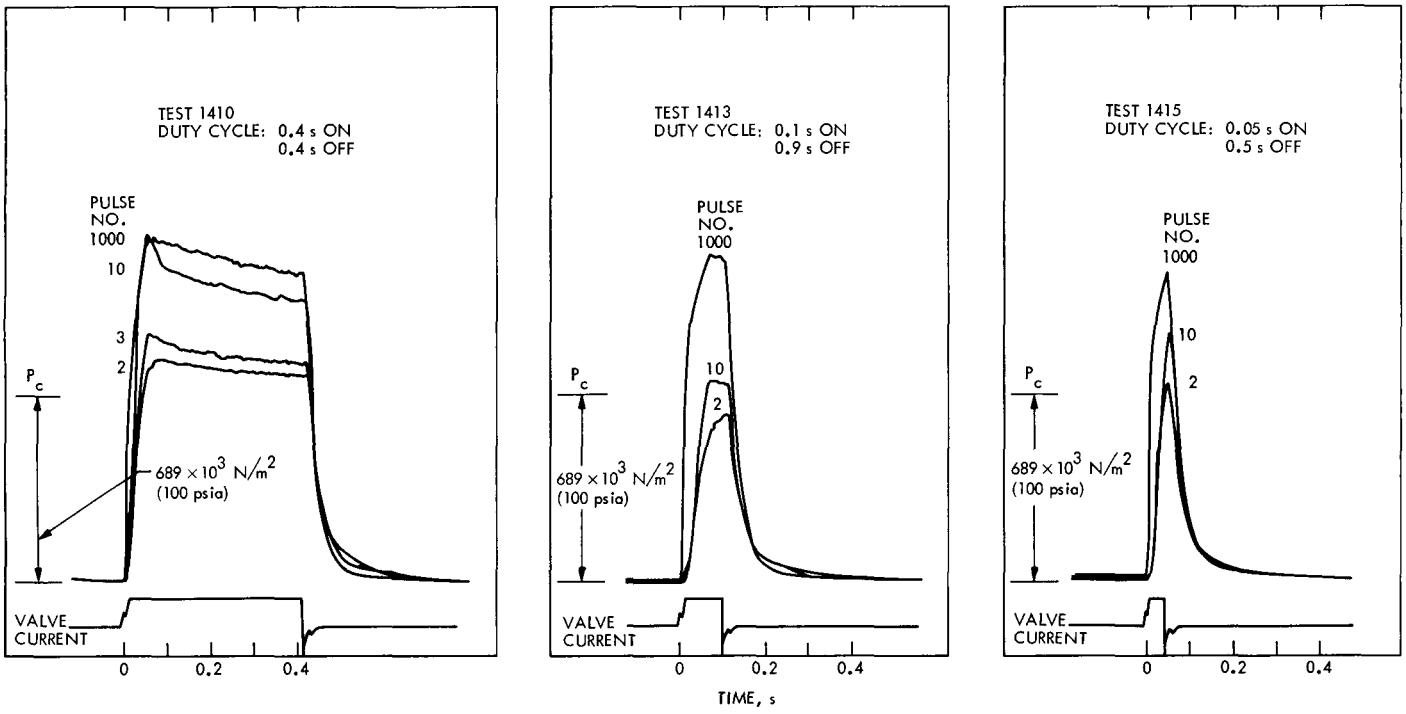

Fig. 26. Typical pulse mode chamber pressure profiles for Rocket Research thruster S/N 02 at 0.44-N (0.1-lbf) thrust

thruster S/N 002, whose disassembly was previously reported in Ref. 6. This thruster was identified as S/N 002A, because it contained a majority of components from the earlier unit (including the injector).

The results of the calibration performance tests are presented in Fig. 27. Again there was no apparent difference in performance data before or after the environmental dynamics test series. The chamber pressure roughness parameter shows improvement at higher chamber pressures and longer operating time. This is apparently caused by variations in the spring-loaded catalyst bed. In general, the calibration test performance of the Marquardt thruster is comparable to that of the other two thrusters.

The steady state performance parameters at the design thrust level of 0.44 N (0.1 lbf), listed in Table 6, show very little change before or after vibration. The similarity in thrust chamber geometry between the Marquardt and the Hamilton Standard thrusters is evident by the parallelism of the performance parameters.

Figure 28 presents the start and stop pressure transients recorded during a 60-s gas sampling test (Test 1418). The resonances noted in injector pressure and Viscojet differential pressure traces at the start of the test are typical examples of a small amount of gas trapped in the propellant line or in the pressure transducer cavities. The chamber pressure trace shows smooth start and stop transients with a 12% increase in peak pressure from the start to the end of the test. A temperature–time history for this same test is presented in Fig. 29. As can be seen in this figure, the thrust chamber wall temperature closely parallels the nozzle throat temperature. This relationship is due to the double-wall construction required of the thruster body to accommodate the integral spring that maintains a constant load on the catalyst bed. Since this spring cavity presents a very large thermal gradient across the catalyst bed, both temperatures essentially equilibrate by conduction to that of the exhaust gas at the exit of the catalyst bed. The thruster temperature is seen to approach steady state equilibrium by the end of the 60-s firing.

The gas sample analysis for the Marquardt thruster, listed in Table 7, shows a 41.5 to 42.0% ammonia dissociation level before and after the vibration testing (Tests 1418 and 1546, respectively). As expected, a larger trace of unreacted hydrazine is recorded for the lower dissociation level. This result is very similar to that obtained for the Hamilton Standard thruster. The observed amount of unreacted hydrazine falls below the lower detectable limit in later tests, when the ammonia dissociation level is increased to above 45%.

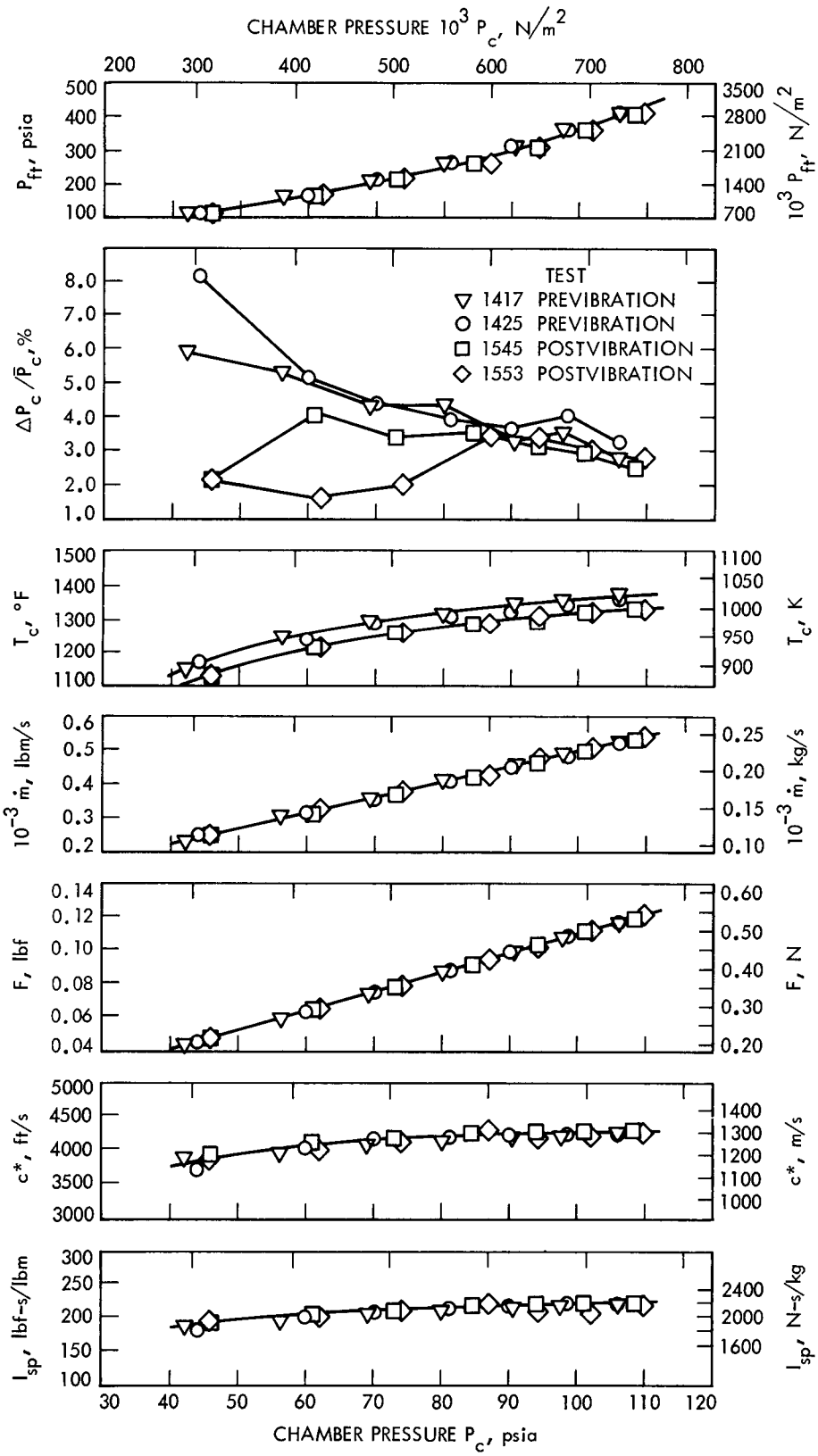

Fig. 27. Calibration test performance of Marquardt thruster S/N 002A before and after vibration tests

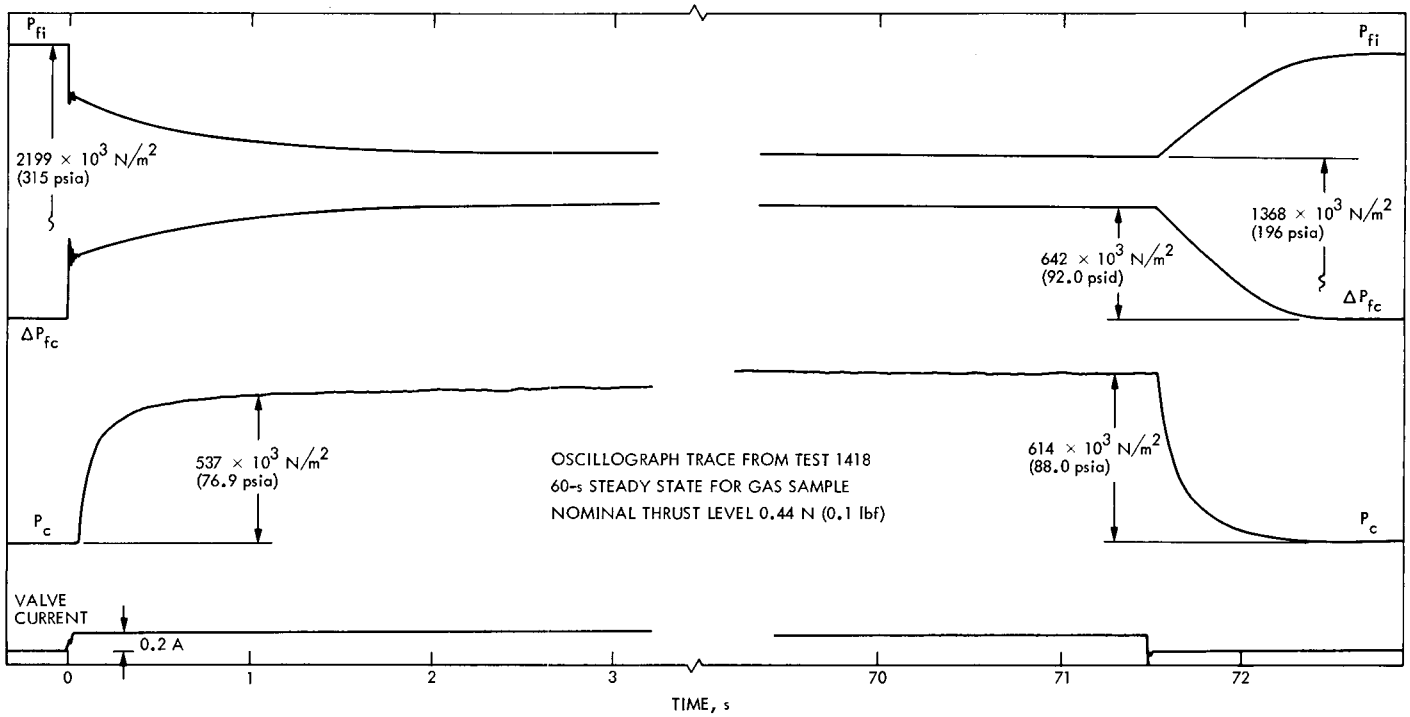

Fig. 28. Typical start and stop transient pressure response of the Marquardt thruster S/N 002A

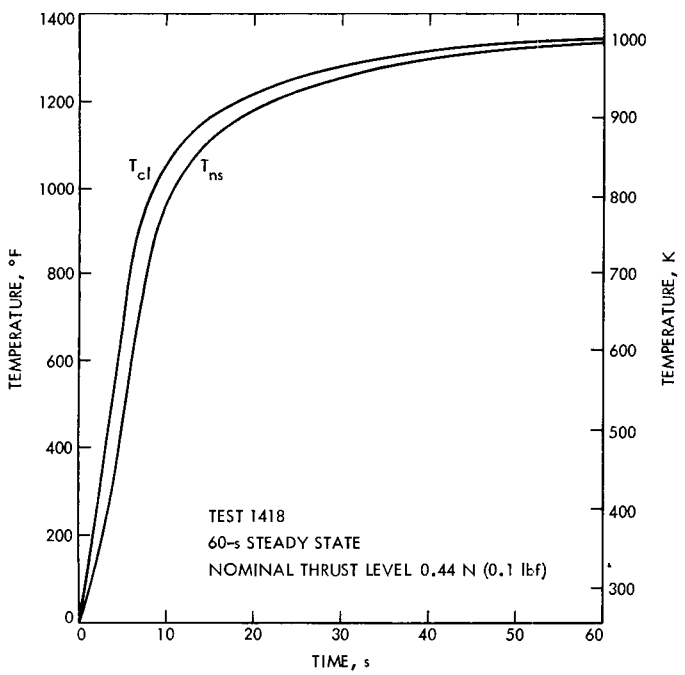

Fig. 29. Typical steady state temperature rise time for Marquardt thruster S/N 002A

A typical set of Marquardt thruster chamber pressure profiles for three pulse mode duty cycles is shown in Fig. 30. These results are similar in shape to the Rocket Research thruster, but reach a lower maximum P_c level. The chamber pressure increased slowly with operating time, most probably because of the thermal lag caused by the mass of the spring-loaded thrust chamber. However, when thermal equilibrium had been obtained, the P_c pulse shape was characterized by a sharp rise and fall with a relatively smooth, flat top. The repeatability and predictability of the chamber pressure profile appears very good at the design operating conditions.

F. Environmental Dynamics Test Results

The following discussion on the results of the environmental dynamics tests will apply to all three thrusters, since there was no discernible difference between the two separate test series. The recorded data apply only to the input parameters. It was not practicable to mount response transducers onto the bodies of the small thruster assemblies, because the size and weight of such an installation would have too great an influence on the final results.

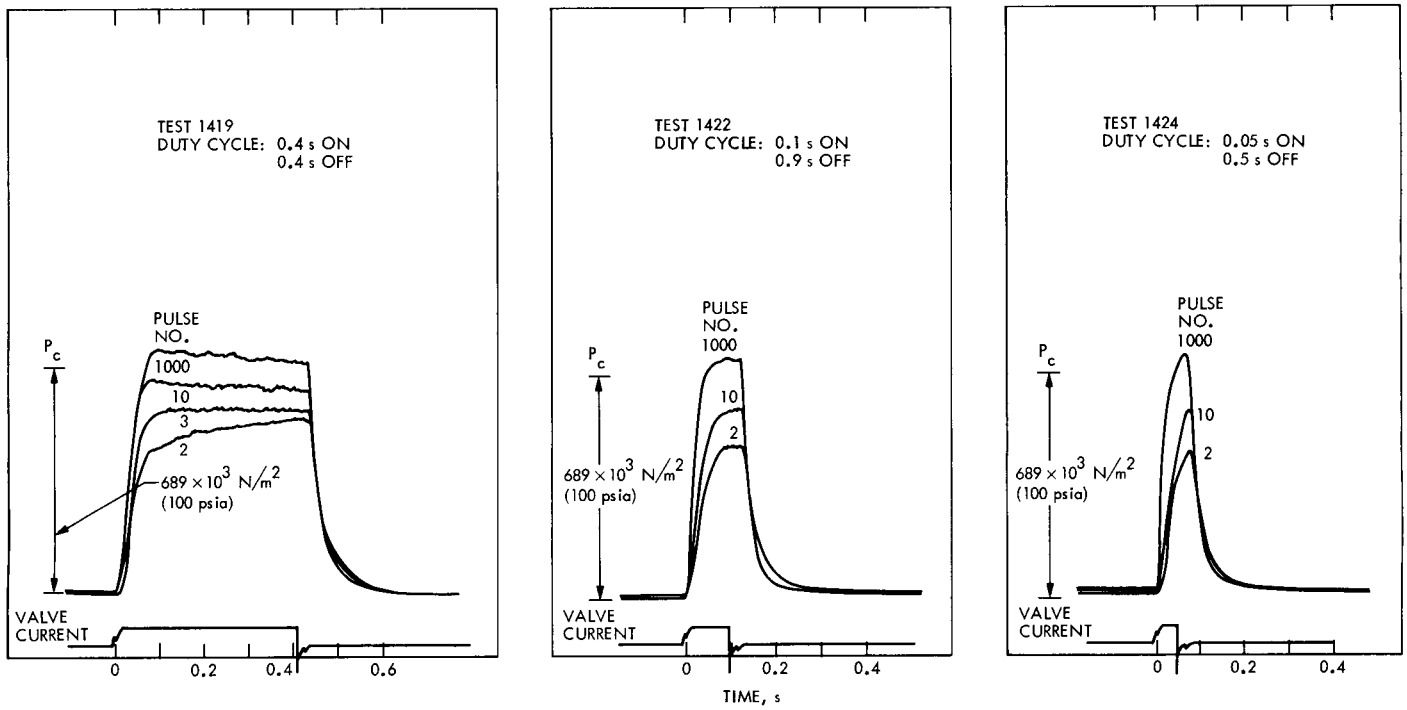

Fig. 30. Typical pulse mode chamber pressure profiles for Marquardt thruster S/N 002A at 0.44-N (0.1-lbf) thrust

Table 8. Typical results of acoustic energy test

1/3 octave band center frequency, Hz	Specified sound pressure level, dB ref. 2×10^{-5} N/m^2 (0.0002 μbar)			Measured sound pressure level, dB ref. 2×10^{-5} N/m^2 (0.0002 μbar)		
	Minimum	Average	Maximum	Minimum	Average	Maximum
40	114	130	135	—	—	122.6
50	124	132	137	129.1	130.5	132.7
63	129	134	139	130.8	133.5	135.6
80	130	135	140	130.9	133.8	135.5
100	131	136	141	132.6	134.8	136.1
125	133	137	141	135.9	137.5	139.0
160	134	138	142	137.1	138.6	139.8
200	135	139	143	137.7	138.8	140.2
250	135	139	143	137.7	139.1	140.8
315	135	139	143	139.1	140.1	140.9
400	136	139	142	138.0	139.0	139.7
500	136	139	142	138.2	138.8	139.5
630	136	139	142	137.8	138.7	139.3
800	135	138	141	137.5	138.0	138.8
1000	134	137	140	136.2	137.1	138.0
1250	134	136	138	134.9	135.3	136.0
1600	132	135	137	133.0	133.8	134.2
2000	130	134	136	131.9	132.5	133.8
2500	128	133	135	130.1	130.8	131.5
3150	126	132	134	127.9	128.7	129.8
4000	124	131	132	125.8	126.6	128.0
5000	122	130	131	122.3	123.5	125.0
6300	120	129	130	120.1	121.4	123.2
8000	118	128	129	—	—	121.6
10,000	116	127	128	—	—	120.2
Overall	148.5	150	151.5	148.8	149.4	149.9

Typical results of the acoustic energy test are summarized in Table 8, which compares the specified sound pressure levels to those that were experimentally measured. The measurements are a compilation and averaging of signals from six control microphones recorded on high-speed tape. Frequency spectrum plots were made from the instantaneous values of sound pressure levels at several time increments, with a detector averaging time of 1 s. Figure 31 is a typical frequency spectrum plot for the control microphone (No. 1) taken at 50 and 250 s into the test. The exposure to this 150-dB overall sound pressure level for a total period of 300 s did not produce any visible damage to any of the three thrusters.

The results of the dynamic vibration tests are shown in the following figures. Figure 32 depicts the acceleration as a function of frequency for the up and down sinusoidal vibration sweep at a rate of 2.0 octaves per minute from 50 to 2000 Hz at a constant 1-g peak. These data, taken with the drive input along the lateral x-axis, show only slight resonance occurring around 60 and 180 Hz. Similar plots for the lateral y-axis and the vertical z-axis show the same results.

Figure 33 is a plot of acceleration as a function of frequency for the up and down sinusoidal vibration sweep at a rate of 2.0 octaves/min from 5 to 10 Hz at 1.93×10^{-2} m (0.76 in.) double amplitude, 10 to 20 Hz at a constant 4.0 g peak, and 30 to 2000 Hz at a constant 10.0 g peak. These data were recorded with the drive input along the lateral y-axis. A low level of resonance is noted at 60, 180, and 1300 Hz. Similar plots for the lateral x-axis and the vertical z-axis show comparable results.

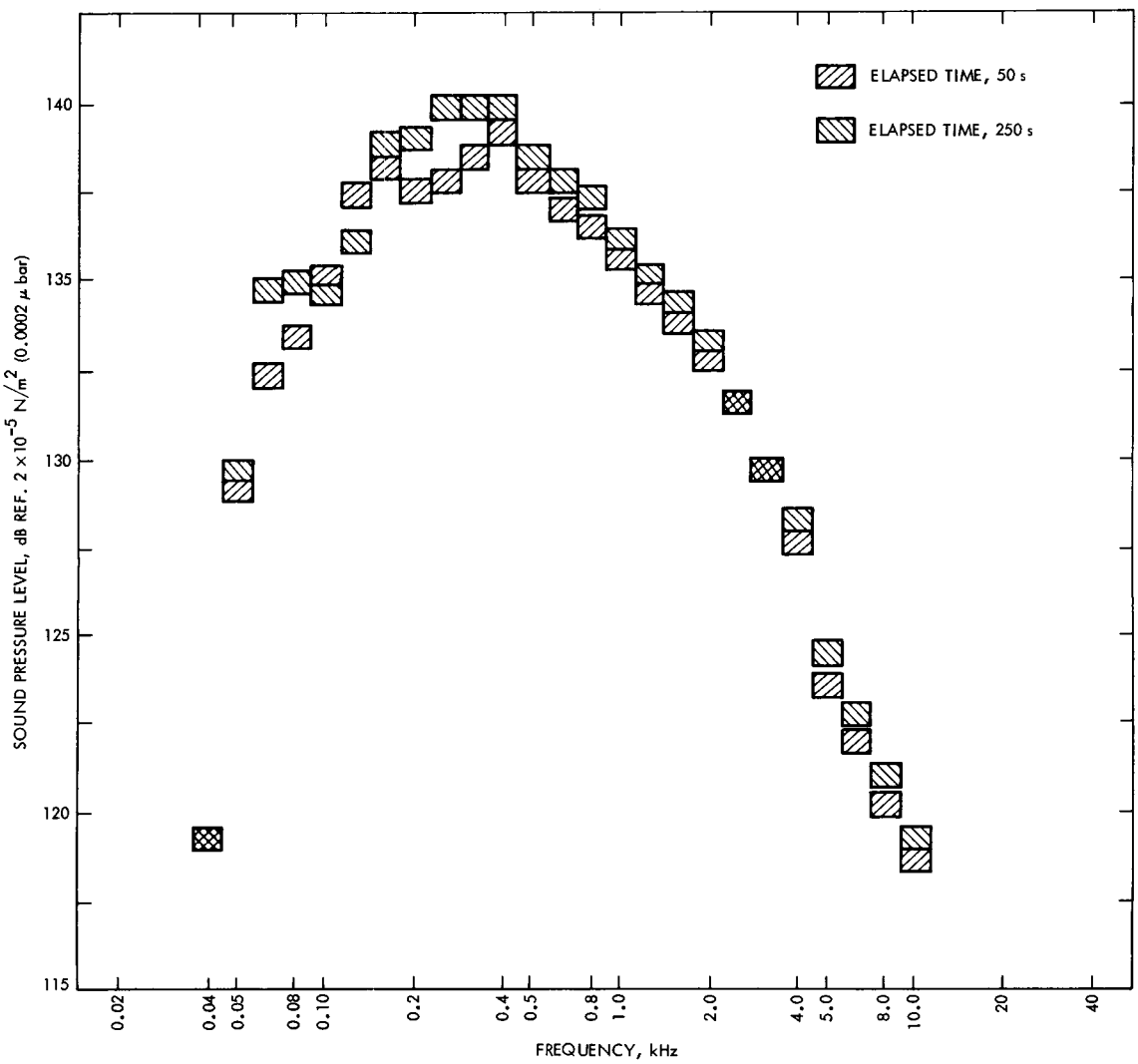

Fig. 31. Sound pressure frequency spectrum plot for control microphone (No. 1)

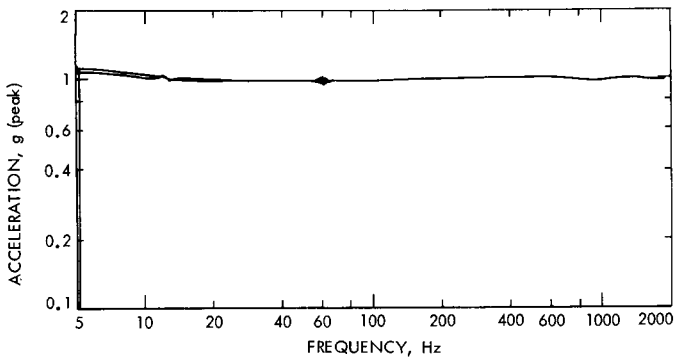

Fig. 32. Typical acceleration response for 1-g constant-amplitude sinusoidal vibration input on lateral x-axis (sweep rate up and down = 2 octaves/min)

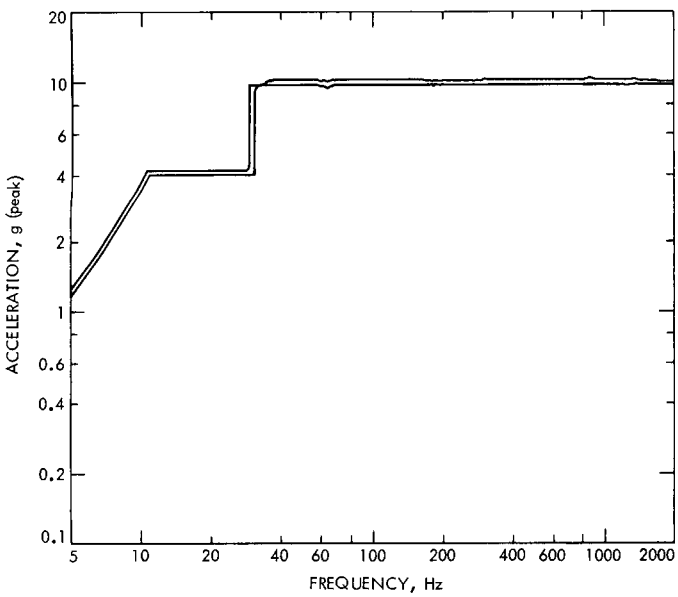

Fig. 33. Typical acceleration response for programmed sinusoidal vibration input on lateral y-axis (sweep rate up and down = 2 octaves/min)

Figure 34 is an analyzer display of decibel level as a function of frequency for the random vibration sweep over the wide-band level of 27.8 g rms from 25 to 50 Hz with roll-off at 24 dB/octave, 50 to 600 Hz at 1.0 g^2/Hz, and 600 to 2000 Hz with roll-off at 12 dB/octave. These data were recorded with the drive input along the vertical z-axis. The same plots for the lateral x-axis and lateral y-axis show similar results.

Typical samples of the oscilloscope trace recording of the acceleration from the applied shock tests are presented in Fig. 35. These pictures, which were recorded on the first in a series of shocks applied to each axis, show a shock pulse shape which approximates a terminal peak sawtooth that rises to a maximum value of 200 g in just over 0.7 ms and decays in less than 0.1 ms. Five of these shocks were applied in each of the three axes for a total of 15 shocks on the test assemblies.

The final test in the environmental dynamics test series was static acceleration. Each thruster test assembly was subjected to a 15-g acceleration on a centrifuge for a

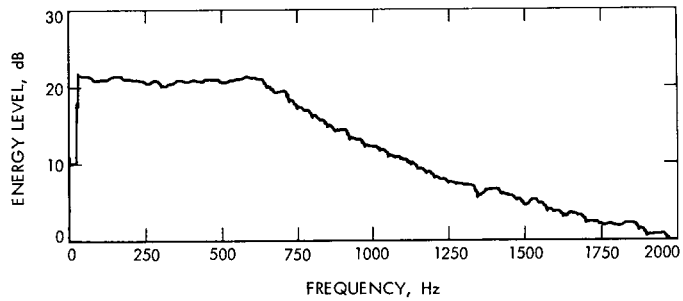

Fig. 34. Typical analyzer display of decibel level to random vibration programmed sweep over wide-band level of 27.8 g rms (input on vertical axis)

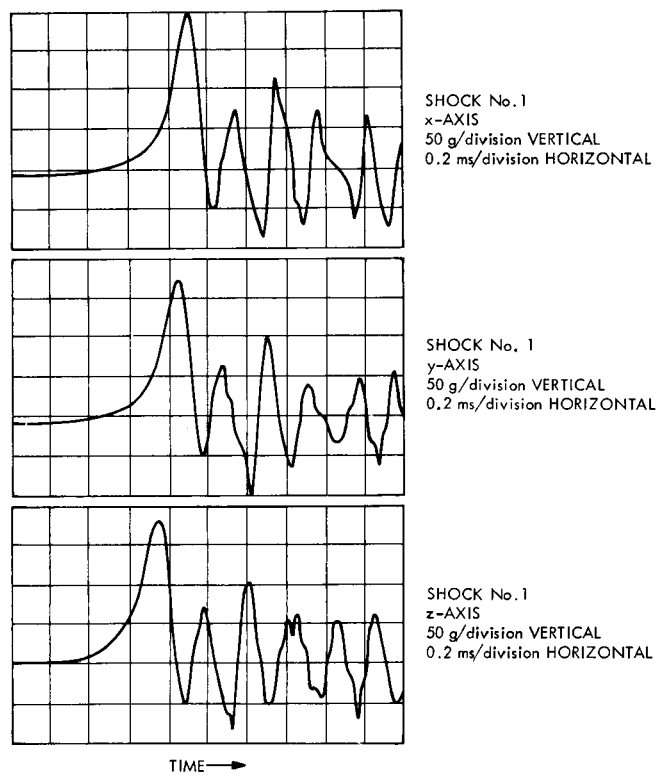

Fig. 35. Typical acceleration response to shock load applied in each of three orthogonal axes

period of 120 s in each of the three axes. The only data recorded during this test were on the speed of rotation of the centrifuge; these data, in conjunction with the known lever arm length, were sufficient to determine the applied acceleration.

Post-test visual inspection of each thruster assembly revealed no structural damage. The tape and plastic film covering the exhaust nozzles were removed, and because of the negligible quantity of catalyst particles present, efforts to collect a sample of fines were of no avail. All three thrusters were determined to be acceptable for the performance validation test sequence.

V. Minimum Operating Temperature Definition Tests

A. Introduction

An explanation is warranted as to why a "minimum" operating temperature is even considered. As mentioned earlier (Section I), there is very strong evidence that a marked increase in catalyst bed structural life expectancy is obtainable if the catalyst bed is warmed prior to thruster operations so that all starts are warm starts. For applications requiring very large numbers of starts, such as spacecraft attitude and position controls, obtaining a high probability of increased life expectancy becomes imperative. Therefore, some form of catalyst bed preheating will be required, and the most likely energy source in the immediate future will be in the form of electrical heaters. For earth satellites and interplanetary spacecraft implemented with solar panels, power availability may be less of a concern. However, for applications to such missions as those to the outer planets, where energy must be generated along the way, electrical power dissipation rates must be carefully controlled.

Therefore, it becomes necessary to establish a minimum catalyst bed temperature, and hence a power requirement, at which the thruster will operate successfully throughout its defined mission. A preliminary analysis shows that a properly thermally controlled 0.44-N (0.1-lbf) thruster (radiation shielded with highly reflective surfaces) can be maintained at approximately 149°C (300°F) for less than 0.5 W of electrical power. Although additional analysis is necessary to determine the heating power requirements at temperatures other than 149°C (300°F), this data point indicates the generally small power consumption required to maintain elevated temperatures for this class of thruster.

As explained in Section I, for hydrazine decomposition to occur spontaneously at lower temperatures, larger surface areas are required to start the reactions. This larger surface area is obtained when either liquid- or vapor-phase hydrazine is absorbed into the very porous catalyst. The decomposition of the hydrazine inside a catalyst particle produces very high local gas pressures and thermal gradients, which can fracture the ceramic particle and generate catalyst "fines." These fines are ejected with the exhaust gases, resulting in a net loosening of the catalyst bed, which can cause a thruster to run "rougher" and aggravate the generation of fines by mechanical abrasions (see Fig. 1).

For duty cycles where the initial temperature is low and where there is insufficient time between starts for the catalyst to outgas and rejuvenate itself, the exhaust gases can adsorb onto the active catalyst sites and present a barrier to any additional hydrazine. This process continues onward downstream until most active sites have been affected. Meanwhile, the upstream catalyst cools down (by transferring heat to the oncoming propellant) and aggravates the reduction of catalyst activity by retarding the desorption rate (see Fig. 4). It is hypothesized, however, that a minimum temperature exists for a given duty cycle whereby the catalyst is "vacuum-baked" between starts in such a way that the chemisorbed gases are driven off, thus rejuvenating the bed.

The objectives of this phase of the test program were:

(1) Define the minimum operating temperature above which the hydrazine decomposition reactions will occur primarily on the outer surface of the catalyst.

(2) Define the minimum operating temperature above which the hydrazine decomposition products will not chemisorb on the active catalyst sites and prevent further hydrazine decomposition. This temperature must be high enough that, coupled with the vacuum condition, it will drive off chemisorbed exhaust gases. This is not necessarily the same temperature as that at which the reaction begins to occur primarily on the outer catalyst surface. (The temperature required to prevent chemisorption will generally be higher, as indicated in Fig. 3.)

B. Tests

The tests to define the lower operating temperature limits were performed in the vacuum test facility described in Section III. Impulse bit data were obtained for catalyst bed temperatures which were varied from ambient temperature to 316°C (600°F) in 27°C (50°F) incre-

ments. Although a pulse train of approximately 10 pulses was executed at each desired temperature, the first pulse of each train was the more representative of a limit-cycle event. The time lapse between temperature changes was sufficient to outgas the major portion of the catalyst bed within the thruster *off*-time, since the thruster remained in a vacuum during the duration of this test series.

For these tests, the desired temperature was obtained by a momentary steady state firing that allowed the thruster to exceed the desired temperature slightly and to cool back to it. (For later tests, an electrical heater made of a winding of chromel high-resistance wire was installed on the thruster body with high-temperature, asbestos-impregnated epoxy cement. Electrical power to the heater was regulated by a temperature controller.) The intent of these tests was to find the point where both an impulse bit (or impulse-bit-related parameter) slope change occurs and a reduction in chamber pressure response occurs as a function of temperature. This change is hypothesized to represent the temperature above which the reaction would take place primarily on the outer surface of the catalyst.

C. Data Analysis

A parametric study was conducted to determine which parameter or combination of parameters would be the most effective or the most representative in depicting the point where a change in slope as a function of temperature occurs. The data were iterated in several forms in an attempt to find a parameter that relates impulse bit and/or chamber pressure response as a function of temperature in such a manner as to exaggerate the change in the curve slope to more clearly display where it occurs. Two parameters that appeared to give the best results were I_{bit}/P_c max and I_{bit}/pulse "area ratio." The term P_c max referred to the maximum reading of the chamber pressure pulse, while the pulse area ratio was defined as the ratio of the primary pulse area to the tail-off area.

Because the tail-off portion of the pulse becomes more significant as the temperature is reduced, a "hot" pulse—greater than 316°C (600°F)—was used as a definition point. The time increment from pulse initiation to the point where chamber pressure had decayed to approximately 10% of its maximum value was defined as the primary pulse area; the remainder was defined as "tail-off." The duration of the primary pulse was held constant as a reference time, even for the lower temperature.

Although the actual impulse bit may not vary significantly with the temperature (it generally becomes a little smaller with lower temperatures), there is a significant pulse centroid shift as temperature is reduced. If the primary pulse reference time is held constant, the pulse mode area ratio changes with the lower temperature. This definition, as it relates to the Rocket Research thruster, is presented in detail in Fig. 36, where the temperature-related difference is more obvious because of the longer valve *on*-time. The identical procedure was followed for the remaining two thrusters, whose hot and cold pulse waveforms are presented in Figs. 37 and 38.

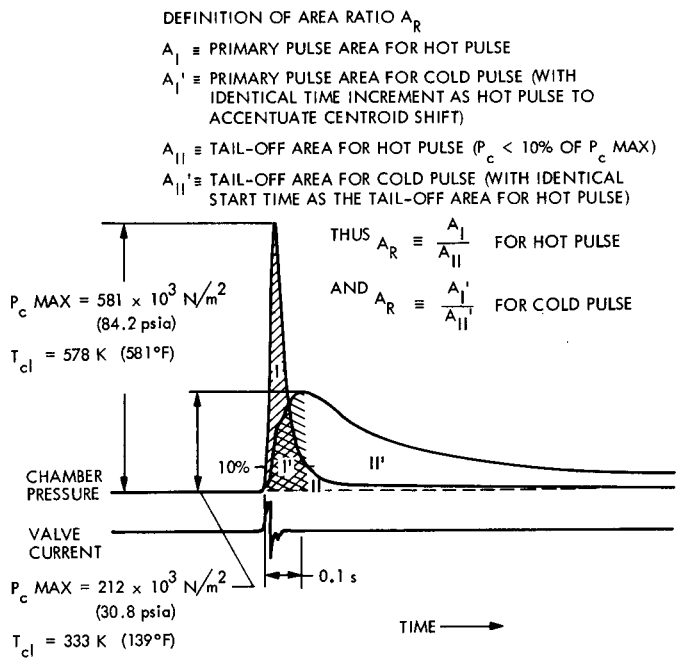

Fig. 36. Comparison of hot and cold pulse for Rocket Research thruster S/N 02 (valve *on*-time = 0.020 s)

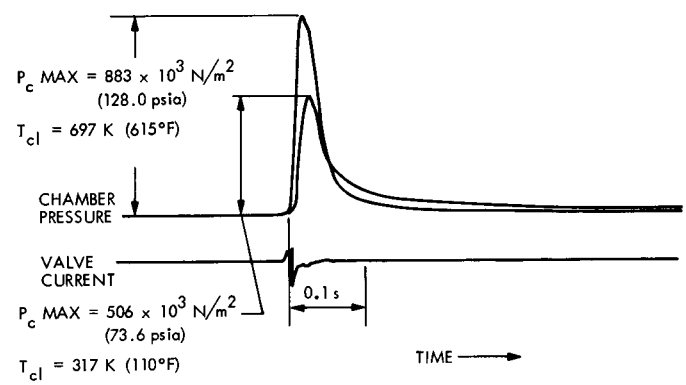

Fig. 37. Comparison of hot and cold pulse for Hamilton Standard thruster S/N 001 (valve *on*-time = 0.010 s)

Thus, the I_{bit}/pulse area ratio as a function of temperature shows a much more exaggerated break in the curve than would be true of a display of impulse bit alone. The point at which this slope change occurs is theorized to be the minimum operating temperature and is also the point above which the pulse waveform becomes normal. (In other words, there is no further indication of ignition delay; see Figs. 39–41). Also, when the pulse centroid shifts toward the tail-off region as the temperature is reduced, the maximum, or peak, chamber pressure is also reduced.

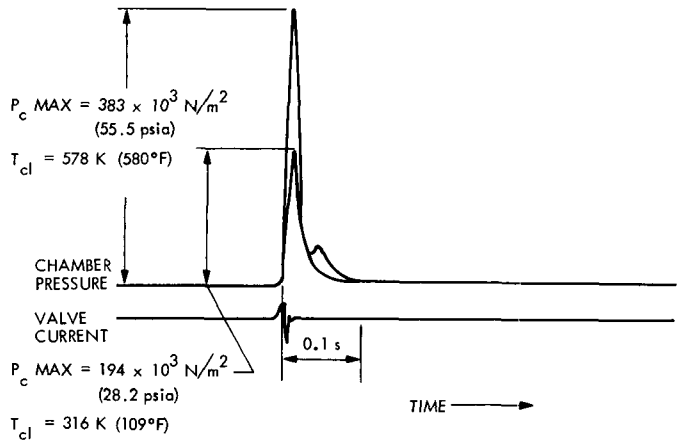

Fig. 38. Comparison of hot and cold pulse for Marquardt thruster S/N 002A (valve on-time = 0.010 s)

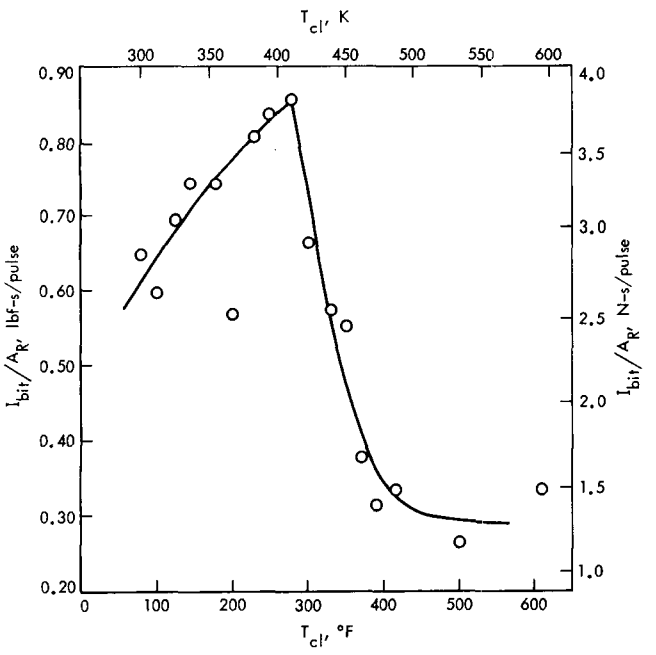

Fig. 39. Impulse bit per pulse area ratio as a function of thruster temperature, Hamilton Standard thruster S/N 001

Therefore, one would expect to see a variation in I_{bit}/P_c max: this parameter would be expected to change slope at the point where ignition delay effects, such as the hydrazine vaporizing and/or absorbing into the catalyst, were no longer felt. This was indeed the case (see Figs. 42–44), and the changed slope of the I_{bit}/P_c max

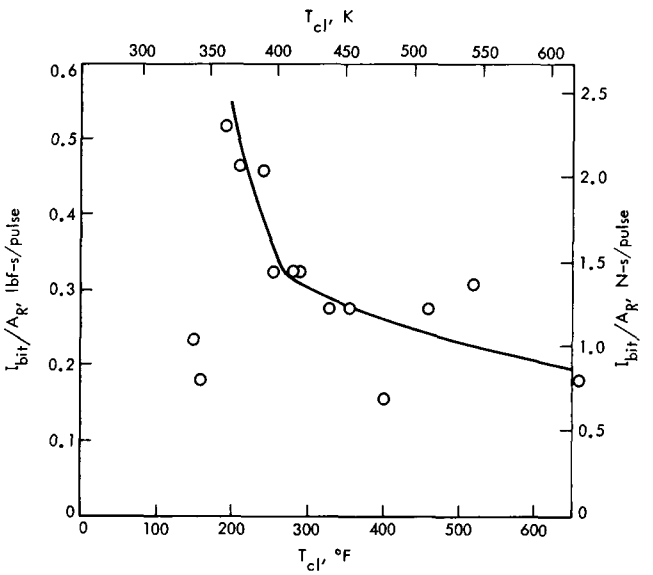

Fig. 40. Impulse bit per pulse area ratio as a function of thruster temperature, Marquardt thruster S/N 002A

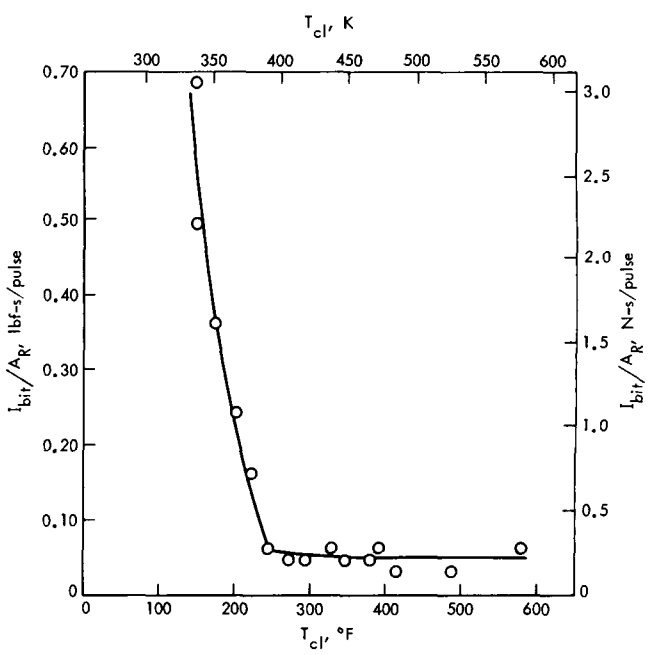

Fig. 41. Impulse bit per pulse area ratio as a function of thruster temperature, Rocket Research thruster S/N 02

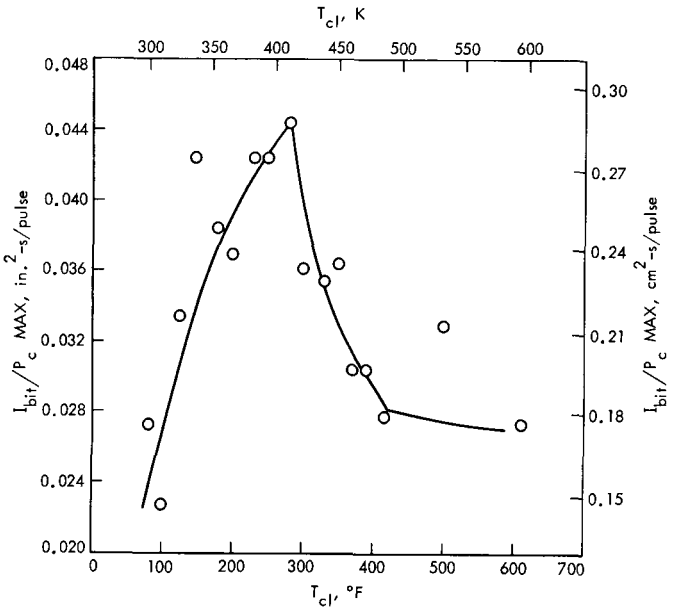

Fig. 42. Impulse bit per maximum chamber pressure as a function of thruster temperature, Hamilton Standard thruster S/N 001

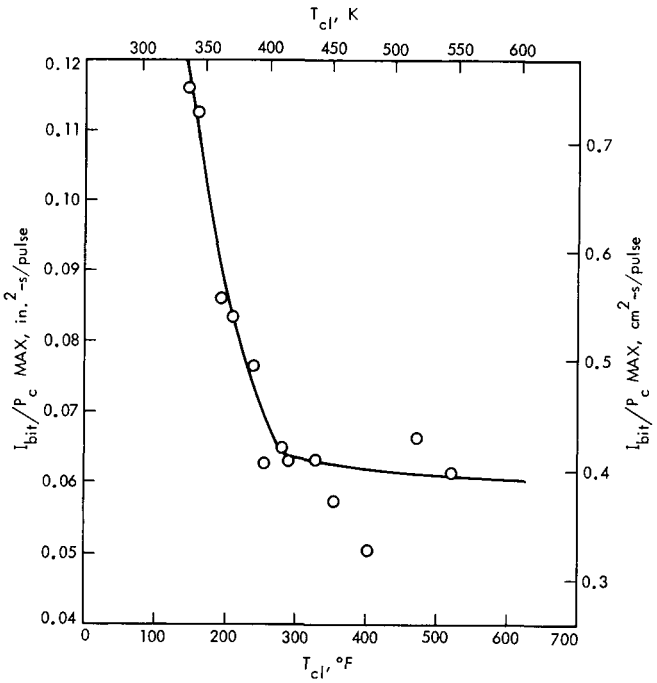

Fig. 43. Impulse bit per maximum chamber pressure as a function of thruster temperature, Marquardt thruster S/N 002A

curve corresponded to approximately the same temperature as the I_{bit}/area ratio point. (Compare, for example, Figs. 41 and 44.)

D. Results

The data from this test series were reduced into the form of impulse bit per maximum chamber pressure (I_{bit}/P_c max) and impulse bit data per area ratio (I_{bit}/A_R); (see the definition in Fig. 36), and are presented for the Hamilton Standard, Marquardt, and Rocket Research 0.44-N (0.1-lbf) thrusters in Figs. 39–44. The slope change as a function of the impulse bit parameters occurred as a maxima for the Hamilton Standard thruster and as a break in a descending curve for the remaining two thrusters. This difference is probably attributable to the fact that the Hamilton Standard thruster had a much larger capillary tube inlet volume (downstream of the thruster valve). The temperatures for both the Hamilton Standard and Rocket Research thruster bodies were obtained directly from thermocouples located near the injector.

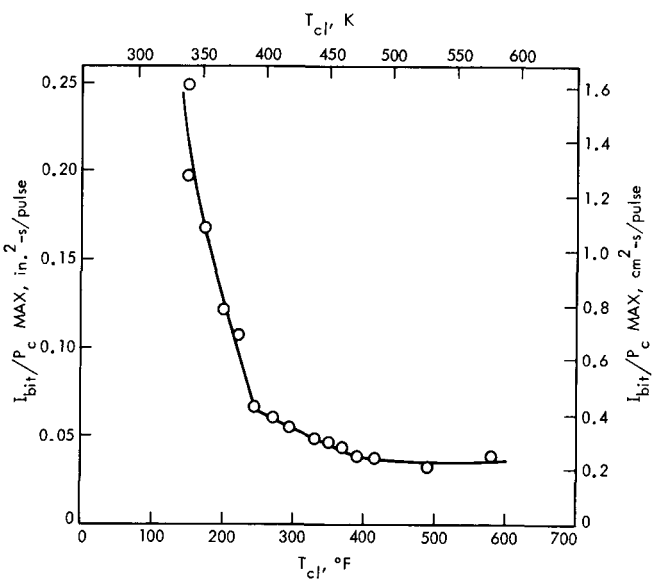

Fig. 44. Impulse bit per maximum chamber pressure as a function of thruster temperature, Rocket Research thruster S/N 02

The catalyst bed temperature for the Marquardt thruster, because of its construction with the inner and outer cylindrical sections sandwiching a TZM (titanium zirconium molybdenum alloy) spring maintained in tension, had to be semi-empirically derived. This derivation was accomplished by a standard heat transfer technique to account for the thermal gradient across the space between the catalyst bed and the outer shell, using the measured outer surface temperature as a reference. However, as a result of inaccuracies from simplifying assumptions necessary for this technique, the reduced data of the impulse bit parameter as a function of temperature in

Figs. 40 and 43 appear more scattered than that of the other two thrusters.

Examination of the reduced data reveals a slope change occurring around 135°C (275°F) for the Hamilton Standard and Marquardt thrusters and around 121°C (250°F) for the Rocket Research thruster. This slope change is hypothesized to represent the point at which the primary propellant decomposition reactions begin to occur primarily on the outer surface of the catalyst, and would, therefore, be the minimum operating temperature required to curtail the generation of catalyst fines. However, a second slope change appears to occur at around 204°C (400°F), as seen from the Hamilton Standard and Rocket Research thruster data in Figs. 39 and 44. (The data from the Marquardt thruster appears too scattered at this temperature to warrant any specific conclusion.)

Although a positive conclusion was not reached as to the significance of the second slope change, it is suspected that this change may represent the point at which the hydrazine has nearly completely changed phase (liquid to vapor) in the injector tube and is being injected into the catalyst bed as a vapor. If this is indeed the case, then it would appear that this temperature would represent a much more efficient and predictable impulse bit for the limit cycle application of the 0.44-N (0.1-lbf) thruster. However, preliminary data from another test program conducted with a 0.44-N (0.1-lbf) thruster in a very-high-vacuum facility (Ref. 7) have also suggested that this slope change at this temperature might possibly represent the temperature at which catalyst bed outgassing becomes predominant and causes a resistance to the incoming flow.

As a conclusion from this test series, it appears that the 0.44-N (0.1-lbf) thruster can be operated at initial temperatures above 121°C (250°F) with minimal concern for the generation of catalyst fines during limit cycle mode application.

However, the second objective of determining the minimum temperature above which the reduced catalyst bed activity from chemisorption of the exhaust gases will not impact the successful completion of any given attitude propulsion system mission requirement is best determined from the results of the life tests, which are discussed in Section VI. The temperature selected as having a very high probability of successful completion of the life test series with a minimal energy expenditure was 204°C (400°F).

VI. Limit-Cycle Life Tests

A. Introduction

One of the most widely applied forms of spacecraft attitude control is the "limit cycle" concept. When spacecraft stabilization and pointing are said to be accomplished by limit cycle mode, the inference is that there are two or more opposing mass expulsion devices that normally operate in pulse mode, with very short pulses from one side of the spacecraft at a time, causing the spacecraft to drift back and forth through a deadband, which is predetermined by the required pointing accuracy. The time between pulses could be as long as 1/2 hour or as short as a few seconds. Since pointing accuracy is inversely proportional to impulse bit, it is desirable to implement an attitude propulsion system that is capable of producing very small impulse bits. Previous JPL spacecraft have made use of gaseous nitrogen systems for this application. However, for spacecraft where the primary propulsion is from a monopropellant hydrazine system, or a bipropellant system where hydrazine is the fuel, it is a logical extension to consider a liquid-fed, monopropellant attitude propulsion system that is in common with the primary hydrazine fuel supply. Prior to this test program, extensive life tests at a minimum thruster/valve *on*-time and relatively low start temperatures to simulate a limit cycle mode of operation had not been demonstrated. Therefore, to verify that the 0.44-N (0.1-lbf) class of thrusters is worthy of consideration for limit cycle applications, a life test demonstration was necessary.

The objectives of this limit-cycle life test program were essentially three-fold. The first part was to determine whether 10^5 starts could be accumulated with minimal difficulty on a 0.44-N (0.1-lbf) thruster, operating at a 0.01-s *on*-time at both 93°C (200°F) and 204°C (400°F) initial temperatures. The marginality of the 93°C (200°F) initial temperature was to be determined during this phase. The questions to be addressed were whether any thruster of this class could sustain 10^5 starts at a 93°C (200°F) initial temperature per start, or whether this capability were entirely a function of design; and, if 10^5 starts were indeed feasible, whether 2.5×10^5 starts were possible at a 93°C (200°F) initial temperature.

The second part of this test objective was to determine whether 2.5×10^5 starts could be accumulated with a minimal performance loss on a 0.44-N (0.1-lbf) thruster at a 0.01-s *on*-time and 204°C (400°F) initial temperature per start.

The third objective was to determine the points, if any, where performance loss may occur from what is hypothesized to be caused from chemisorption of exhaust gases by the catalyst particles.

B. Test Installation

The test installation for the limit-cycle tests was identical to that described in Section II, where the schematic diagram of the test facility was presented as Fig. 7. Photographs of each of the three thrusters, as installed, (Hamilton Standard, Marquardt, and Rocket Research, respectively) are presented in Figs. 10–12. Before the limit cycle life tests were started, the test facility was upgraded to operate continuously for a 24-h day. The upgrading consisted primarily of the following additional safety features: (1) the installation of a thrust chamber maximum-temperature emergency shutdown device; (2) the replacement of normally closed solenoid safety valves with latching solenoid valves in the propellant feed system; and (3) the installation of an automatic fire-fighting sprinkler system in the test area.

In the absence of an adequate temperature feedback circuit, the thruster duty cycle was established and maintained by a repeat-cycle programmed timer which was set to actuate the thruster valve when the thruster temperature had approximately recovered to the level of the desired start temperature. In order to accelerate the cool-down to the desired temperatures of 93°C (200°F) and, later, 204°C (400°F) and to shorten the overall time to perform these life test series, a small aluminum block, cooled by a low flow of gaseous nitrogen through it, was installed at the injector end of each thruster (see Fig. 45). This additional heat sink had negligible effect on the chamber pressure profile because of the very short valve *on*-time (0.01 s). However, it did aid in reducing the required *off*-time by a few seconds.

C. Test Procedure

Before and immediately after each life test on each thruster, a calibration test was performed to define the thruster performance and to determine whether there had been any performance changes as a result of the life tests. As described in Section II, the calibration test consisted of operating over a range of steady state chamber pressure values (tank pressure varied from 690×10^3 N/m^2 (100 psig) to 2760×10^3 N/m^2 (400 psig) in 345×10^3 N/m^2 (50 psid) increments) to determine the variation of the performance parameters. Any deviation revealed by the calibration test conducted after the life test would indicate a quantifiable performance change. A chronology of

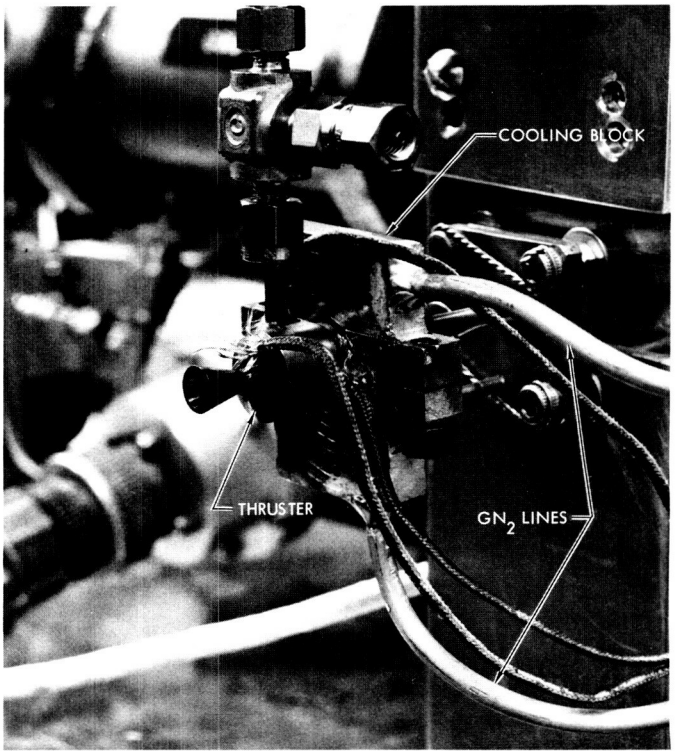

Fig. 45. Rocket Research thruster S/N 02 with aluminum heat sink block installed

this test series is presented in Table 5 of Section IV. Figures 46–49 depict the performance results of calibration tests conducted before and after the life tests on the Hamilton Standard, Marquardt, and Rocket Research (S/N 01 and 02) thrusters, respectively. As can be seen from the I_{sp} and c^* values, only a slight net performance loss was experienced by either the Hamilton Standard or the Rocket Research thruster. However, a meaningful post-life-series calibration test could be obtained only for the lower temperature life on the Marquardt thruster because of the very low flow rates that resulted from the partial plugging of the injector tube, which occurred during the higher temperature life test. The unusually high pressure drop between the tank pressure P_{ft} and the thruster chamber pressure P_c for the Marquardt thruster for Test 1571 was caused by the facility valve VFL (see Fig. 7) having been opened only approximately 10% after a propellant transfer. The chamber pressure roughness ($\Delta P_c/\bar{P}_c$) was nominal for each of the three thrusters, with the Rocket Research unit demonstrating the greatest value. This was consistent with the results reported in Ref. 1.

An indication of the performance variation as a function of the number of starts throughout the life test sequences

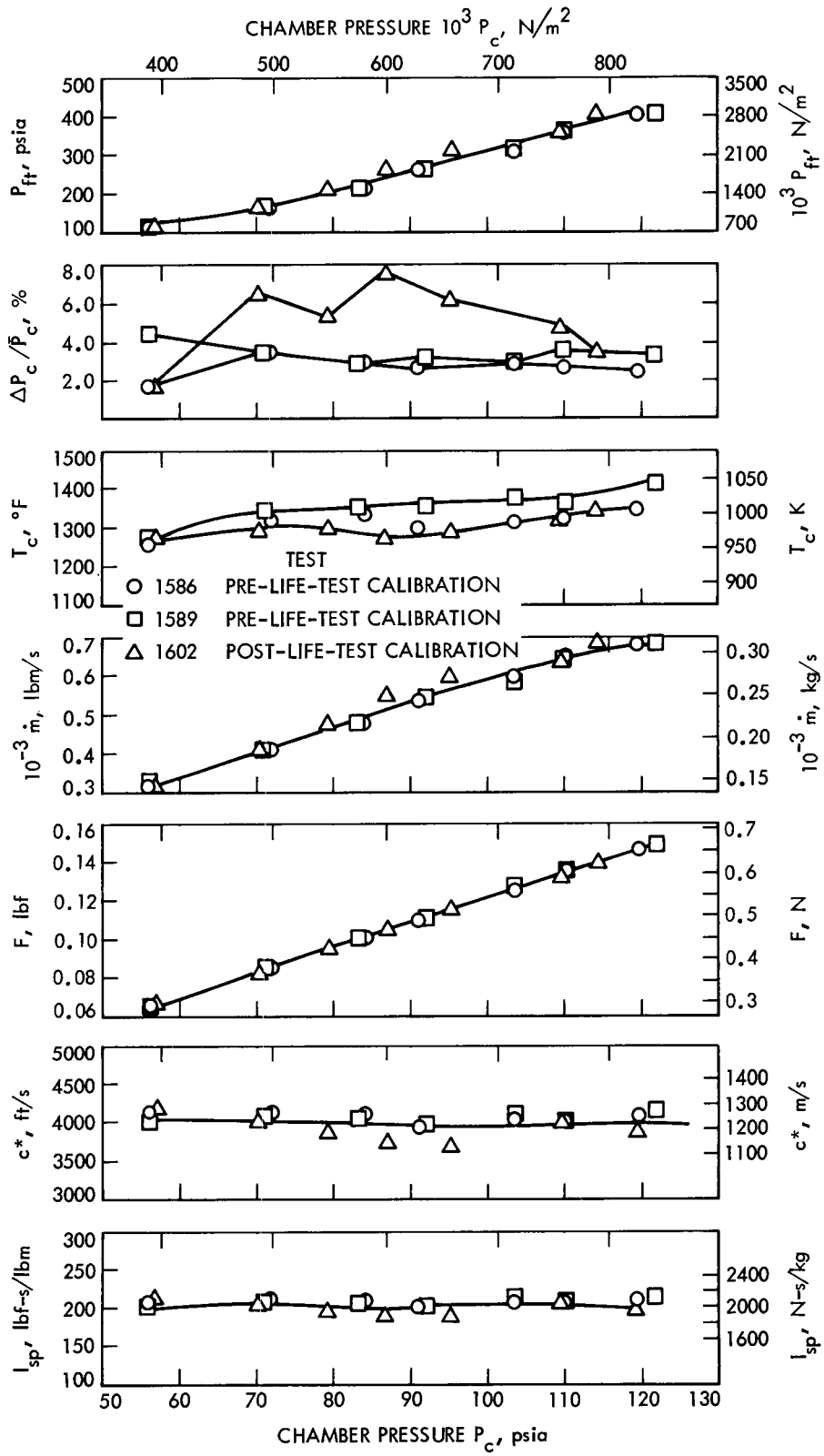

Fig. 46. Calibration test performance of Hamilton Standard thruster S/N 001 before and after limit-cycle life tests at 206°C (400°F)

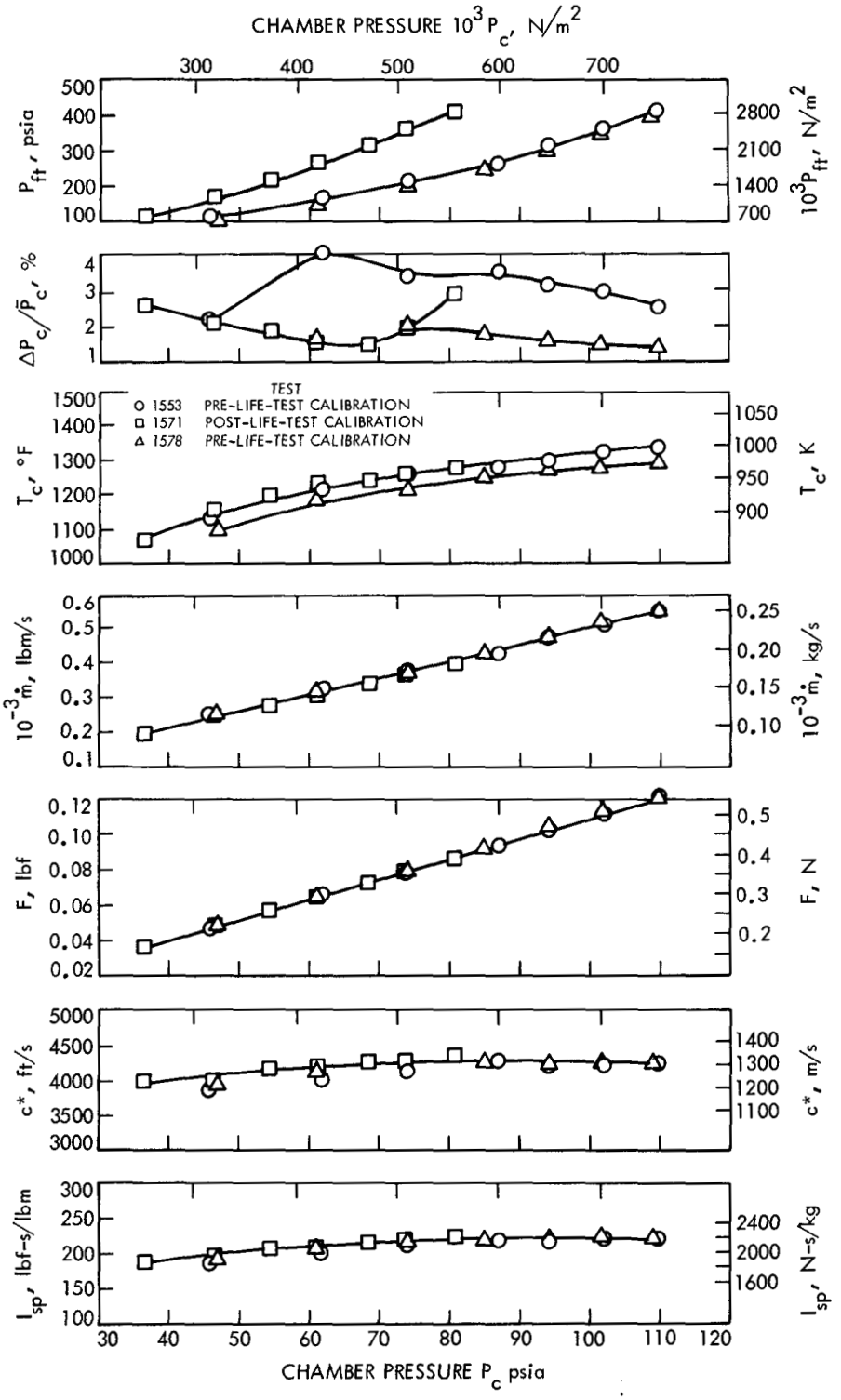

Fig. 47. Calibration test performance of Marquardt thruster S/N 002A before and after limit-cycle life tests at 96°C (200°F) and 206°C (400°F)

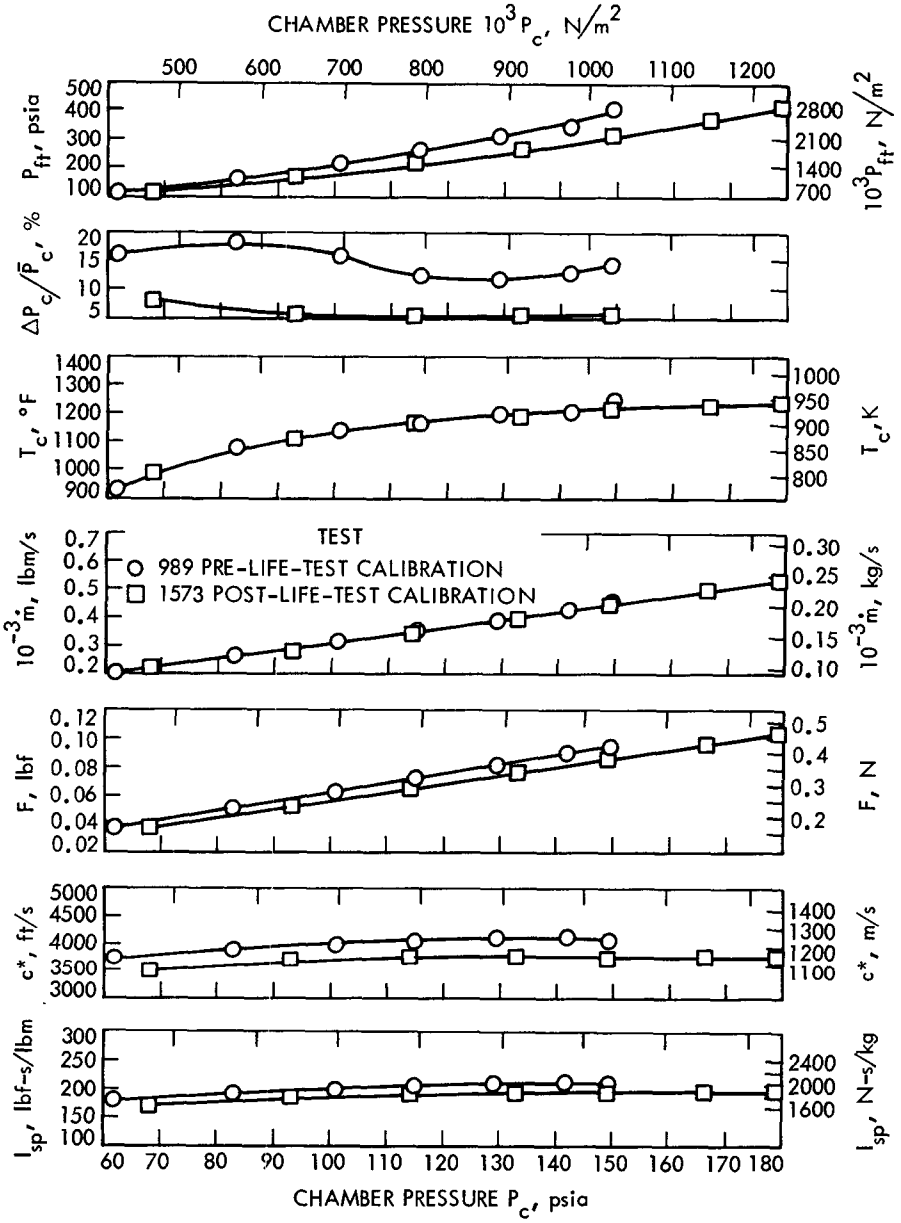

Fig. 48. Calibration test performance of Rocket Research thruster S/N 01 before and after limit-cycle life tests at 206°C (400°F)

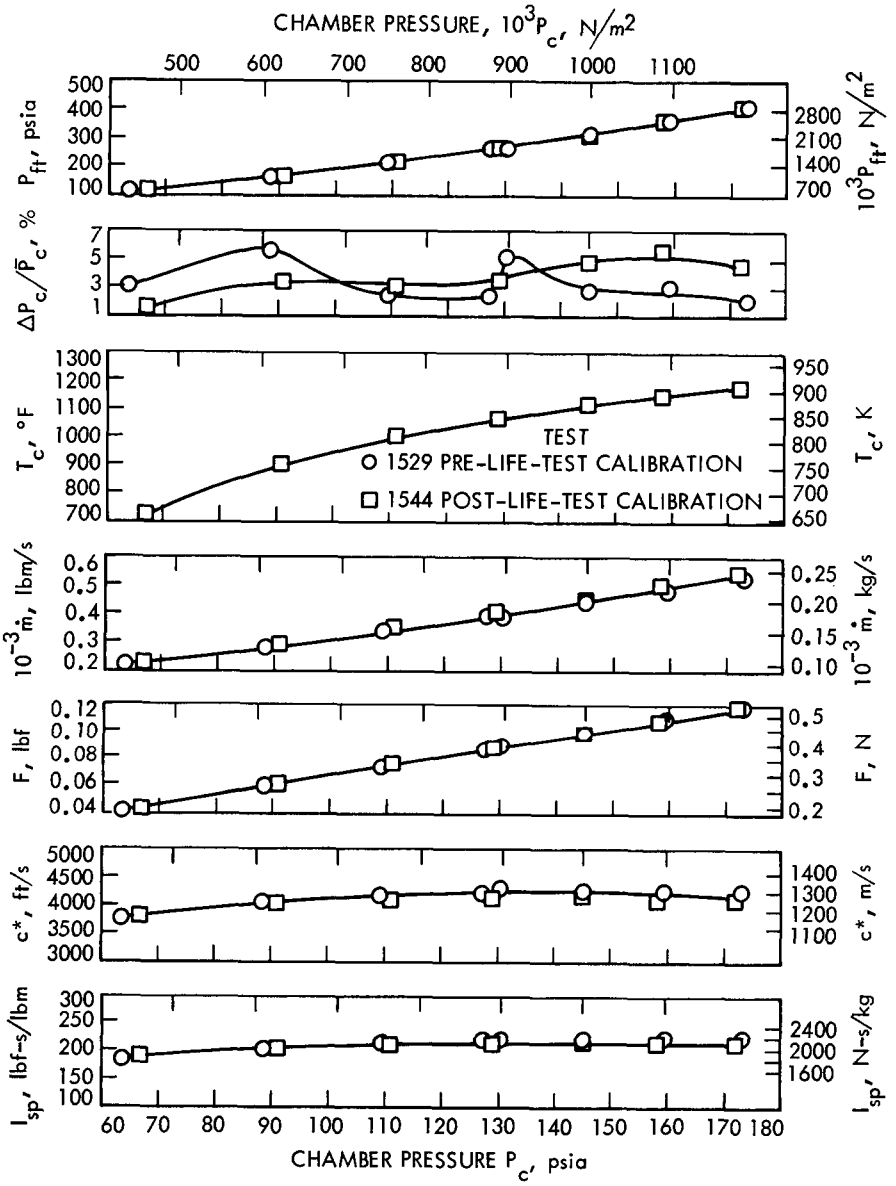

Fig. 49. Calibration test performance of Rocket Research thruster S/N 02 before and after limit-cycle life tests at 96°C (200°F)

is presented for the Hamilton Standard thruster in Fig. 50. A 30-s steady state firing at the nominal thrust level was made at the points indicated in the figure as a reference of the progress of the thruster. The decision to make these reference point tests came sufficiently late in the life test series that only the Hamilton Standard thruster was affected. A marked performance degradation would have been cause to terminate the life test.

A summary of the nominal start temperatures and the final duty cycles for the life test series performed with each thruster is presented in Table 9. A total of 100,216 starts at a nominal initial temperature of 210°C (410°F) was executed by Rocket Research thruster S/N 01 (with a 0.02-s valve *on*-time) at the very beginning of this test program to demonstrate the feasibility of a 0.44-N (0.1-lbf) hydrazine catalytic thruster to accomplish a large number of starts with a slightly preheated catalyst bed. This test occurred while the environmental dynamics tests (Section IV) on the mating thrusters were underway. (Rocket Research thruster S/N 01 had previously participated in the TOPS attitude propulsion system test program reported in Ref. 1).

Table 9. Thruster starting temperatures and duty cycles for limit-cycle life tests

Thruster and serial number	Start temperatures K	°F	Number of starts	Duty cycle *on/off* time, s	Comments
Rocket Research S/N 01	483	410	100,216	0.020/14.0	
Rocket Research S/N 02	394	250	48,983	0.010/25.0	
	372	210	56,219	0.010/9.0	Cooled[a]
Total			103,202		
Marquardt S/N 002A	394	250	30,831	0.010/16.0	
	375	215	221,417	0.010/10.0	Cooled
Total			252,248		
Marquardt S/N 002A-1	480	405	100,465	0.010/8.0	Heated[b]
Hamilton Standard S/N 01	535	503	35,620	0.010/16.5	Heated
	483	409	221,045	0.010/13.0	Cooled
Total			256,665		Heated

[a]Cooled thruster had an aluminum heat sink block attached to the thruster body. Gaseous nitrogen was continuously circulated through the heat sink block.

[b]Heated thruster had electrical resistance heating elements wrapped around the thrust chamber, which were energized only when the temperature dropped below 478 K (400°F) and de-energized above 483 K (410°F).

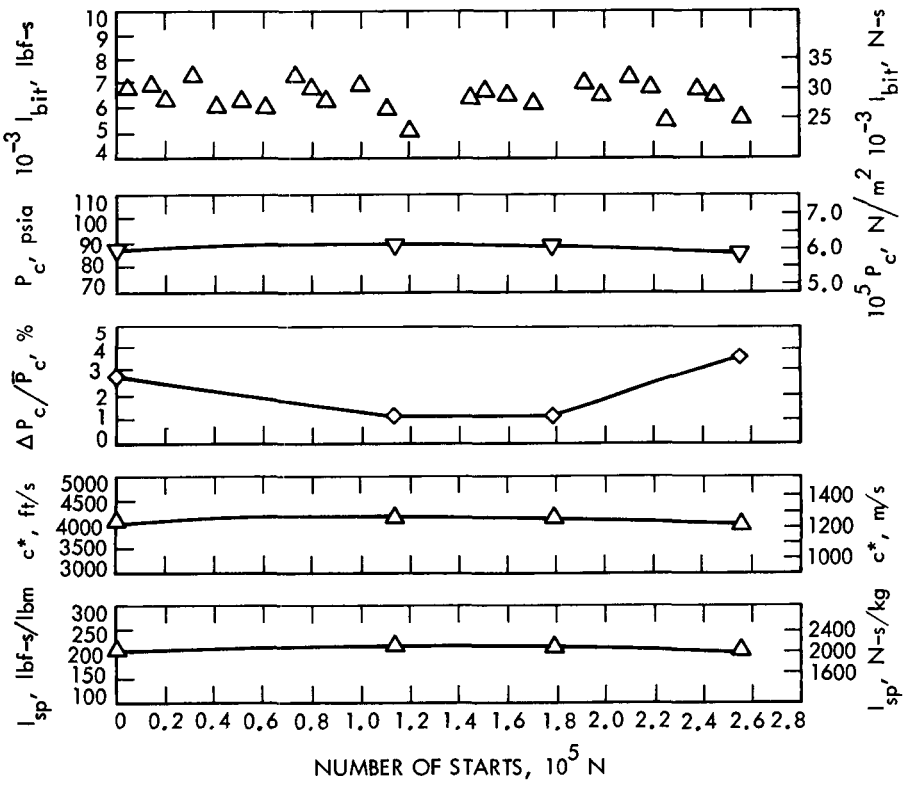

Fig. 50. Performance variation as a function of number of starts for Hamilton Standard thruster S/N 001, nominal temperature = 262°C (409°F)

After the environmental tests and the tests to define the minimum operating temperature, Rocket Research thruster S/N 02 was installed and subjected to 103,202 starts, 48,983 of which were at 121°C (250°F) while the remainder were at a nominal 99°C (210°F) start temperature. All pulse widths for this test series were governed by a 0.01-s valve *on*-time. The first indication of thrust/performance decay from the hypothesized catalyst bed chemisorption was observed during this specific test series at start 96,353.

Difficulty was experienced in restarting the thruster with the control system set in the automatic limit-cycle mode after a propellant transfer, prior to which the catalyst bed temperature was allowed to drop to ambient (21°C, or 70°F). The thruster was restarted by short, manually controlled, steady state actuations of the thruster valve to bring the catalyst bed temperature back up to operating conditions. The impulse bits for both Rocket Research thrusters are presented in Figs. 51 and 52.

Marquardt thruster S/N 002A was installed next. The primary objectives of this test were to demonstrate 2.5×10^5 starts at a nominal 93°C (200°F) start temperature and 0.01-s valve *on*-time, as well as to determine where performance loss from catalyst bed chemisorption would occur and what type of rejuvenation process would be effective. The resulting impulse bits as a function of number of starts are presented in Fig. 53. As indicated in this figure, there were five performance losses from catalyst bed chemisorption. Since an unsuccessful restart attempt was made after the first occurrence, the thruster

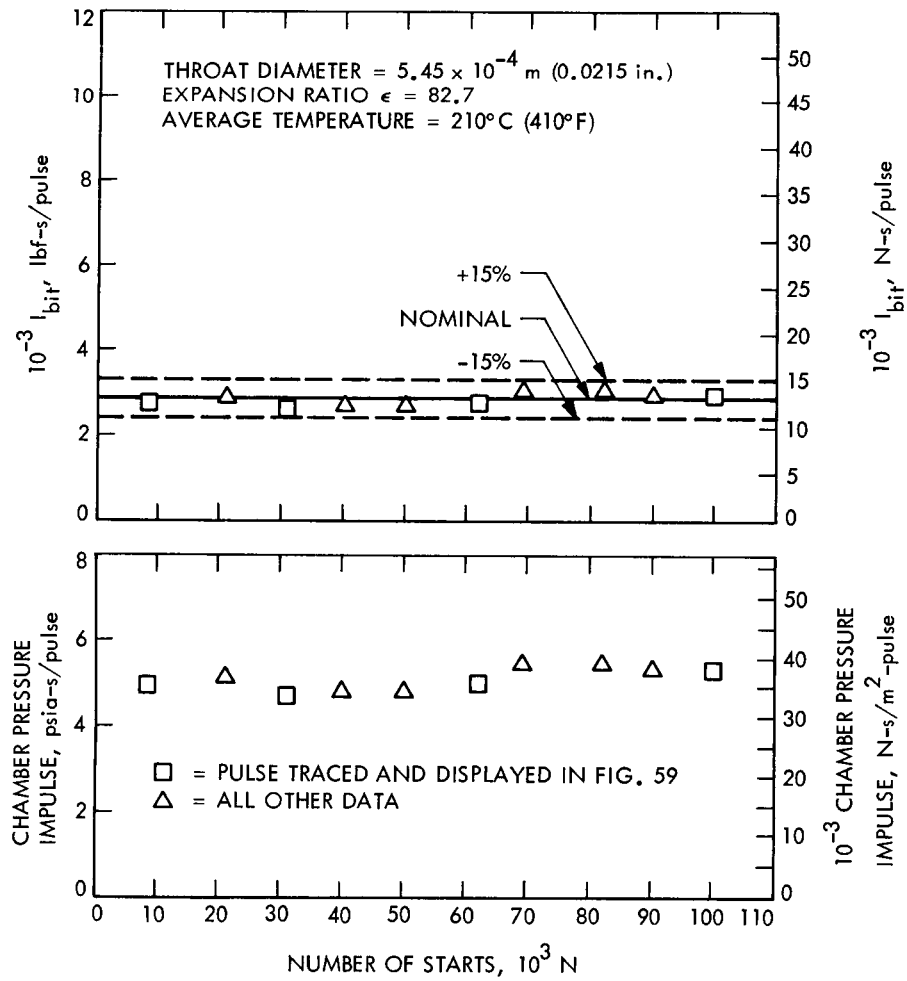

Fig. 51. Impulse bit as a function of number of starts for Rocket Research thruster S/N 01

body was externally heated to approximately 260°C (500°F) for about 30 minutes prior to any further restart attempts and immediately after each subsequent performance loss. This procedure, although only an expedient, reactivated a sufficient number of catalyst sites to rejuvenate performance and enable the test to continue.

Because of the success of this procedure, at the completion of this test series the thruster (with the valve removed) was baked in a 260°C (500°F) oven for 48 h to reactivate the catalyst bed for the next test series. This process was performed at atmospheric pressure, since a vacuum oven capable of this higher temperature was not available at the time. However, it is recommended that this method of catalyst bed rejuvenation be conducted in a vacuum oven so as to provide for the continual removal of the evolved gases, as well as to prevent further nitriding and/or oxidation of the catalyst bed by the atmosphere.

At the completion of the bake-out procedure, the reassembled Marquardt thruster was scheduled to be reinstalled into the test system to demonstrate 2.5×10^5 starts at 204°C (400°F). Calibration Test 1575 (see Table 5) was conducted with the intent of determining the effect the oven baking may have had on thruster performance. However, a flow restriction through the injector assembly was observed. (The earlier problem with the propellant system valve VFL had been corrected.) The possibility of a restriction in the solenoid valve was eliminated when the valve was removed and flow-checked and was found to be unrestricted. The 1.43×10^{-4} m (5.6×10^{-3} in.) ID injector tube, the suspected cause of the flow restriction, was probed full length with wires

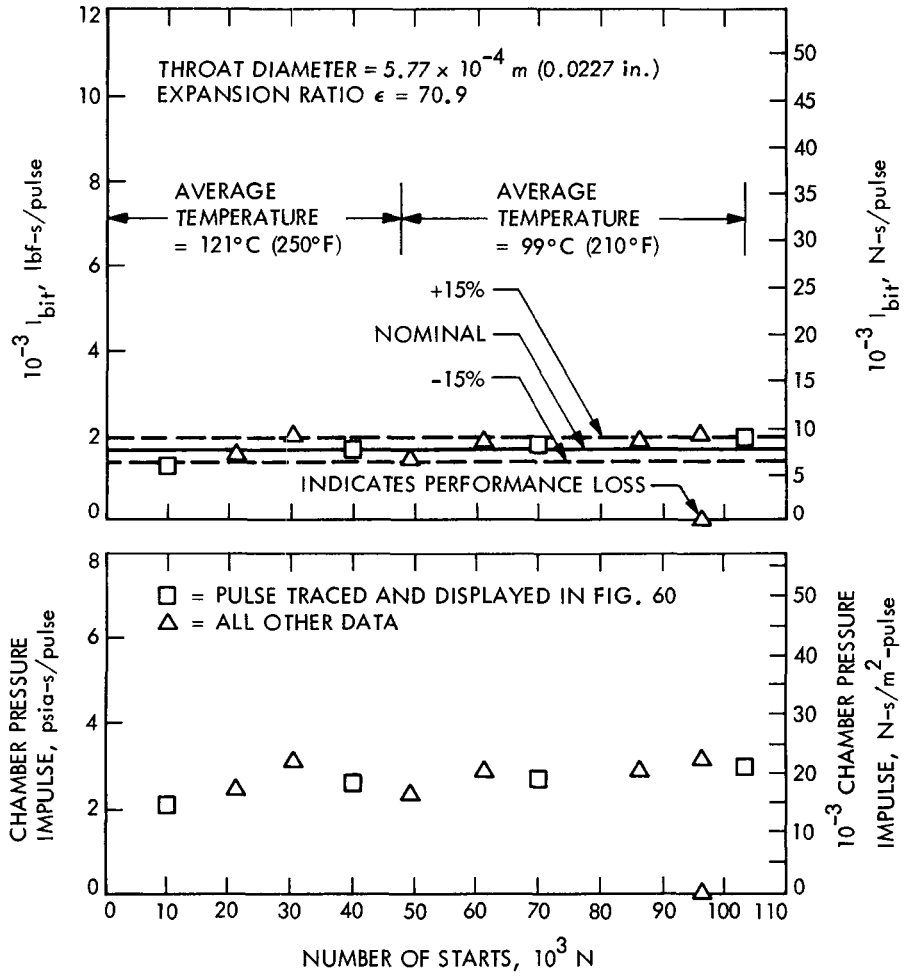

Fig. 52. Impulse bit as a function of number of starts for Rocket Research thruster S/N 02

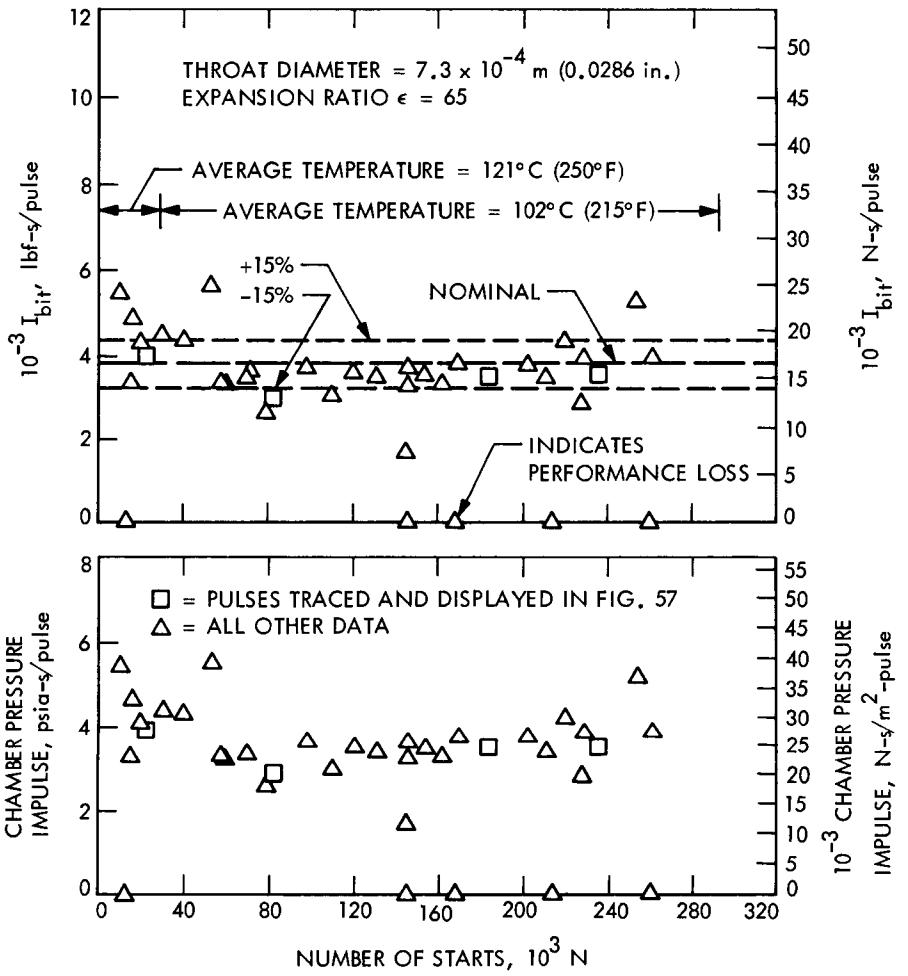

Fig. 53. Impulse bit as a function of number of starts for Marquardt thruster S/N 002A

ranging in size from 7.65×10^{-5} m (3×10^{-3} in.) to 1.15×10^{-4} m (4.5×10^{-3} in.) in diameter.

Although some resistance to the passage of the wire was noted at first, the injector tube appeared to be fully opened after probing. The thruster was reassembled and test-fired (Test 1577) to verify performance. Calibration Test 1578 was then conducted to document the thruster characteristics before the 204°C (400°F) limit-cycle simulation test. The results of the calibration test, presented in Fig. 47, demonstrate performance characteristics comparable to previous calibration tests on this thruster, indicating a full recovery of the catalyst bed.

In preparation for the 204°C (400°F) limit-cycle simulation test, a chromel heater wire attached to a temperature controller was bonded to the Marquardt thruster with an asbestos-impregnated epoxy. During the operational checkout of this modified assembly, the solenoid valve was found to have a broken lead wire just below the surface of the valve body, rendering repair very difficult. Hence this valve was replaced by the spare valve from Marquardt thruster S/N 001 that was not in use (each thruster was delivered with a valve attached). The thruster serial number was then modified from S/N 002A to S/N 002A-1 to reflect this minor change. The 204°C (400°F) limit-cycle life test on the Marquardt thruster S/N 002A-1 was terminated after 100,465 starts, short of the 2.5×10^5 start goal, because of progressive loss of chamber pressure caused by a partial plugging of the capillary injector tube.

The post-life-test calibration test of this thruster showed an 80% loss in flow rate. Wire probing of the injector tube located the blockage at the downstream end past the thruster body inlet and immediately upstream of the injector screen attachment point. The cause of the flow restric-

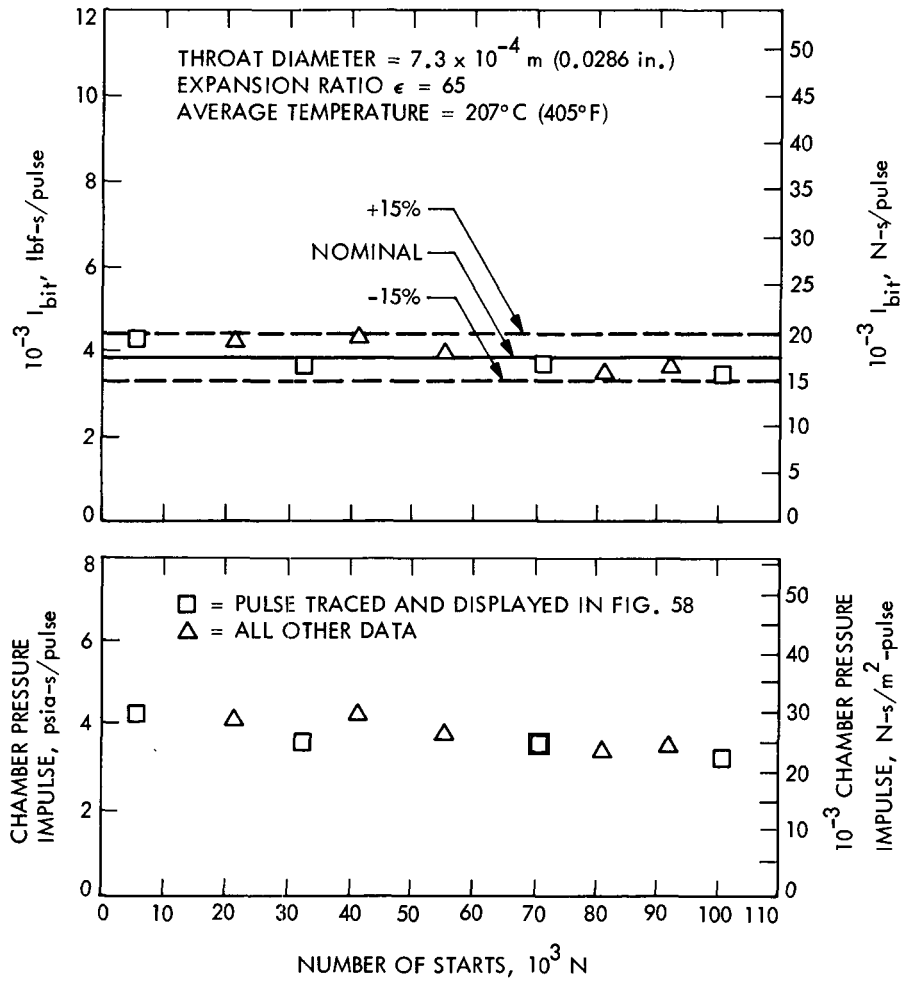

Fig. 54. Impulse bit as a function of number of starts for Marquardt thruster S/N 002A-1

tion was under detailed investigation at the time of this report, but was suspected to be from a buildup of contamination. Upon removal of the Marquardt thruster, the facility propellant feed system filters were disassembled and cleaned to remove any contamination which may have accumulated.

The Hamilton Standard thruster was installed (also with the thruster heater and temperature controller) to demonstrate the 2.5×10^5 starts of 204°C (400°F). This test proceeded without incident until around start 218,187, when the very small P_c pressure transducer line (approximately 0.008 m (1/32 in.) OD, 0.004 m (1/64 in.) ID, and approximately 0.025 m (1 in.) long), constructed of 321 CRES tubing), which had been used for other thruster installations during the program, became partially plugged. (The tube is located between the thrust chamber P_c tap and the transducer inlet in Fig. 10.) This plugging was possibly due to a stray catalyst particle or to local nitriting of the pressure tube, although the quantity of material was too small for the JPL Chemistry Laboratory to obtain a detailed analysis. This partial restriction had no effect on the steady state performance reading, but it did act as a "snubber" for the dynamic pulse output, causing a suppression of the recorded chamber pressure waveform shape. The trace of the P_c pulse output returned to normal when this transducer line was replaced.

The variation of impulse bit with number of starts is presented in Figs. 51–55 for the Rocket Research, Marquardt, and Hamilton Standard thrusters, respectively. Chamber pressure impulse in units of psia-second/pulse is also presented for comparison, since impulse in units of lbf-second is obtained by multiplying the integral of chamber pressure by the thrust coefficient C_f and throat area A_t. The C_f and A_t values used in this calculation are based on an

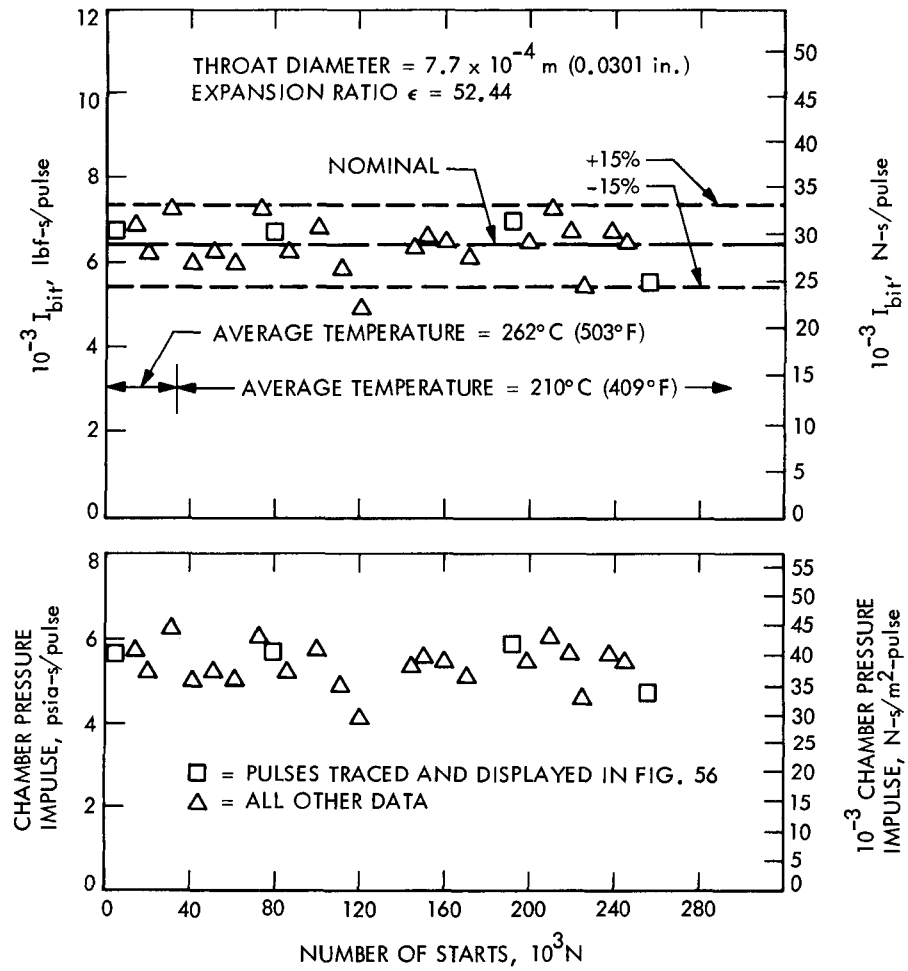

Fig. 55. Impulse bit as a function of number of starts for Hamilton Standard thruster S/N 001

earlier steady state test conducted on each thruster. Thus, the resulting impulse bit in units of force-second is slightly larger, and therefore more conservative for limit cycle mode, than that which really existed. The corresponding integral of chamber pressure (P_c bit) is presented as the unconverted raw data. All integrating of the chamber pressure pulse wave form was done with a planimeter directly from the oscillograph recorder traces, and, as can be seen from the figures, the general body of data falls within an obtainable limit of approximately ±15% of the nominal value for a 0.01-s *on*-time limit cycle operation of a 0.44-N (0.1-lbf) hydrazine catalytic thruster.

A sampling of typical chamber pressure profiles is presented for each thruster in Figs. 56–60 to depict more explicitly the variation of pulse profile with start number. For ease of cross reference, each pulse traced for these figures is the point indicated by a square symbol in Figs. 51 and 55. As can be seen, there was very little variation in chamber pressure profile for either the Hamilton Standard thruster at the 209°C (409°F) start temperature or the Rocket Research S/N 01 thruster at 210°C (410°F) start temperature, as was predicted from the results of the minimum operating temperature tests presented in Section V.

A noticeable variation in pulse waveform was indicated, however, for the lower-temperature starts on both the Marquardt S/N 002A and the Rocket Research S/N 02 thrusters. The variation was less pronounced on the Rocket Research thruster, primarily because of the longer catalyst bed, which tends to stabilize the pressure dynamics for short pulses, and the shorter overall sampling range (10^5 starts as compared with 2.5×10^5 starts on the Marquardt thruster).

The partial plugging of the Marquardt thruster S/N 002A-1 injector tube resulted in a very noticeable change

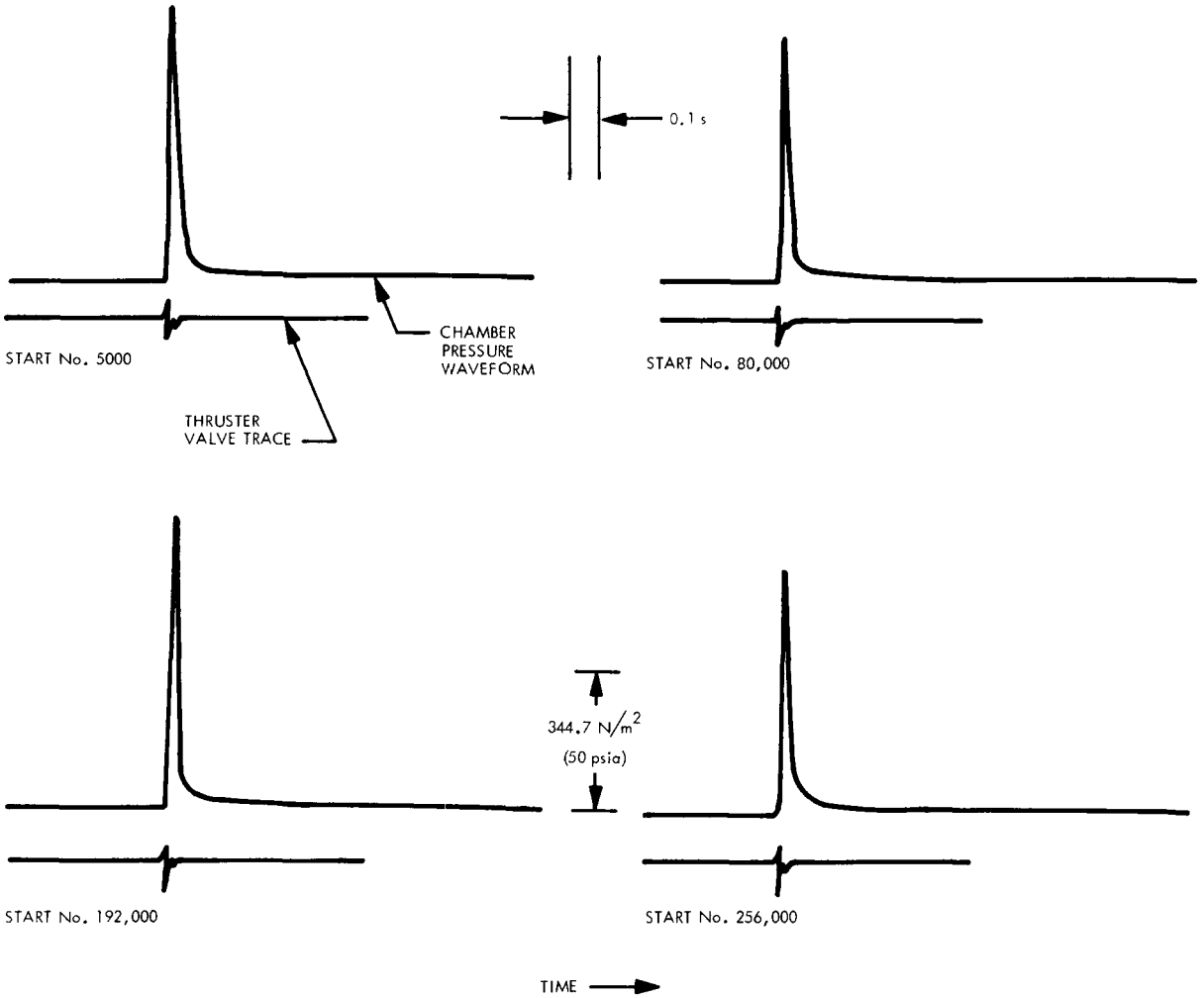

Fig. 56. Pulse trace from limit-cycle life test of Hamilton Standard thruster S/N 001 at a starting temperature of 209°C (409°F)

in chamber pressure profile (Fig. 58), although only a slight change in impulse bit (Fig. 54). This apparent discrepancy is explained by the fact that although a large flow impedance exists, most of the required quantity of hydrazine was still being injected into the catalyst bed (though more slowly), rendering approximately the same available energy and hence impulse bit.

VII. Exhaust Product Tests

A special test was conducted to determine the composition of the thruster exhaust products and to attempt to quantify any unreacted hydrazine that may have been present during pulse mode operation. Past JPL experience from similar test programs has shown that some trace amounts of unreacted hydrazine are usually present in the exhaust products, even for steady state thruster operations (catalyst bed temperature of approximately 760°C, or 1,400°F), and that the presence of these small traces is considered normal (see Table 7, Section IV). It was suspected that because of the relatively low start temperatures (approximately 204°C, or 400°F max), and the very short valve *on*-times (0.01 s), larger quantities of unreacted hydrazine would probably be present.

The exhaust gas samples taken for this evaluation were extracted with an evacuated 10-cm³, valved, stainless steel cylinder attached to the thruster P_c port. (This procedure is described in detail for the steady state tests in Ref. 1.) The exhaust nozzle was capped with a blowout insert to ensure maximum capture of the exhaust products by the sampling cylinder. The thruster valve was energized for a maximum of 1 s to ensure sufficient *on*-time to collect the exhaust product sample of the complete start transient.

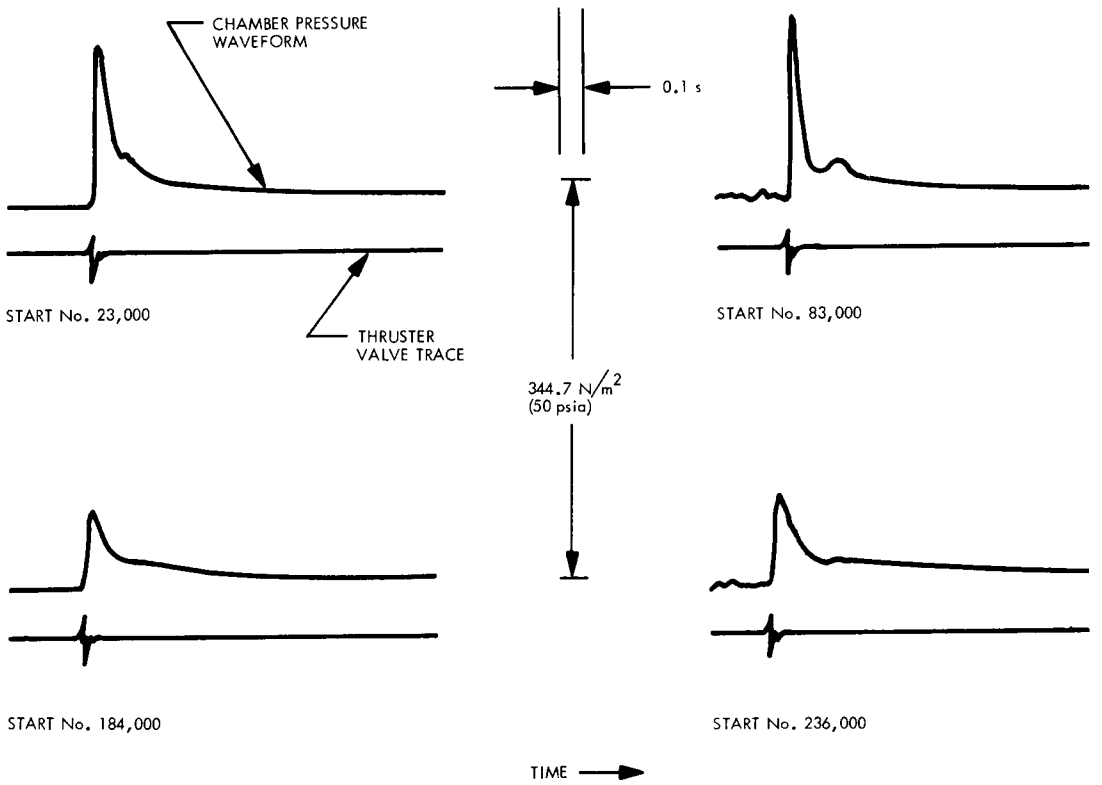

Fig. 57. Pulse trace from limit-cycle life test of Marquardt thruster S/N 002A at a starting temperature of 111°C (231°F)

The results of the sample collections are presented in Table 10. For all cases, the quantity of ammonia was extracted and defined from the total gas present. The percentage of nitrogen and hydrogen present in the remaining fraction of the gas sample was determined as a reference for two cases. (Test 1610 was a standard gas sample taken near the end of a 60-s steady state operation.) As can be seen, trace amounts of unreacted hydrazine were always present but were not consistent from sample to sample. Unfortunately, time did not permit a refinement of the sampling procedure, and hence the inconsistency of the results is not surprising.

The primary factor affecting the final quantification is the fact that the unreacted hydrazine is collected while in the vapor phase, and, prior to final analysis in the chemistry laboratory, condenses to a very small volume inside the sampling cylinder. It then becomes very difficult for the analyst to ensure that he has removed all of the condensed hydrazine (with the application of heat) when the analysis is performed, or that he has not decomposed some in the process. However, the samples shown in Table 10 present some indication of the quantity of hydrazine existing in the exhaust products during pulse mode. It is felt intuitively that quantities on the order of 600–900 μg are more in line with what might be expected for these test conditions.

For the last three samples only, an attempt was also made to quantify the amount of water vapor present. These results, which are subject to similar randomness because of the sampling technique, are also presented in Table 10. As a comparison with what might be an expected quantity of water, the batch of hydrazine used for this specific test demonstrated a water assay of 0.67%. Using Test 1610 in Table 10 as a reference, the generation of the quantity of gases collected (58.45 cm^3) would require 38.1 mg of hydrazine. For the water assay indicated above, 38.1 mg of hydrazine would have approximately 255 μg of water associated with it. This calculated value of 255 μg is in very good agreement with the experimental value of 283 μg. The first two water sample analyses appear to be in error on the high and low sides, respectively.

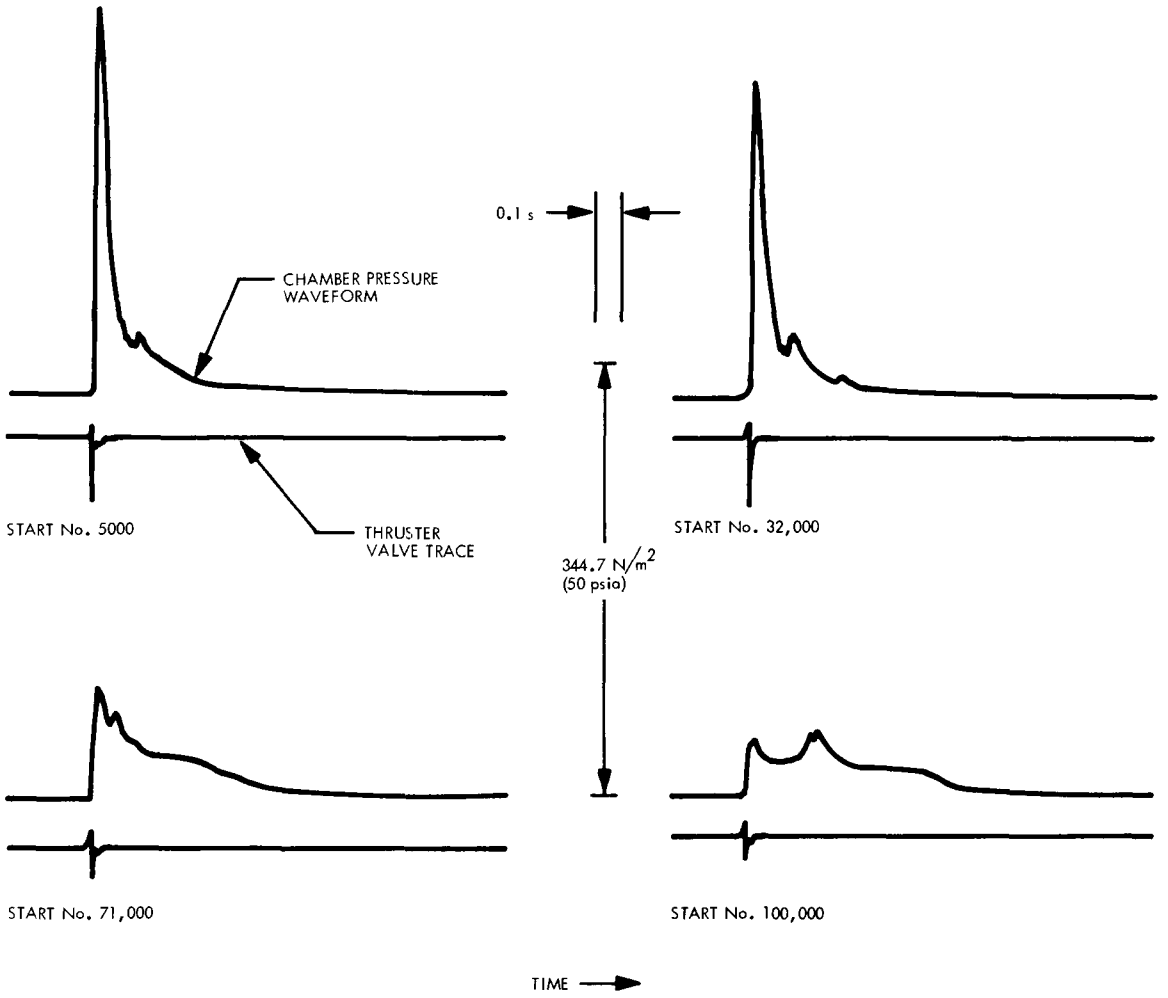

Fig. 58. Pulse trace from limit-cycle life test of Marquardt thruster S/N 002A-1 at a starting temperature of 207°C (405°F)

Table 10. Hydrazine and water detected in the exhaust gases of Hamilton Standard thruster S/N 01

Test number	Total gas, cm^3	NH_3, cm^3	NH_3, %	N_2, %	H_2, %	$N_2 + H_2$, %	N_2H_4, μg	H_2O, μg
1604	63.94	39.06	61.1	—[a]	—	38.9	10	—
1605	63.33	38.53	60.8	—	—	39.2	390	—
1606	62.76	38.58	61.9	21.8	16.2	38.0	40	—
1607	62.23	38.08	61.2	—	—	38.8	980	—
1608	62.63	37.99	60.7	—	—	39.3	5	675
1609	62.29	39.31	63.1	—	—	36.9	7	161
1610	58.45	22.41	38.3	26.4	35.1	61.5	600	283

Nominal thruster chamber pressure = 581×10^3 N/m^2 (85 psia).
Thruster initial temperature = 204°C (400°F).
Propellant tank pressure = 1650×10^3 N/m^2 (240 psia).
Valve *on*-time = 1.0 s.
[a]Dash indicates quantity not measured.

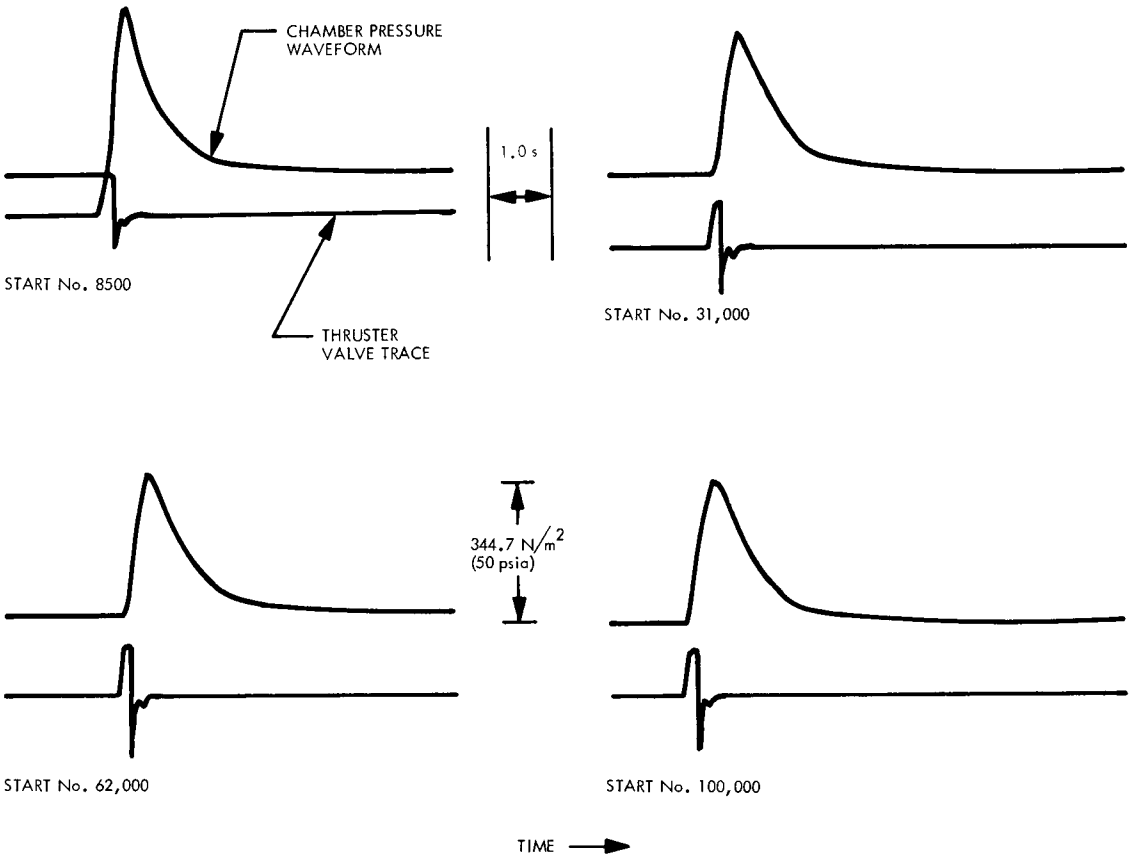

Fig. 59. Pulse trace from limit-cycle life test of Rocket Research thruster S/N 01 at a starting temperature of 210°C (410°F)

VIII. Conclusions

As a result of this test program, the following conclusions have been reached:

(1) The thruster/valve assembly can readily sustain a nominal launch dynamic environment with no mechanical or performance degradation.

(2) The 0.44-N (0.1-lbf) hydrazine catalytic thrusters can be used for spacecraft attitude propulsion limit cycle operations for an extensive number of starts if the thruster body is maintained at an elevated temperature, such as 205°C (400°F), since up to 2.5×10^5 starts were demonstrated at this temperature with no resulting deleterious effects on the thruster.

(3) Start temperatures of more than 121°C (250°F) should result in minimal mechanical damage to the catalyst particles.

(4) Since chemisorption of the exhaust product gases by the catalyst bed active sites appears to be a real but curable cause of reduced catalyst bed activity at lower temperatures, the continual maintenance of these thrusters at temperatures of 205°C (400°F) or greater while in space would allow the catalyst bed to "vacuum bake" and outgas between starts. This procedure should sufficiently retard the buildup of chemisorbed gases to ensure a successful completion of a nominal mission where this class of thruster must demonstrate an extensive number of starts.

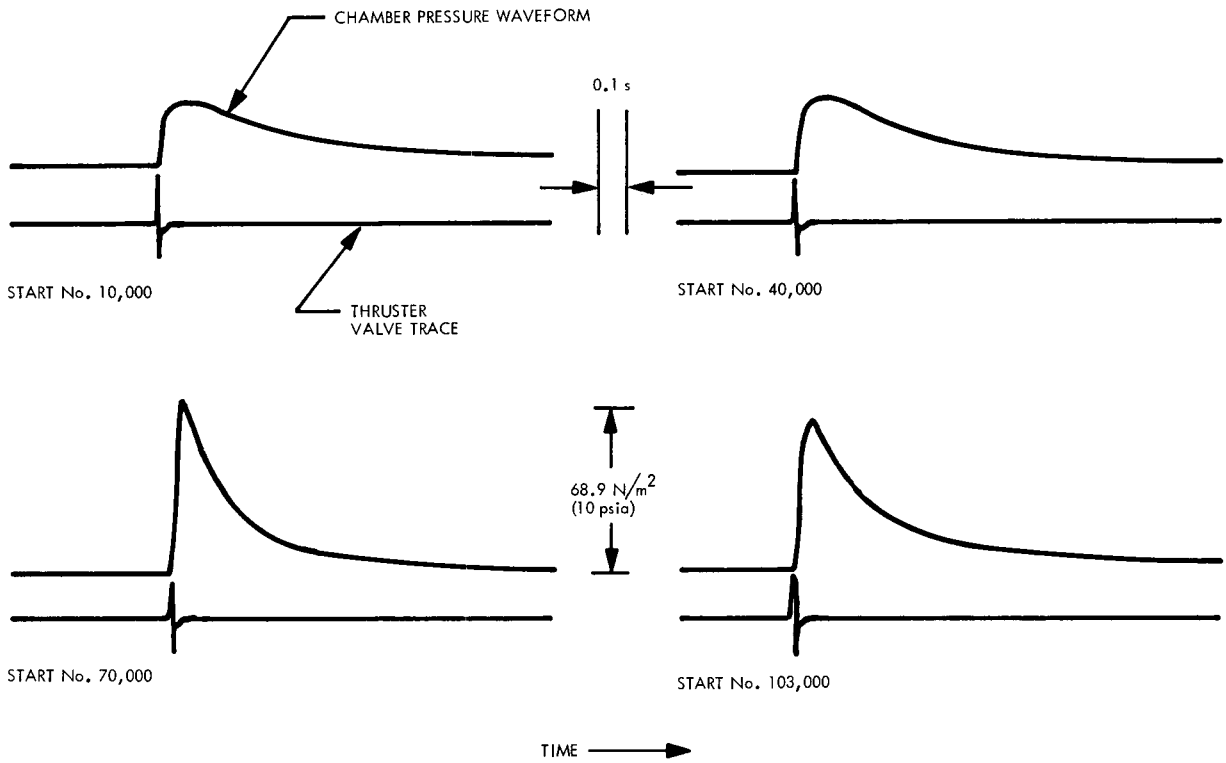

Fig. 60. Pulse trace from limit-cycle life test of Rocket Research thruster S/N 02 at an average starting temperature of 110°C (230°F)

Nomenclature

A_R ratio of primary pulse area to pulse tailoff area

A_t nozzle throat area

c^* characteristic velocity

C_f thrust coefficient, dimensionless

d_e effective passage diameter

d_t nozzle throat diameter

F thrust

g gravitational acceleration of earth

g_c Newton's constant relating force and mass

I_{sp} specific impulse

I_{bit} unit of impulse per pulse

$\dot{m}$ propellant mass flowrate

N_{pl} pressure loss modulus, dimensionless, $\equiv g_c \rho d_e^3 \Delta P / \mu^2 \lambda$

N_{Re} Reynolds number, dimensionless, $\equiv 4\dot{m}/\pi d_e \mu$

P_a ambient pressure

P_c chamber total pressure

P_{fi} fuel injector pressure

P_{ft} fuel tank pressure

ΔP differential pressure

$\Delta P_c/\bar{P}_c$ relative chamber pressure roughness (peak to peak)

ΔP_{fc} Viscojet differential fuel pressure

T_{fl} fuel temperature

T_{cl} lower catalyst bed temperature

T_{ns} nozzle throat temperatures

ΔT temperature difference

X ammonia dissociation fraction

Nomenclature (contd)

α	coefficient of thermal expansion	λ	effective length of passage
ϵ	nozzle expansion-area ratio, dimensionless	μ	absolute viscosity
ηc_f	thrust coefficient efficiency, dimensionless	ρ	density

References

1. Moynihan, P. I., *Attitude Propulsion Technology for TOPS*, Technical Report 32-1560, Jet Propulsion Laboratory, Pasadena, California, Nov. 1, 1972.
2. Gordon, P. G., *300 lb Thrust Rocket Engine Assembly, Viking Orbiter 1975 Flight Equipment, Detail Specification for*, Specification ES505919, Jet Propulsion Laboratory, Pasadena, California, Nov. 14, 1972 (JPL internal document).
3. Long, H. R., and Bjorklund, R. A., *Trajectory Correction Propulsion for TOPS*, Technical Report 32-1571, Jet Propulsion Laboratory, Pasadena, California, Nov. 15, 1972.
4. Drenning, C. K., *Refurbishment of Marquardt R-25 0.1-lb Monopropellant Rocket Engine*, Letter Report 152/19669, The Marquardt Company, Van Nuys, California, Apr. 19, 1972.
5. Drenning, C. K., *Post Test Analysis of TMC R-25A 0.1-lb Thrust Monopropellant Engine (P/N T-17412, S/N 002)*, The Marquardt Company, Van Nuys, California, Mar. 21, 1972.
6. Moynihan, P. I., "Minimum Impulse Tests of 0.45-N Liquid Hydrazine Catalytic Thrusters," in *JPL Quarterly Technical Review*, Vol. 2, No. 1, Jet Propulsion Laboratory, Pasadena, California, July 1972.
7. Chirivella, J. E., and Moynihan, P. I., "Hydrazine Rocket Engine Plume Deposits Measured with Quartz Crystal Microbalances," presented at the 7th JANNAF Plume Technology Meeting, U.S. Army Missile Command, Redstone Arsenal, Alabama, Apr. 3–5, 1973.

Bibliography

Cannon, W. A., English, W. D., and Robson, J. H., *Pressurization Systems Design Guide, Vol. III, Pressurant Gas Solubility in Liquid Propellants*, Report DAC-60510-F1 (NASA Contract NAS7-548), National Aeronautics and Space Administration, Washington, D. C., July 1968.

Chirivella, J. E., Moynihan, P. I., and Simon, W., "Small Rocket Exhaust Plume Data," in *JPL Quarterly Technical Review*, Vol. 2, No. 2, Jet Propulsion Laboratory, Pasadena, California, July 1972.

Bibliography (contd)

Chirivella, J. E., "Boundary Layer Expansion Around the Nozzle Lip," presented at the 7th JANNAF Plume Technology Meeting, U.S. Army Missile Command, Redstone Arsenal, Alabama, Apr. 3–5, 1973.

Chirivella, J. E., "Operation of Small Rocket Engines in the JPL High Vacuum Space Simulator (Molsink)," in *JPL Quarterly Technical Review,* Vol. 3, No. 1, Jet Propulsion Laboratory, Pasadena, California, July 1973.

Chirivella, J. E., and Simon, W., "Molecular Flux Measurements in the Back Flow Region of a Nozzle Plume," presented at the 7th JANNAF Plume Technology Meeting, U.S. Army Missile Command, Redstone Arsenal, Alabama, Apr. 3–5, 1973.

Coulbert, C. D., and Yankura, G., *Survey of Materials for Hydrazine Propulsion Systems in Multicycle Extended Life Applications,* Technical Memorandum 33-561, Jet Propulsion Laboratory, Pasadena, California, Sept. 15, 1972.

Holcomb, L. B., *Satellite Auxiliary Propulsion Selection Techniques,* Technical Report 32-1505, Jet Propulsion Laboratory, Pasadena, California, Nov. 1, 1970.

Appendix
0.44-N (0.1-lbf) Thruster Performance Calculations

The following is a listing of test data parameters and equations used for the computerized performance calculation of the 0.44-N (0.1-lbf) thrusters. (The equations expressed herein were derived and used with the English system of units. Prior to their direct use with the SI system of units, the numerical constants should be recalculated.)

(1) A_{th}, hot nozzle throat area, m^2 ($in.^2$).

$$A_{th} = \frac{\pi d_t^2}{4}\left[1 + 2\alpha\left(\frac{T_{cl} + T_{ns}}{2} - 70\right)\right] \qquad \text{(A-1)}$$

where

d_t = measured nozzle throat diameter at ambient temperature, m (in.)

α = linear coefficient of thermal expansion of nozzle material, m/m K (in./in. °F)

T_{cl} = measured lower chamber skin temperature, K (°F)

T_{ns} = measured nozzle throat skin temperature, K (°F)

(2) P_{ft}, fuel tank pressure, N/m^2 (psia).

$$P_{ft} = P_{ftg} + P_a \qquad \text{(A-2)}$$

where

P_{ftg} = measured fuel tank gage pressure, N/m^2 (psig)

P_a = measured ambient pressure, N/m^2 (psia)

(3) P_c, corrected thrust chamber absolute pressure downstream of catalyst bed, N/m^2 (psia).

$$P_c = P_{c1} + 0.01934\,P_{vc} \qquad \text{(A-3)}$$

where

P_{c1} = measured thrust chamber pressure, N/m^2 (psia) (or use P_{c2})

P_{vc} = measured vacuum test chamber pressure, N/m^2 (torr)

(4) $\Delta P_c/\overline{P}_c$, relative chamber pressure roughness, % (peak to peak).

$$\Delta P_c/\overline{P}_c = \frac{P_c\,\text{max} - P_c\,\text{min}}{\overline{P}_c} \times 100 \qquad \text{(A-4)}$$

where

P_c max = maximum chamber pressure measured, N/m^2 (psia)

P_c min = minimum chamber pressure measured, N/m^2 (psia)

$\overline{P}_c$ = average chamber pressure measured, N/m^2 (psia)

(5) $\dot{m}$, propellant mass flow rate, kg/s (lbm/s).

(a) For the Viscojet ΔP flowmeter, the nondimensional parameters are

$$N_{Re} = \frac{4\dot{m}}{\pi d_e \mu} = \text{Reynolds number} \qquad \text{(A-5)}$$

$$N_{pl} = \frac{g_c \rho d_e^3 \Delta P}{\mu^2 N_s d_s} = \text{pressure modulus} \qquad \text{(A-6)}$$

where

d_e = measured effective orifice passage diameter, 3.82×10^{-4} m (1.5×10^{-2} in.)

ΔP = measured pressure differential across the Viscojet, N/m^2 (psid)

d_s = measured diameter of Viscojet disc element, 1.01×10^{-2} m (0.40 in.)

N_s = number of Viscojet disc elements (3)

ρ = propellant density at measure inlet temperature (T_{fl}, °F), kg/m^3 ($lbm/in.^3$)

μ = propellant viscosity at measure inlet temperature, kg/m-s (lbm/in.-s)

g_c = Newton's constant relating force and mass, $9.8\ \frac{\text{kg-m}}{\text{N-s}^2}$ (3.86×10^2 lbm-in./lbf-s^2)

The Viscojet model 38VL3CM used in this program was calibrated with water and verified with hydrazine after installation into the test system. The calibration curve for this flowmeter showing a plot of N_{Re} as a function of N_{pl} is given in Fig. A-1. Since the plot is linear on a log–log

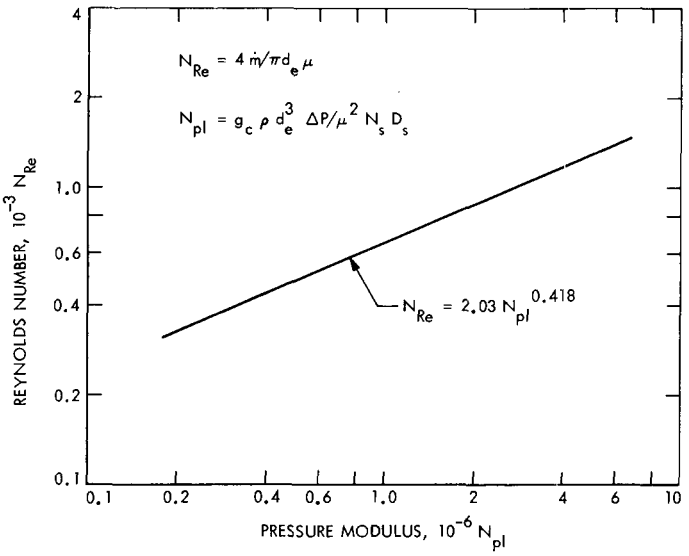

Fig. A-1. Calibration of Viscojet flowmetering device (Model 38VL3CM), with hydrazine at 14°C (57°F)

scale, the equation representing this line was determined to be

$$N_{Re} = 2.03\, N_{pl}^{0.418} \tag{A-7}$$

Solving this equation for $\dot{m}$ produces the final Viscojet flowmeter equation:

$$\dot{m} = 1.379 \times 10^{-3}\, \mu \left(\frac{\rho \Delta P}{\mu^2}\right)^{0.418}, \text{kg/s (lbm/s)} \tag{A-8}$$

(b) For turbine flowmeters, the nondimensional parameters are

$$N_{dc} = \frac{f\rho d^3}{\dot{m}} = \text{discharge coefficient} \tag{A-9}$$

$$N_{Re} = \frac{f\rho d^2}{\mu} = \text{Reynolds number} \tag{A-10}$$

where

f = measured turbine blade output frequency, pulse/s

d = characteristic inside diameter of flowmeter, m (in.)

ρ = propellant density at measured inlet temperature (T_{fl}), kg/m³ (lbm/in.³)

μ = propellant viscosity at measured inlet temperature, kg/m-s (lbm/in.-s)

The Omniflo Model FTM-0.4-LJS, S/N 850425, used in this program was calibrated with water and was also verified with hydrazine in the test system at ambient temperature conditions. The calibration curve of N_{Re} as a function of N_{dc} is presented in Fig. A-2. Since the plotted curve was not linear, it was reduced to tabular form and inserted into the computer program as a subroutine. Propellant mass flow rate was determined by first calculating N_{Re} using Eq. (A-10). The value of N_{dc} was then determined from the flowmeter calibration table and finally $\dot{m}$ was calculated from Eq. (A-9).

(6) c^*, characteristic velocity, m/s (ft/s).

$$c^* = \frac{A_{th} P_c g_c}{\dot{m}} \tag{A-11}$$

where

A_{th} = Eq. (A-1)

P_c = Eq. (A-3)

$g_c = 9.8 \dfrac{\text{kg-m}}{\text{N-s}^2}$ (3.86 × 10², lbm-in./lbf-s²)

(7) $C_{fv\,(calc)}$, calculated vacuum thrust coefficient.

$$C_{fv\,(calc)} = \sqrt{\frac{2\gamma^2}{\gamma - 1}\left(\frac{2}{\gamma + 1}\right)^{(\gamma+1)/(\gamma-1)}\left[1 - \left(\frac{P_e}{P_c}\right)^{(\gamma-1)/\gamma}\right]} + \frac{P_e - P_v}{P_c}\epsilon \tag{A-12}$$

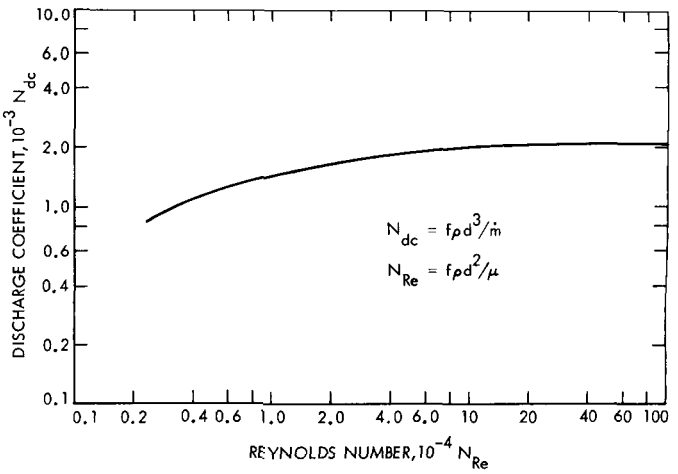

Fig. A-2. Calibration of Omniflo turbine flowmeter (Model FTM-0.4-LJS, S/N 850425), with hydrazine at 14°C (57°F)

where

γ = ratio of specific heat capacities of exhaust products determined from the measured ammonia dissociation level ($X\%$) by the relationship presented in Fig. A-3

P_c = Eq. (A-3)

P_v = 0.01934 P_{vc} (torr) nozzle backpressure, N/m² (psia)

ϵ = nozzle expansion area ratio, A_e/A_t

P_e = nozzle exit pressure, N/m² (psia), determined from

$$P_e = P_c \left(\frac{1}{1 + \frac{\gamma - 1}{2} M_e^2} \right)^{\gamma/(\gamma-1)}$$

where

M_e = exit Mach number calculated from

$$\epsilon^2 = \frac{1}{M_e^2} \left(\frac{1 + \frac{\gamma - 1}{2} M_e^2}{1 + \frac{\gamma - 1}{2}} \right)^{(\gamma+1)/(\gamma-1)}$$

(8) $C_{fv\,(act)}$, actual or corrected vacuum thrust coefficient.

$$C_{fv\,(act)} = C_{fv\,(calc)} - P_v \epsilon / P_c \qquad \text{(A-13)}$$

where

$C_{fv\,(calc)}$ = Eq. (A-12)

P_v = 0.01934 P_{vc} (torr) nozzle backpressure, N/m² (psia)

ϵ = Eq. (A-3)

P_c = nozzle expansion ratio, A_e/A_t

(9) F_v, vacuum thrust, N (lbf).

$$F_v = C_{fv\,(act)} A_{th} P_c \qquad \text{(A-14)}$$

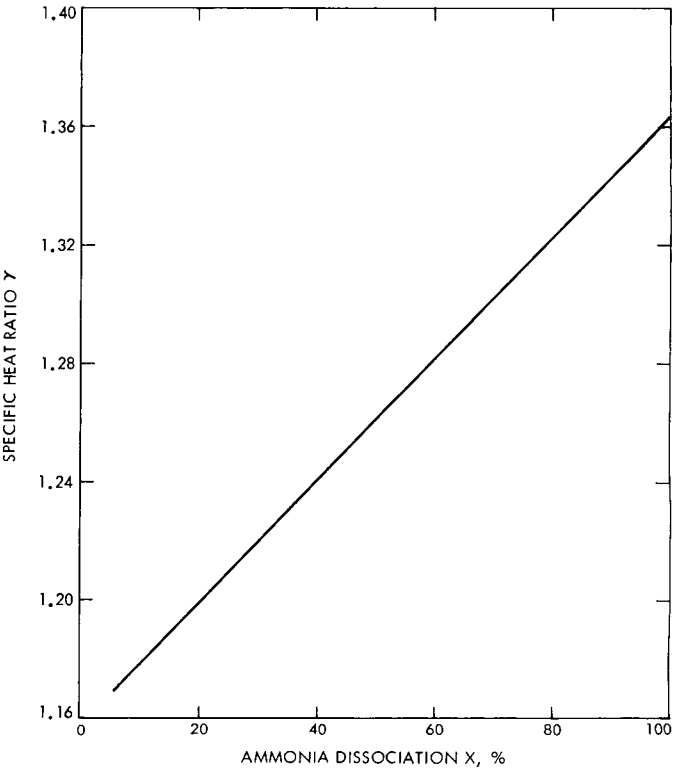

Fig. A-3. Specific heat ratio γ for dissociated products of anhydrous hydrazine as a function of ammonia dissociation X

where

$C_{fv\,(act)}$ = Eq. (A-13)

A_{th} = Eq. (A-1)

P_c = Eq. (A-3)

(10) I_{sp}, specific impulse, N-s/kg (lbf-s/lbm).

$$I_{sp} = C_{fv\,(act)} c^* / g_c \qquad \text{(A-15)}$$

where

$C_{fv\,(act)}$ = Eq. (A-13)

c^* = Eq. (A-11)

g_c = 9.8 kg-m/N-s² (3.86 × 10² lbm-in./lbf-s²)

NASA — JPL — Coml., L.A., Calif.